$^{40}Ar/^{39}Ar$ Ages of Feldspar and Muscovite from the Source and Detritus of the French Broad River, North Carolina

by

Di Fan

A thesis submitted to the Graduate Faculty of
Auburn University
in partial fulfillment of the
requirements for the Degree of
Master of Science

Auburn, Alabama
August 6th, 2016

Keywords: muscovite, K-feldspar, $^{40}Ar/^{39}Ar$,
geochronology, Blue Ridge, French Broad River

Approved by

Willis E. Hames, Chair, Professor of Geosciences
Mark G. Steltenpohl, Professor of Geosciences
Haibo Zou, Associate Professor of Geosciences

Abstract

As the westernmost metamorphic belt of the Appalachians, the Blue Ridge has been the subject of many geochronology studies. The Blue Ridge experienced high-grade deformation and peak metamorphism during Taconic orogeny, followed by a low-grade metamorphic overprint during the Acadian orogeny. The Alleghanian orogeny is the last collisional stage of the Appalachians and associated regional metamorphism and ductile deformation is documented along most of the Piedmont and the Carolina Slate belt. There is still debate, however, as to the extent of Alleghanian metamorphism in the western Blue Ridge. This concern is made more difficult to evaluate because previous work generally did not characterize the history of low-temperature metamorphism of the Blue Ridge in the region between western North Carolina and Tennessee.

To address the cooling history of the Blue Ridge, samples were collected in the area of the French Broad River catchment in North Carolina. Single crystals of muscovite from basement and stream sediment samples and K-feldspar from the basement, were dated in this project to avoid the ‘inherited’ ages often associated with high-temperature geochronometers. Muscovite from basement rock samples in the catchment area yield single crystal $^{40}Ar/^{39}Ar$ ages that typically range from 315 Ma to 400 Ma. K-feldspar crystals from basement rocks yield single crystal ages as young as ca. 270 Ma and up to ca. 1100 Ma. Results for the two mineral phases show similar age distribution patterns: easterly basement samples, within and near the Brevard fault zone, yield Carboniferous

age distributions characterized by simple, single modes, but basement samples collected near and west of Asheville are more complex. The incremental heating experiments for K-feldspar show variable discordance. The variation in ages of microcline and orthoclase crystals from a single basement sample collected west of Asheville covers a wide range of 800 million years from late Mesoproterozoic to Permian. Comparing the results of the present study to published data for higher temperature thermochronometers (e.g., U-Pb ages for zircon, $^{40}Ar/^{39}Ar$ ages for hornblende and micas), it is remarkable that the low temperature record of K-feldspars can be used to characterize a greater range of cooling history rather than the higher temperature thermochronometers. The $^{40}Ar/^{39}Ar$ age signature of detrital muscovite mineral samples collected along the French Broad River catchment becomes dramatically more complex within lower grade rocks downstream (northwest). Our work on basement samples in the catchment shows the complexity is not only due to the increasing sediment input of various local tributaries into the trunk stream, but also to the intra-sample complexity of polymetamorphic history recorded in the metamorphic rocks west of the Brevard fault zone.

Acknowledgments

This project was funded by Geosciences Advisory Board Research Awards and Spencer Waters and Dan Folse Memorial Award. Financial support was also provided through National Science Foundation (grant # NSF 0911687) for the isotopic analyses and the Geological Society of America for conference travel. Special thanks to Dr. Willis Hames for the guidance in the field trips and the lab work and the great help to compile this thesis. This work cannot be done without his help. He is always very patient and meticulous helping in editing my thesis draft and conference abstracts. Thanks are also due to the members of my committee, Dr. Mark Steltenpohl and Dr. Haibo Zou for all the help and suggestions on this study and meaningful comments on this thesis. I have learned a lot from these fabulous professors. The author would like to thank the graduate students James Gunn and Kayla Griffin for the help during the field trip in 2015. Lastly, thanks to my parents and my boyfriend living on the opposite side of the earth for their endless love and support. I hope this thesis is the best gift to them after two and half years of waiting.

Table of Contents

List of Figures

List of Appendices

1 INTRODUCTION

1.1 Introduction

The southern Appalachians record three episodic contractive Paleozoic events, comprising, from earliest to latest, the Taconic, Acadian and Alleghanian orogenies (e.g., Hatcher, 2005). The Blue Ridge Province of the Appalachians is located in the eastern United States, extending from Georgia northward to Pennsylvania. As the western-most high-grade metamorphic belt of the Appalachians, the Blue Ridge has been the subject of many geochronology studies that document high-grade deformation and peak metamorphism during the Taconic orogeny, followed by a low-grade metamorphic overprint during the Acadian orogeny (Goldberg and Dallmeyer, 1997; Corrie and Kohn, 2007). Widespread Alleghanian (325 Ma – 260 Ma) deformation and metamorphism in the southern Appalachians, resulting from culminating Laurentia-Gondwana collision, also overprint and obscure the Taconic and Acadian record (Dallmeyer, 1975a). The Blue Ridge and Piedmont thrust sheets were translated westward onto Laurentia creating the foreland fold-thrust belt, now represented as the Valley and Ridge (Hatcher, 2005).

The maximum temperature that metamorphosed rocks experience can serve as a proxy for their maximum crustal depth during orogenesis. Figure 1 presents a compilation of different temperature-time records for the southern Appalachians (Fan et al., 2015). Conodont color and texture alteration index (CAI) is used to evaluate the

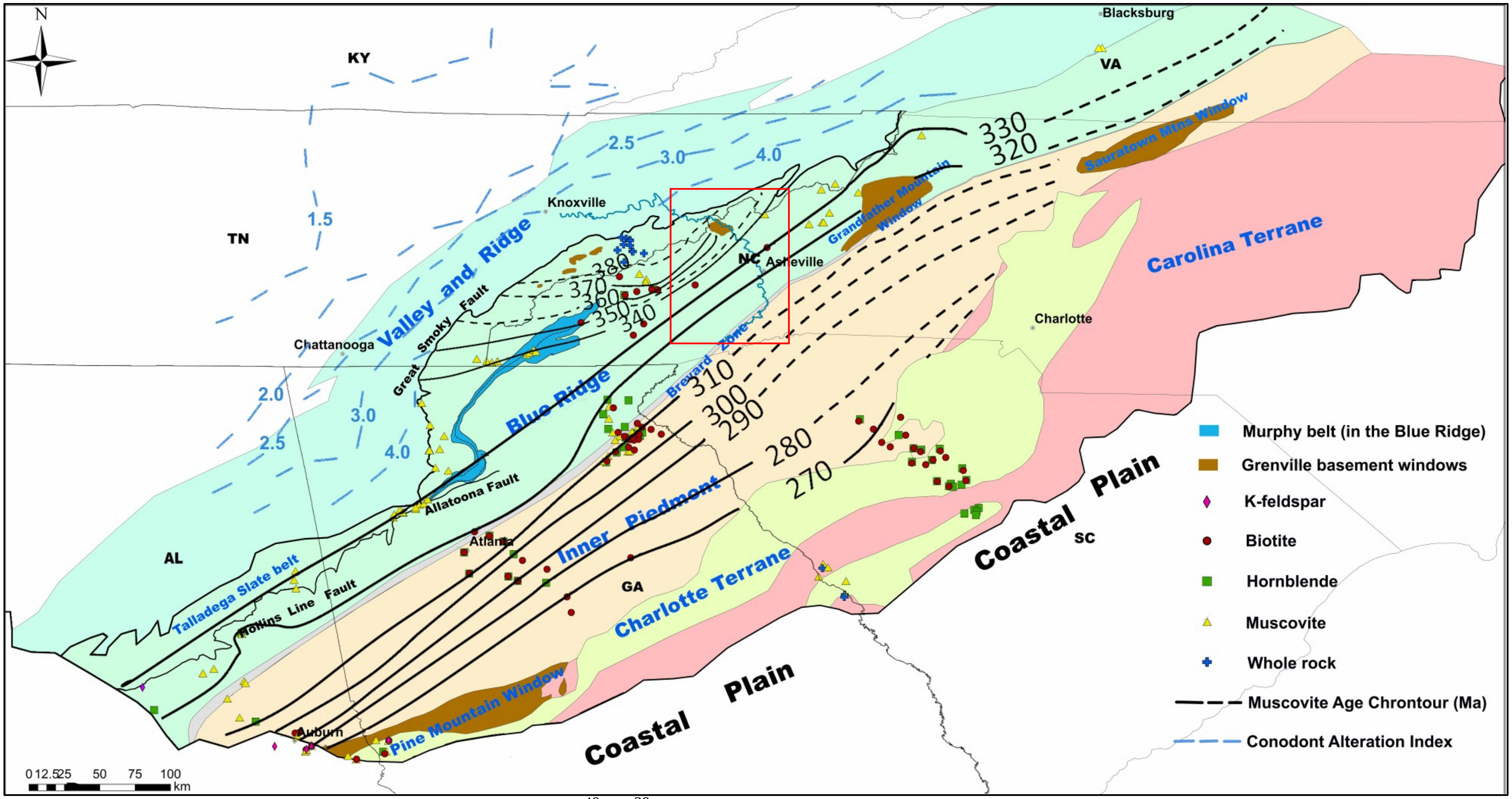

Figure 1. Terrane map of the southern Appalachians and $^{40}Ar/^{39}Ar$ muscovite age chrontours (Fan et al., 2015). Muscovite age chrontours (dashed where extrapolated along strike) in southern Appalachians show the "along-strike" pattern of cooling age in metamorphic and igneous rock. The conodont alteration index represents the thermal maturity of foreland sedimentary sequences. $^{40}Ar/^{39}Ar$ age data of minerals are from previous geochronology studies (Dallmeyer, 1975a; Steltenpohl et al., 2013; sources of additional age data are noted in the references with an asterisk mark '*'). The study area is outlined by the red square.

thermal maturity and estimate the maximum temperature reached by the foreland strata (Rejebian et al., 1987). Studies in the southern Appalachian foreland fold-thrust belt (e.g., Harris et al., 1978) indicate the range of CAI from 1.5 to 4.0 (Fig. 1), which can be correlated to a temperature range of 50 ºC to 300 ºC. Considering the conodont data for the foreland basin, one may infer that the lowest grade rocks of the western Blue Ridge (WBR) experienced Appalachian metamorphic temperatures of at least 300 ºC. $^{40}Ar/^{39}Ar$ age data of various minerals can be applied for the estimation of a temperature-time history in metamorphic rocks. Cooling age 'chrontours', based on the $^{40}Ar/^{39}Ar$ ages of muscovite and other minerals, tend to parallel regional strike and young across strike of the rock units (Fig. 1). This pattern seems compatible with Alleghanian crustal thickening and Barrovian metamorphism in the terranes from the Talladega belt of Alabama to the WBR of southwestern Virginia.

Many previous studies have improved our understanding of the metamorphic history of the Blue Ridge mountains with different petrologic and geochronologic methods (e.g., Carpenter, 1970; Dallmeyer, 1975a; Connelly and Dallmeyer, 1993; Goldberg and Dallmeyer, 1997; Corrie and Kohn, 2007), but the record of the middle-to-low temperature-time history is not well established. Portions of the WBR experienced maximum temperatures of 300-400 ºC. Minerals with different closure temperature record different histories. High-temperature chronometers (such as U-Pb zircon ages, and $^{40}Ar/^{39}Ar$ hornblende ages) may preserve 'inherited ages' and are difficult to apply for dating the metamorphic events in this region. $^{40}Ar/^{39}Ar$ age dating of muscovite and K-feldspar provides an opportunity to look into the cooling history and thermal activity of the low temperature metamorphic rocks. Combined with previous data, a more complete tectonic and cooling history can be constrained.

Detrital samples have the potential to represent all the rocks in a catchment basin in a single sample. A few samples can contain detritus from a large region for more information. Comparing the age data of detrital samples with the source metamorphic and igneous rocks from discrete sites in the catchment basin can constrain the cooling history of the rocks underlying the basin.

1.2 Significance of this Study

Data in this report provide new constraints on the metamorphic history and development of the Blue Ridge. Previous works did not report any geochronological data on K-feldspar in this region. K-feldspar and muscovite $^{40}Ar/^{39}Ar$ ages are reported to evaluate the ~350-150 ºC temperature-time history of the sampling region and the medium-low temperature history can help us understand the shallow crustal tectonic history. The results can be combined with the cooling history based on the previous data at higher temperatures for a more complete pattern of cooling.

The previous published literature is not sufficient to demonstrate the scales of intercrystalline variation in feldspars and micas from single source-rock samples. An age distribution for detrital samples can be correlated to derive a representative source distribution. Furthermore, previous studies do not address how weathering and erosion may mechanically or chemically modify a detrital age distribution from that of the source area. By comparing the age data and the composition of the rock samples and detrital sediments, the application of the two mineral phases as geochronometers can be evaluated.

2 GEOLOGIC SETTING

The Brevard fault zone is a southeastern boundary of the Blue Ridge, separating it from the Piedmont province (Odom and Fullagar, 1973; Fig. 1). The Blue Ridge fault systems, including the Holston-Iron Mountain-Stone Mountain, Great Smoky, and Cartersville Faults, are to the northwest of the Brevard zone (Connelly and Dallmeyer, 1993). The Ocoee Series, a sequence of Late Precambrian quartzo-feldspathic rift-facies sedimentary rock, is conformably overlain by Chilhowee Group of rift-to-drift-facies sandstones and interbedded shales. Metamorphosed rocks of the Murphy syncline are on the southeastern margin of the Ocoee series (Dallmeyer, 1975b). The Ocoee Series nonconformably overlies a Grenville basement complex of polymetamorphic gneisses and plutonic rocks (Fig. 2), both of which were polymetamorphosed and polydeformed during the Paleozoic (Dallmeyer, 1975b; Goldberg and Dallmeyer, 1997). These units have been translated westward by thrust faulting during the Alleghanian orogeny onto the Paleozoic foreland sediments (Connelly and Dallmeyer, 1993).

The Blue Ridge, as a west-verging, overturned anticline, is separated to two parts with contrasting lithostratigraphy, the western Blue Ridge (WBR) and the eastern Blue Ridge (EBR). The east-dipping Hayesville-Burnsville fault, which is a Taconic suture, is the boundary between WBR and EBR (Fig. 3; Dallmeyer, 1988; Miller et al., 2000; Trupe et al., 2003). Among the thrust sheets in the Blue Ridge, the Fries thrust sheet (Fig. 4) is structurally highest (Trupe et al., 2003), and comprises the Grenville basement,

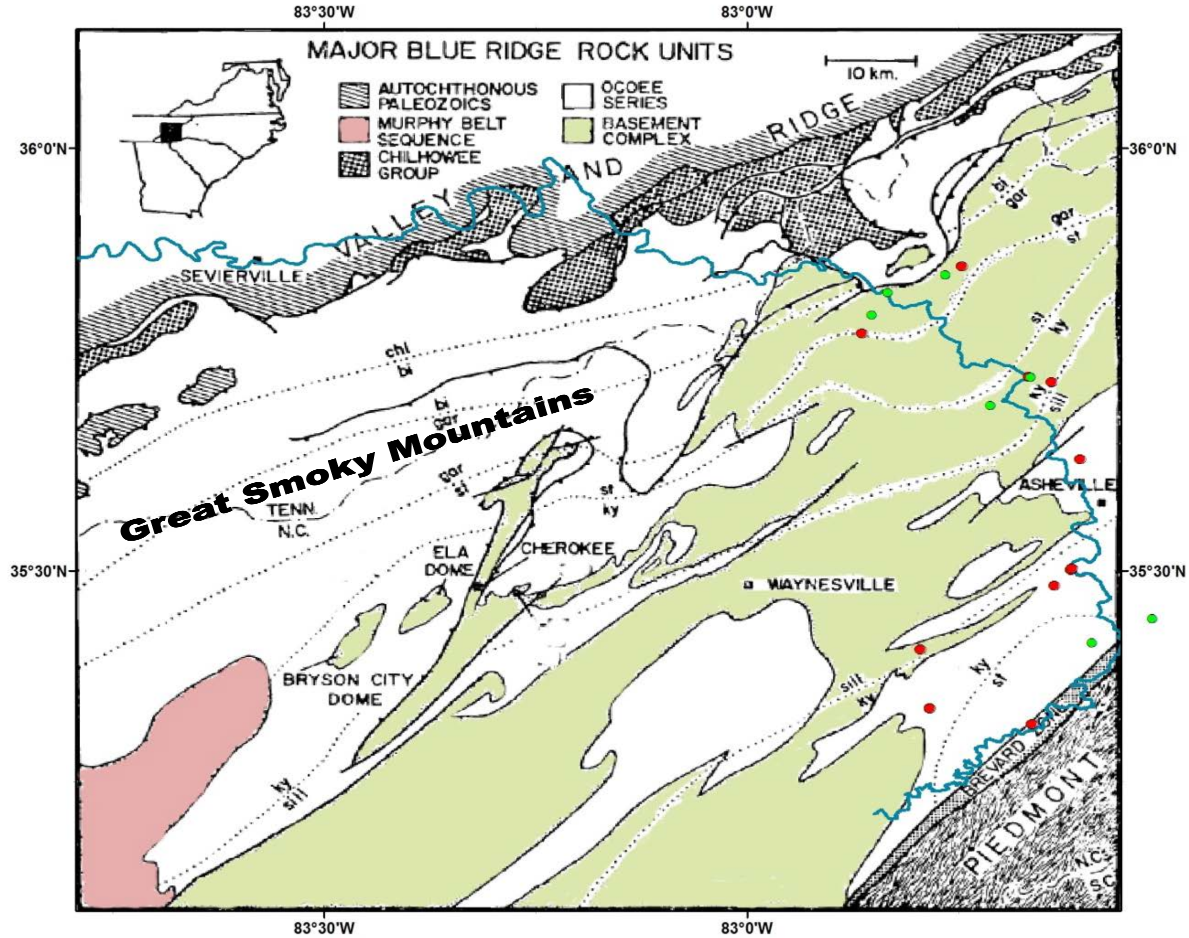

Figure 2. Geologic map of the study area shows the major rock units of the Blue Ridge and the metamorphic zones (modified from Carpenter, 1970, with additions by Dallmeyer, 1975b). The French Broad River is showed in blue. The basement rock samples (red dots) and the detrital samples (green dots) were collected in the French Broad River catchments.

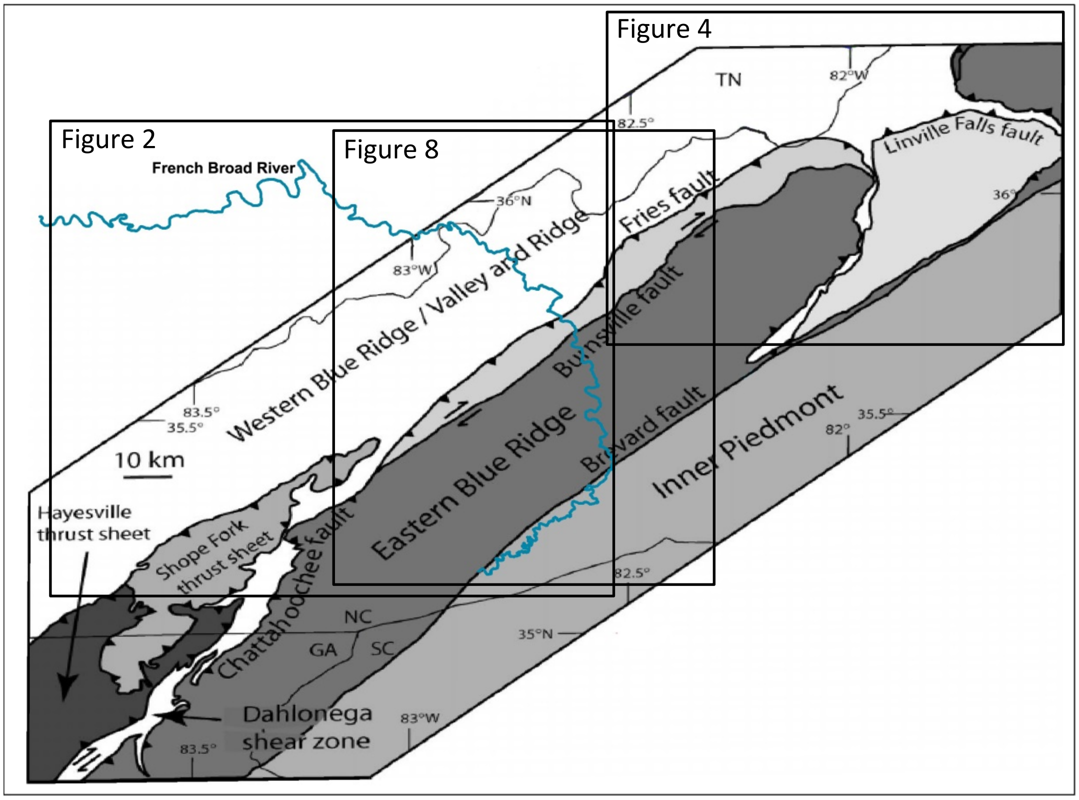

Figure 3. Tectonic map showing the division of the Blue Ridge (Trupe et al., 2003).

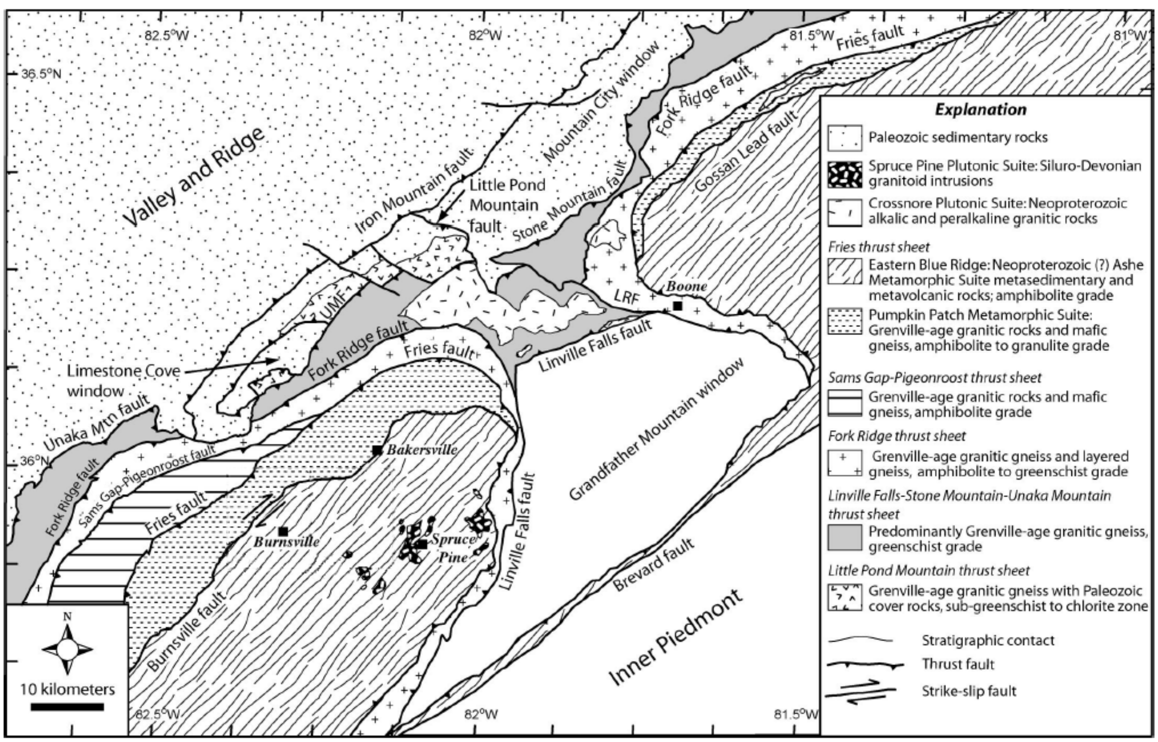

Figure 4. Tectonic map showing the thrust sheets and lithology of the Blue Ridge (Trupe et al., 2003). The thrust sheets extend southeastward to the area of the present study.

the Pumpkin Patch thrust sheet (WBR), and the Ashe Metamorphic Suite (EBR; named Spruce Pine thrust sheet in Goldberg and Dallmeyer, 1997). The thrust sheets to the northwest are below the Fries thrust sheet and are dominated by amphibolite- to granulite-facies basement rocks.

3 PREVIOUS WORK

3.1 Literature Review on the Metamorphic History of the Blue Ridge

Carpenter (1970) used panned alluvial samples (from 354 localities) to construct a metamorphic isograd map of the Blue Ridge (represented in Fig. 2). Carpenter (1970) inferred that the Precambrian metamorphic events occurred at 1300 Ma and 1050 Ma, and the major Paleozoic metamorphic event occurred between 375 Ma to 320 Ma. The sillimanite zone forms a high-grade Barrovian metamorphic core in the region.

Dallmeyer (1975a) used the $^{40}Ar/^{39}Ar$ incremental heating method to analyze biotite and hornblende in gneisses from the Blue Ridge Precambrian basement terrane in northern Georgia, with the assumption that the $^{40}Ar/^{39}Ar$ spectra can distinguish thermally altered samples. Dallmeyer reported that retrograded samples that were not severely affected by Paleozoic metamorphism yield undisturbed age spectra with plateau ages similar to the hornblende and biotite of non-retrograded portions with ages of approximately 1000 Ma and 790 Ma, respectively (Dallmeyer, 1975a). Hornblende retains argon at a higher temperature than biotite, and biotite in turn retains argon at a higher temperature than K-feldspar (Fig. 5). If a sample of Proterozoic rock is not overprinted by Paleozoic metamorphism, we would expect to find K-feldspar ages to be middle to late Neoproterozoic (perhaps 800 Ma – 600 Ma). For the samples that were disturbed by Paleozoic metamorphism, the ages could be affected by diffusive argon loss

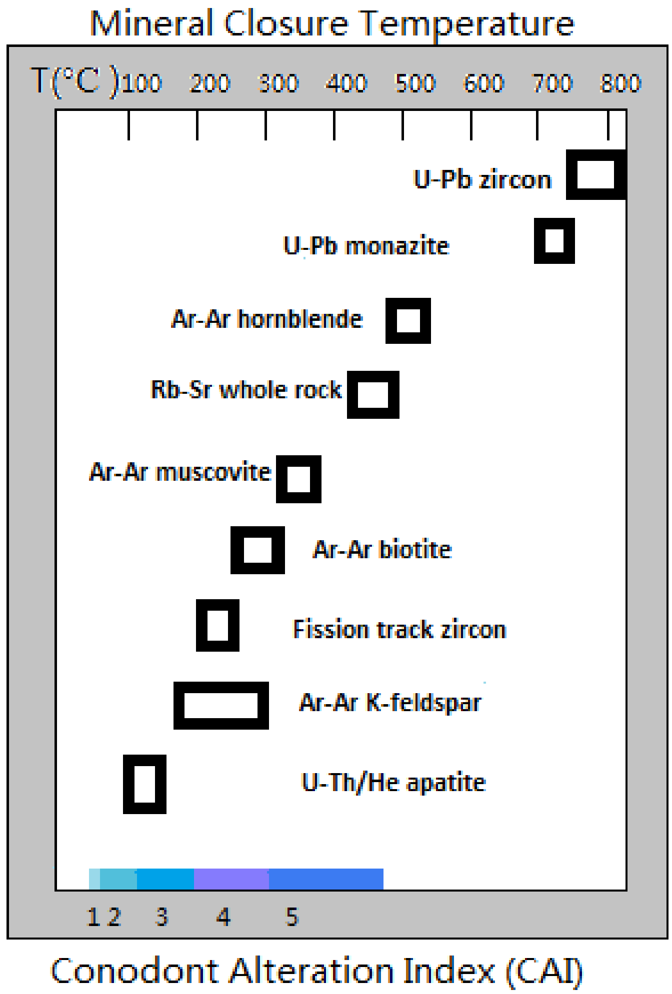

Figure 5. Closure temperatures of different minerals using different dating methods (Hodges, 1991; McDougall and Harrison, 1999; Zeitler et al., 1987) and the conodont alteration index with the corresponding temperature range (Harris et al., 1978; Rejabian et al., 1987).

during Paleozoic reheating. Dallmeyer (1975b) showed that biotite (ca. 345 Ma) and hornblende (ca. 415 Ma) collected from Grenville basement near Cherokee in North Carolina have ages that were "reset" by Paleozoic metamorphism (Fig. 2). Based on the $^{40}Ar/^{39}Ar$ age data, he interpreted the results to reflect a peak metamorphic event in Ordovician (at ca. 480 Ma).

In the last two decades, the poly-metamorphic evolution history of the Blue Ridge and Talladega belt has been documented by several studies, but there are conflicting interpretations in the timing of the Paleozoic metamorphic events. Fossils found within Talladega slate belt (Tull et al., 1988; Gastaldo et al., 1993) suggest post-Devonian to early Mississippian metamorphism. Connelly and Dallmeyer (1993) dated whole rock slate and phyllite samples from the lower metamorphic grade zones, and muscovite concentrates from the higher-grade metamorphic rocks in the western Blue Ridge (WBR), to test the long-standing controversy. The whole-rock samples collected from the chlorite zone yield ages of ca. 440-460 Ma, while the whole-rock samples from biotite and garnet zones yield younger ages of 340-380 Ma (Fig. 1). These results were interpreted to indicate two distinct tectonothermal episodes (Connelly and Dallmeyer, 1993). Their samples of muscovite concentrates yielded $^{40}Ar/^{39}Ar$ ages of 360 Ma to 380 Ma, and the oldest age was interpreted to record the timing of peak metamorphism in this area (Connelly and Dallmeyer, 1993). Corrie and Kohn (2007) published ID-TIMS data for monazite inclusions in garnet, and found a mean U-Pb age of ca. 450 ± 5 Ma. They interpreted this age to represent garnet growth during peak metamorphism of the Taconian orogeny in the Great Smoky Mountains (WBR), requiring the isograds of the Great Smoky Mountains to be Taconian in age. Corrie and Kohn (2007) suggested that previously reported Silurio-Devonian fossils (Unrug and Unrug, 1990) cannot exist in this region. Because of the structural position equivalent of the Talladega slate belt and the WBR, Tull et al. (1988) proposed that the fossil data and associated siliciclastics in the Talladega slate belt can be extrapolated to correlate with the WBR. The Silurian – Early Devonian fossils of the Talladega slate belt, therefore, cannot be reconciled with the U-Pb monazite ages for the region of the Great Smoky Mountains on the basis of the data available currently.

3.2 Dating of Detrital Minerals

Dating of detrital minerals such as zircon, muscovite, feldspar, and garnet is widely applied for providing age constraints for geologic events. Different minerals may record different temperatures of closure from igneous and metamorphic events as well as their cooling histories (Fig. 5). The limitation of using detrital minerals is that the minerals in the sediments may be mixed from several source areas, so the results from different sources can overlap, making the record difficult to interpret.

Muscovite is common in regionally metamorphosed sediments and is stable over a wide range of pressure-temperature conditions. $^{40}Ar/^{39}Ar$ dating of detrital muscovite has been utilized in many previous studies (e.g., Copeland and Harrison, 1990; Goldberg and Dallmeyer, 1997; Najman et al., 1997; Brewer et al., 2006). Feldspar is also a logical choice for $^{40}Ar/^{39}Ar$ detrital studies because of its abundance in nature, but the $^{40}Ar/^{39}Ar$ systematics of feldspar are much more complicated than muscovite. In a simplest model, muscovite crystals form single diffusion domains, with diffusion of ^{40}Ar along the [001] surface (e.g., Hames and Bowring, 1994). Feldspars have more complicated diffusion geometries, and tend to yield results that can be explained by multiple diffusion domains (Lovera et al., 1989).

Hietpas et al. (2010) compared the fidelity of detrital zircon and monazite ages as tools for the investigation of provenance of modern and ancient sediments of the French Broad River (Fig. 6 and Fig. 7). They found these minerals were largely derived from weathering of Proterozoic crystals from lithologies of the southern Appalachian Blue Ridge and western Inner Piedmont. The data from zircon recorded the Grenville and

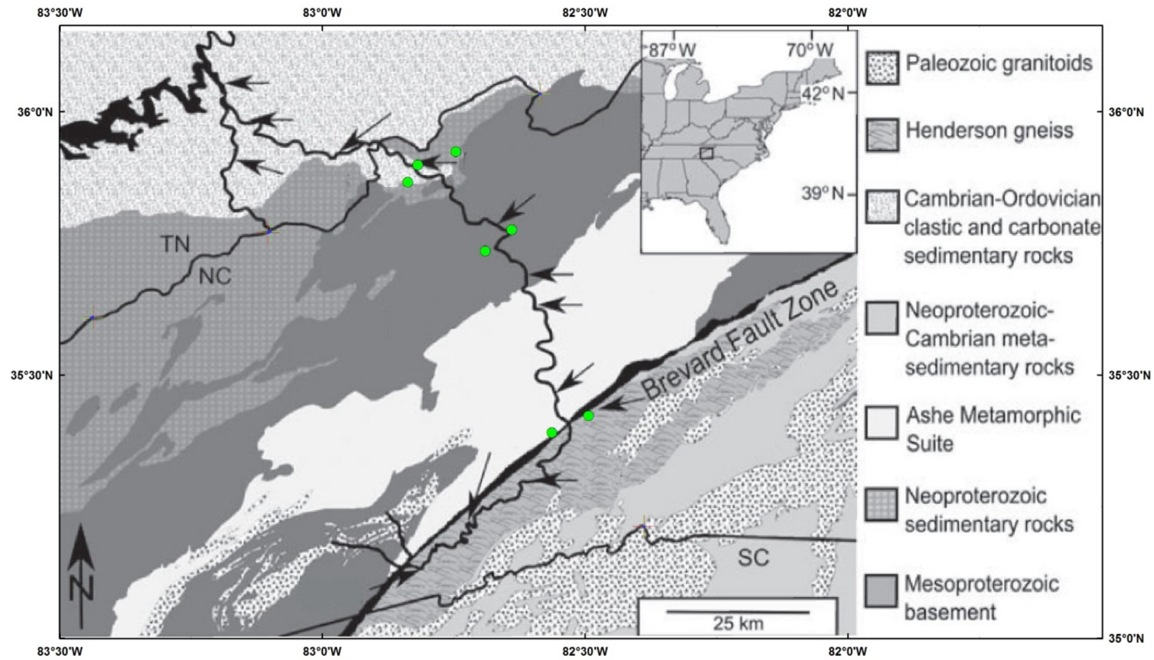

Figure 6. Map of the French Broad River (FBR) catchment region with the locations of 12 sampling sites (arrows) for detrital zircon and monazite (Hietpas et al., 2010) and the detrital sample locations for this project (six of them are from the tributaries of the FBR). This figure is modified from Hietpas et al. (2010).

Figure 7. The main stream of the French Broad River. Detrital samples were collected from the point bars or directly from the river bed.

Taconian events, while monazite sample ages mainly record Taconian and Acadian metamorphism; monazite age data also recorded the 300 m.y. old Alleghanian event that did not appear in the zircon age data. Detrital muscovite in modern stream sediment collected from the French Broad River yield $^{40}Ar/^{39}Ar$ age distributions with a prominent mode at 320 Ma (Hames et al., 2012). The age data on detrital minerals from the French Broad River indicate craton evolution back to the Grenville and the subsequent Paleozoic tectonic events of the southern Appalachians (Hames et al., 2012). However, little geochronologic work has been done in the basement lithologies along the French Broad River, and earlier datasets do not contain $^{40}Ar/^{39}Ar$ ages of feldspar and generally lack muscovite.

4 SAMPLE PETROGRAPHY

4.1 Introduction

The main objectives of the petrographic analysis in this project are to check the micro-structures that are not visible in the hand sample and to provide a strong basis for the interpretation of the mineral relationships. The analysis mainly focuses on the textures of the minerals and their mutual grain boundary relationships to help interpret the age data. Minerals from a sample with a simple history can be expected to yield a simple age distribution. However, a sample that has been subjected to multiple reheating or recrystallization events can be expected to yield more complex distributions of age. The mineral microstructures can also be correlated with the metamorphic conditions. By evaluating the feldspar and quartz microstructures in terms of different types of deformation mechanisms, the temperature history can be constrained more fully.

In this project, minerals from both basement rocks and stream sediments are dated, and an accurate understanding of the mineralogy and mineral textures is necessary for the determination of the sediment sources. To understand the correlation between the ages determined for minerals from the rock samples and from the detrital samples is one of the key objectives of this investigation. We can then estimate correlations between the rock samples and the detrital samples.

4.2 Sampling Sites

The French Broad River flows 213 miles from Transylvania County in North Carolina north to near Knoxville, Tennessee. A total of twelve rock samples (mostly biotite gneiss or muscovite-biotite schist, Appendix A) were collected from the basement near the French Broad River (Fig. 8). Basement rock sample locations were selected on the basis of lithology with available minerals (muscovite and K-feldspar) for $^{40}Ar/^{39}Ar$ analysis, metamorphic grade and location within the stream catchment area. The locations of sample sites were recorded using a hand held GPS.

Eleven of the twelve samples are from the Blue Ridge, and one sample is from the Henderson gneiss in the Inner Piedmont. The samples from the Blue Ridge are mainly biotite gneiss, mica schist, and some low-grade metasedimentary rocks. The petrography of these samples is discussed for the Inner Piedmont and then the eastern Blue Ridge followed by the western Blue Ridge, progressing from higher to lower grades of metamorphism.

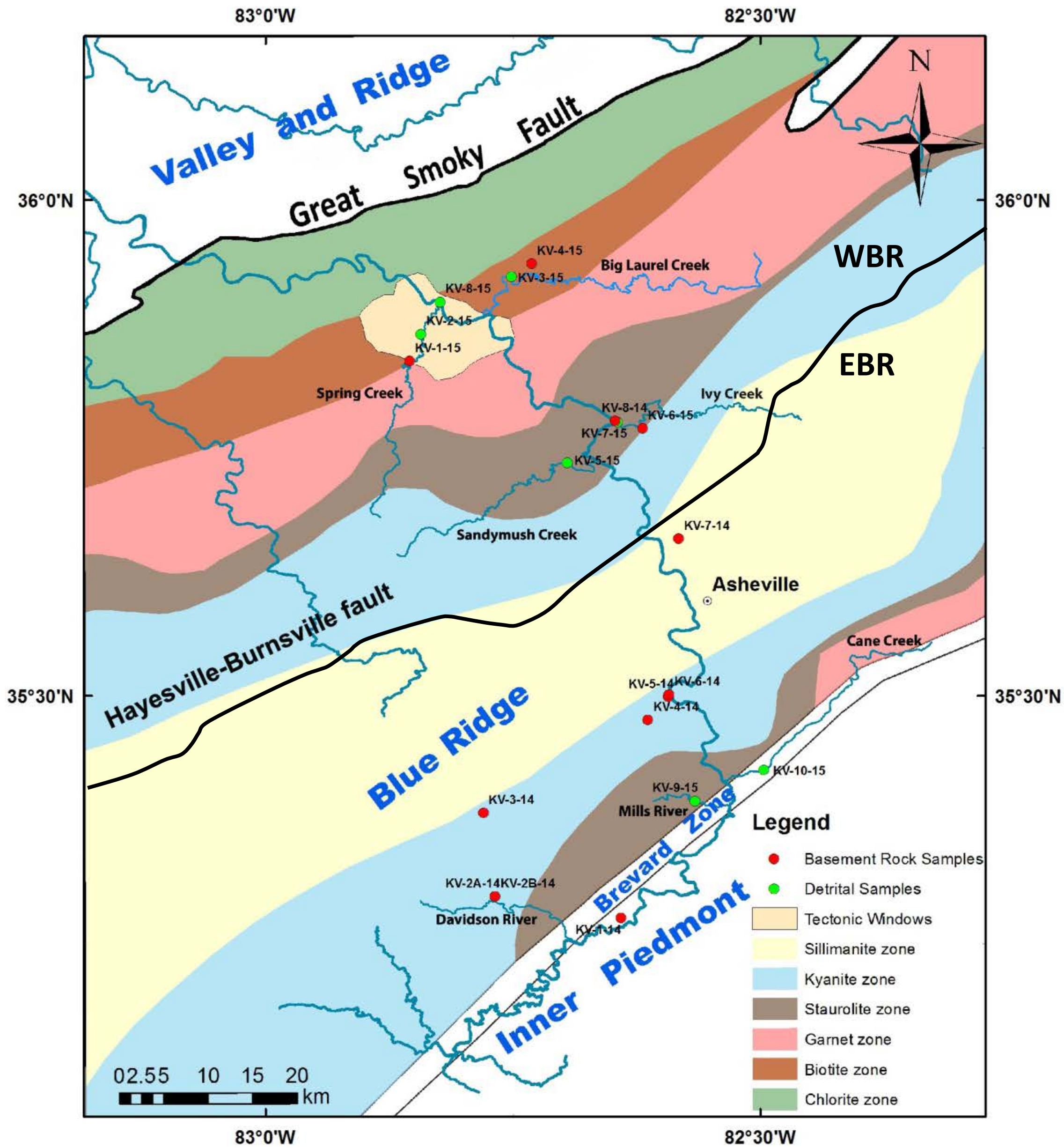

Figure 8. Map of the French Broad River, its main tributaries, and metamorphic zonations illustrating the sample localities (The isograds are modified from Carpenter, 1970; Dallmeyer, 1975b; Hatcher and Goldberg, 1991; Tull and Holm, 2005; Corrie and Kohn, 2007; Tull et al., 2012).

4.3 Petrography analysis

Inner Piedmont (Henderson Gneiss)

The Henderson Gneiss is a large, batholith-scale unit of the Inner Piedmont. It is a quartz monzonite with a crystallization age of ca. 535 Ma (Odom and Fullagar, 1973; Harper and Fullagar, 1981) that was subsequently metamorphosed. The Henderson Gneiss is exposed near the Brevard Zone, and has experienced variably intense deformation and retrogression (Odom and Fullagar, 1973; Davis, 1993). The gneiss is dominated by quartz, plagioclase, biotite, and microcline and some muscovite.

Sample KV-1-14 (Fig. 9) was collected from the Henderson Gneiss adjacent to the Brevard Zone. The sample is a biotite augen gneiss which typifies the Henderson Gneiss. The mineral assemblage is microcline + quartz + biotite + plagioclase + sericite. The rock is overall medium-to-coarse grained (0.5 – 1.5 mm) with inequigranular texture. The gneissosity is defined by distinct biotite layers that alternate with feldspar-quartz layers, and this fabric is pervasive in the whole thin section. Microcline is characterized by tartan-plaid twinning. Myrmekitic intergrowths can be observed near the microcline crystals. Quartz occurs as large single crystals (approximately 0.5mm) with local subgrains and as polycrystalline elongate masses within the foliation. Quartz typically has weakly undulose extinction. Locally, sericite is developed at the expense of feldspars. This sample of Henderson Gneiss is interpreted to be mylonitic, and to have experienced deformation at temperatures sufficient for the dynamic recrystallization of quartz and feldspar and development of gneissosity (i.e., amphibolite facies conditions).

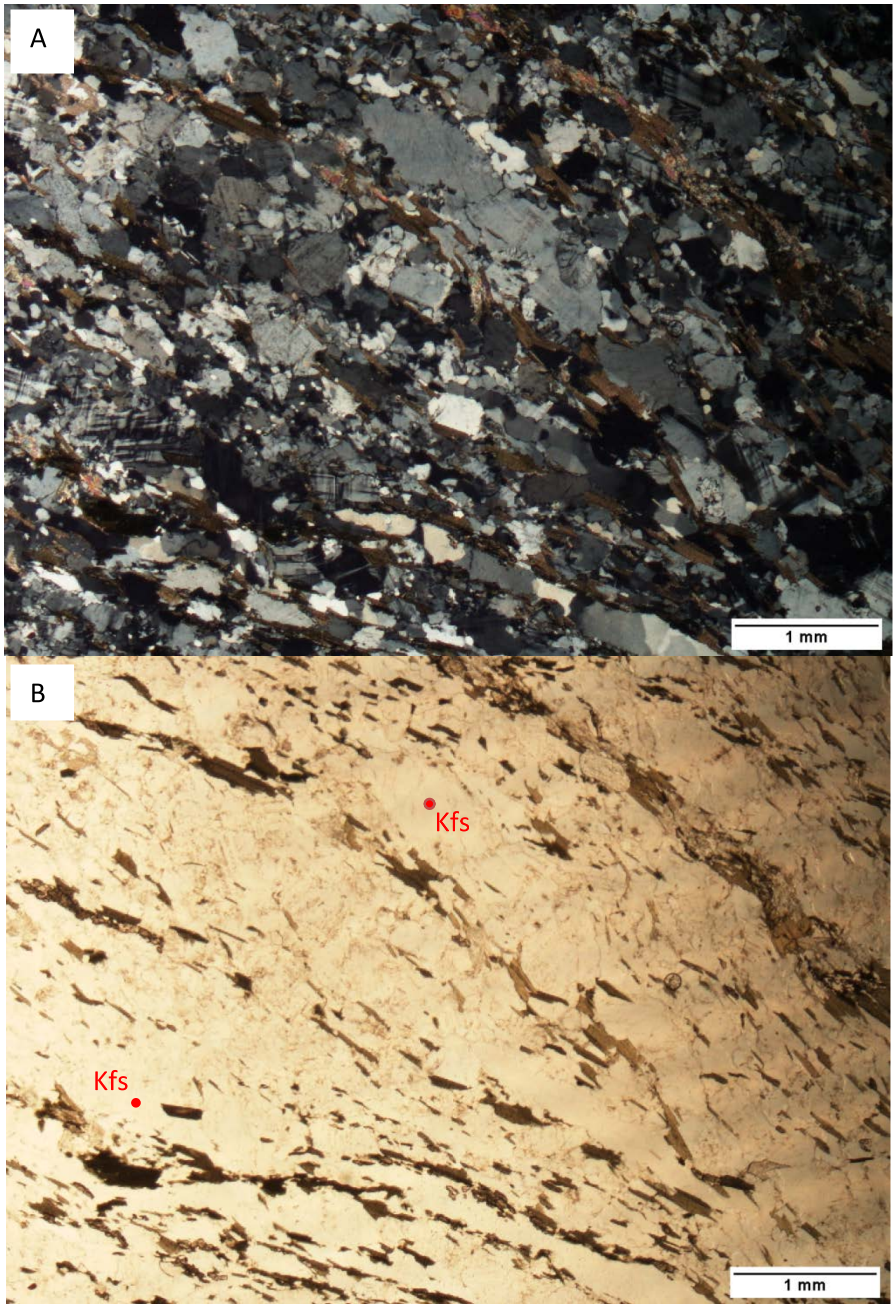

Figure 9. Thin section photomicrography of sample KV-1-14 from the Inner Piedmont (Henderson Gneiss). A: Cross-polarized view, showing an obvious gneissosity. Microstructures indicate that he sample is a mylonite. B: Plane-polarized photomicrograph of the area in A. Biotite appears to define the foliation in this view. Two deformed, porphyroclastic microcline crystals (Kfs) are labeled.

Eastern Blue Ridge

The eastern Blue Ridge and the western Inner Piedmont have similar lithologies and have been collectively defined as the Tugaloo terrane (Hatcher, 2005). The eastern Blue Ridge contains a variety of medium- to high-grade metamorphosed igneous and sedimentary rocks, including numerous felsic plutons (Dallmeyer, 1975b; Miller et al., 2006). Part of the Grenvillian basement is also exposed in the eastern Blue Ridge (Fig. 2). Volcanic and sedimentary rocks overlying the basement units (Ashe Metamorphic Suite) developed with the closure of the Iapetus and Rheic Oceans during the early to middle Paleozoic (Miller et al., 2006). The eastern Blue Ridge rocks are locally migmatitic, recording very-high temperatures reached by these rocks during the Paleozoic (Trupe et al., 2003).

Samples collected from the eastern Blue Ridge are from the Ashe Metamorphic Suite and some associated intrusive rocks. Sample KV-2B-14 is a muscovite-biotite-graphite schist with mica that defines a single-generation fabric (Fig. 10). KV-2A-14 was collected from an adjacent deformed igneous rock. It is a metadiorite with biotite, muscovite and garnet. Quartz textures record deformation through undulose extinction and subgrain rotation. Sample KV-3-14, KV-4-14, and KV-5-14 are biotite gneisses that are similar to KV-2A-14. Sample KV-3-14 is characterized by an anastomosing foliation that wraps around plagioclase and quartz porphyroclasts. The fabric shows muscovite as a fabric forming mineral and as porphyroclasts (Fig. 10C, D). Sample KV-4-14 and KV-5-14 (Fig. 11) are characterized by elongated feldspar and multiple generations of mica showing different orientations to the principle foliation.

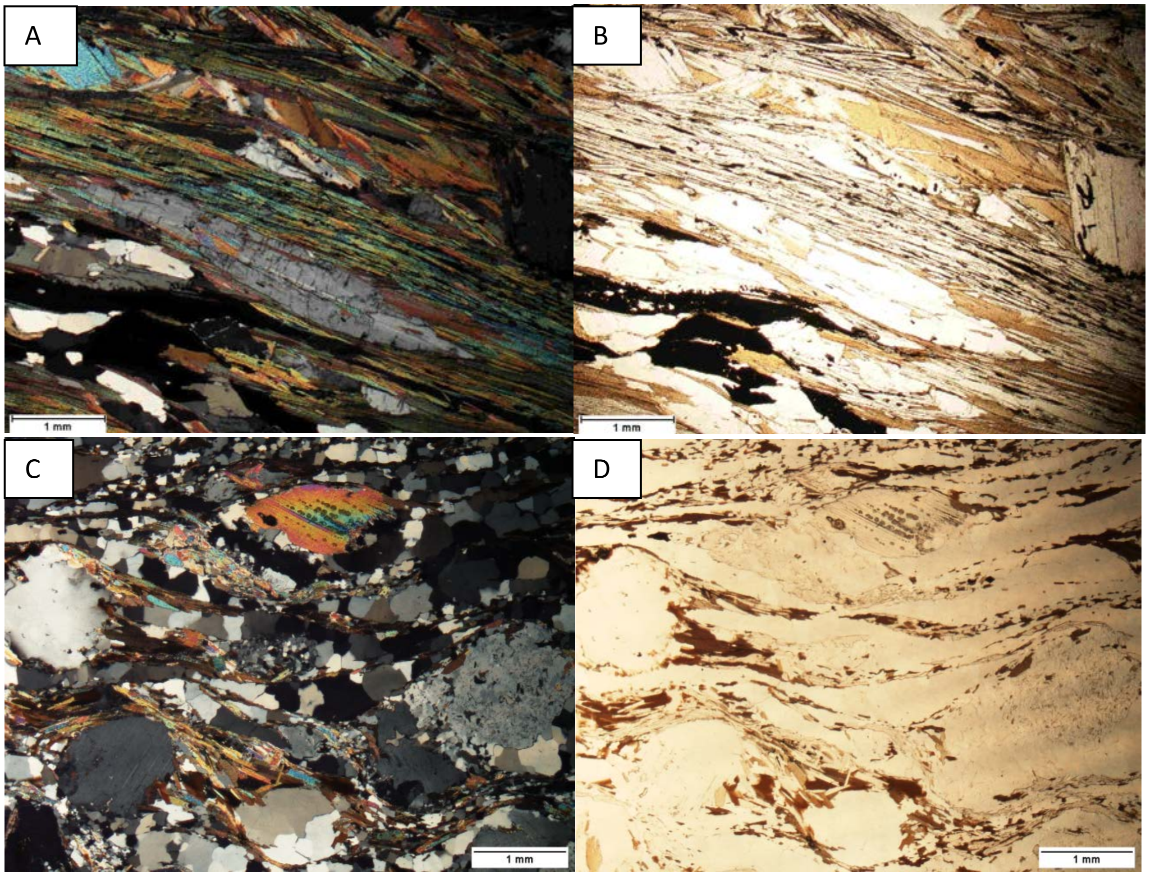

Figure 10. Thin section photomicrographs of the samples from the eastern Blue Ridge. A: Cross-polarized view of sample KV-2B-14, showing an elongated plagioclase along the mica-defined fabric. B: Plane-polarized view of the area in A. Opaque mineral is graphite. C: Cross-polarized view of sample KV-3-14, showing porphyroclasts of feldspar, quartz, and muscovite in an anastomosing foliation. D: Plane-polarized photomicrograph of the area in C.

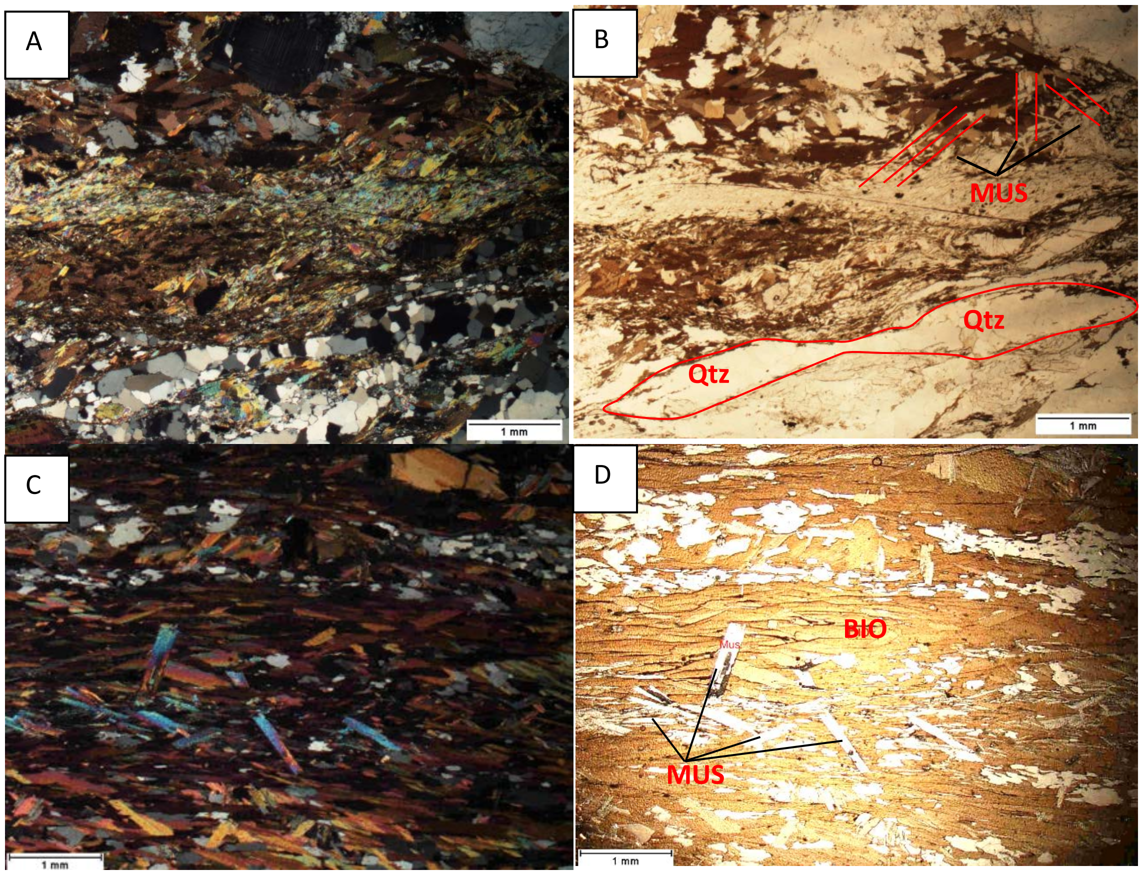

Figure 11. Thin section photomicrographs of the samples from the eastern Blue Ridge.
A: Crossed-polarized view of sample KV-4-14, showing multiple-generation of muscovite. B: Plane-polarized view of the area in A. S-C fabric of quartz can be observed.
C: Cross-polarized photomircrograph of sample KV-5-14, showing a principal foliation defined by muscovite and biotite, and a later generation of cross-cutting muscovite. D: Plane-polarized view of the area in C. This sample is rich in biotite.

KV-5-14 is very rich in biotite (>70%), and biotite also defines the foliation. Sample KV-6-14 and KV-7-14 are mica schists with the mineral assemblage muscovite + biotite + plagioclase + quartz + garnet ± rutile. They are characterized by multiple-generation of muscovite and undulose extinction in the muscovite crystals around the garnet porphyroblasts. Garnet porphyroblasts have inclusions that define an internal surface that differs from the main schistosity. Collectively, the eastern Blue Ridge samples appear to have experienced an earlier metamorphic event that produced garnet, followed by deformation and metamorphism sufficient to deform and recrystallize muscovite and biotite.

Western Blue Ridge

The western Blue Ridge consists of numerous imbricated thrust sheets bounded by faults that were active during Alleghanian movements (Goldberg and Dallmeyer, 1997; Trupe et al., 2003). The western Blue Ridge in North Carolina is dominated by low- to high-grade metamorphosed sedimentary rocks of late Precambrian to early Paleozoic age and polymetamorphosed basement rocks (Connelly and Dallmeyer, 1993). The basement rocks are mainly granitic gneiss and associated granitic intrusions (Goldberg and Dallmeyer, 1997; Miller et al., 2006). The metamorphic grade in the western Blue Ridge generally increases from the northwest to the southeast (Fig. 8).

Samples collected for this study in the western Blue Ridge represent diverse lithologies. Sample KV-8-14 and KV-6-15 are granitic biotite gneisses with the mineral assemblage quartz + plagioclase + biotite + K-feldspar + sphene ±garnet ± sericite (Fig. 12). In both of the samples, quartz and K-feldspar show granoblastic interlobate texture. Single grains of quartz have undulose extinction and subgrain rotation is very common. Some fine-grained quartz crystals have boundaries curved into the neighboring grains as a result of dynamic recrystallization through grain-boundary bulging (Passchier and Trouw, 1996). Chlorite is locally present, forming after biotite. Sample KV-1-15 was collected from the Max Patch Granite near the Spring Creek. The mineral assemblage is quartz + K-feldspar + plagioclase +biotite + epidote+myrmekite. Myrmekite is very common in this sample, likely induced by strain. The large grains of feldspar and quartz (around 1mm) show bright rims under cross polarized light (Fig. 12) and feldspar has fractures. Sample KV-4-15, which is the northernmost rock sample, is a quartzite at very low metamorphic grade. Large quartz crystals (1 – 5 mm) and plagioclase

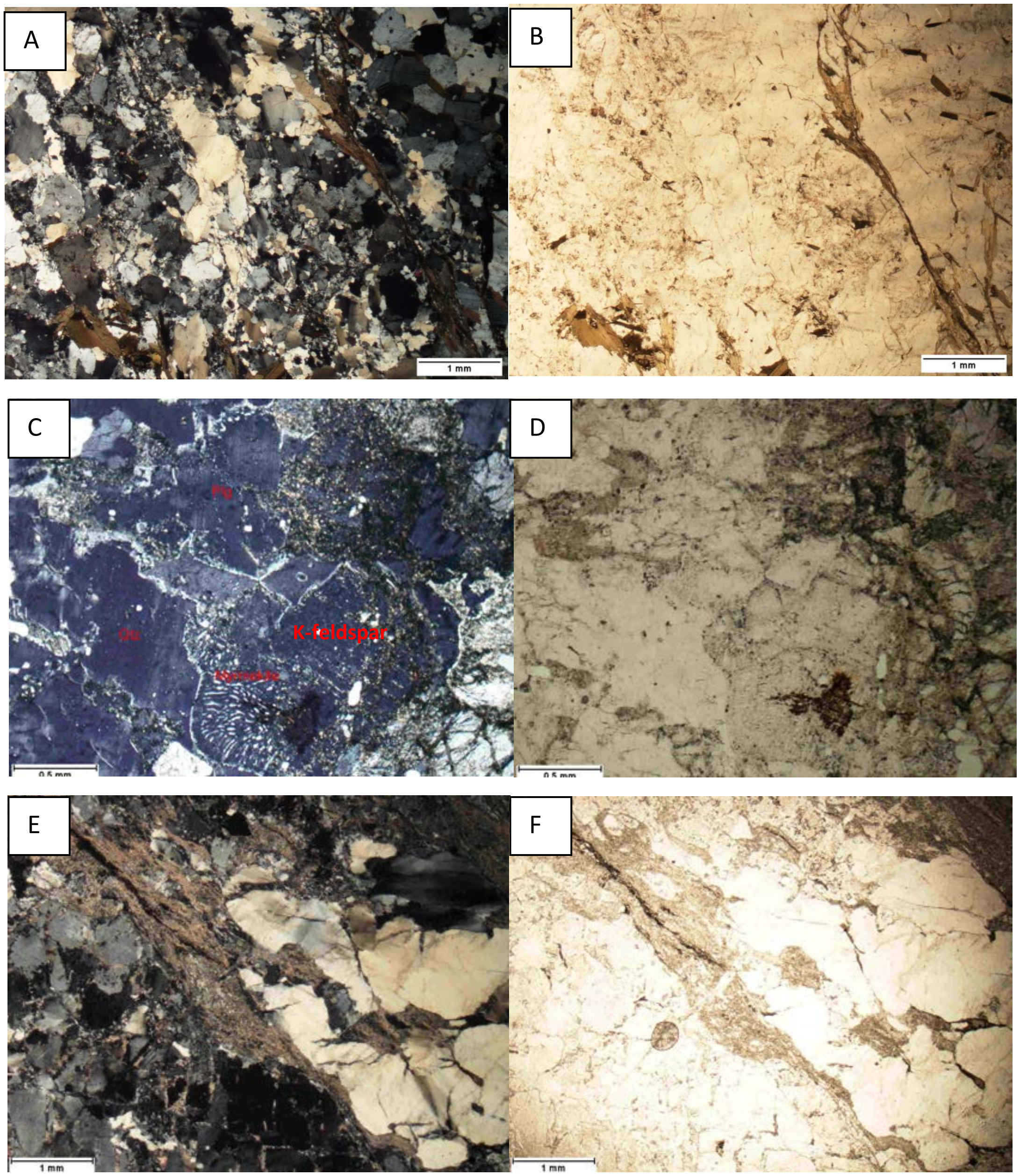

Figure 12. Thin section photomicrographs of samples from the western Blue Ridge. A: Cross-polarized photomicrograph of sample KV-6-15. This granitic biotite gneiss shows granoblastic texture. B: Plane-polarized view of the area in A. C: Cross-polarized photomicrograph of sample KV-1-15, showing myrmekite grown at the boundary of large K-feldspar crystal. The grains show bright rims that may be late (hydrothermal) quartz. D: Plane-polarized view of the area in C. E: Cross-polarized photomicrograph of sample KV-4-15, a metasedimentary rock. F: Plane-polarized view of the area in E, showing fractures in quartz crystals.

crystals (1 – 2 mm) have fractures filled with fine-grained mica and feldspar. Muscovite was not common within the lithologies observed in the western Blue Ridge.

5 $^{40}Ar/^{39}Ar$ ANALYSIS RESULTS

5.1 Introduction

In the $^{40}Ar/^{39}Ar$ method, the sample to be dated is first irradiated in a nuclear reactor with fast neutrons to transform ^{39}K to ^{39}Ar and then fused in an ultrahigh vacuum system to extract argon for purification and analysis in a mass spectrometer (Merrihue and Turner, 1966; see details in McDougall and Harrison, 1999).

Following corrections for interfering isotopes, the age can be calculated by the equations below.

$$t = \frac{1}{\lambda}\ln\left(1 + J\,\frac{^{40}Ar^{*}}{^{39}Ar_{K}}\right) \qquad J = \frac{e^{\lambda t} - 1}{^{40}Ar^{*}/^{39}Ar_{K}}$$

In the two equations above, λ is the decay constant of ^{40}K with a value of 5.543 $\times 10^{-10} yr^{-1,}$ and J is the irradiation parameter which is proportional to the amount of ^{39}Ar produced during irradiation.

5.2 Experimental methods

Feldspar and muscovite grains were separated from rock samples following disaggregation and sieving by hand-picking from the 18 – 40 mesh size range (420 – 1000 μm). Stream sediments were first air-dried in the lab room, and then the feldspar and muscovite crystals were handpicked under a binocular microscope. These samples were dated in the ANIMAL lab under the direction of Dr. Willis Hames at Auburn University (Fig. 13). Further details of the $^{40}Ar/^{39}Ar$ analyses are in Appendix C.

Two different experiment methods are applied for the $^{40}Ar/^{39}Ar$ analysis of muscovite and K-feldspar. This is based on the different lab behaviors of these two types of minerals.

Single crystal total fusion (SCTF) was used for muscovite, to heat single crystals with a fixed power until fused, and then the total released gas from the crystals is measured. This approach to evaluate 'total gas' ages for muscovite is justified, as muscovite in low-grade and Barrovian metamorphic rocks generally does not contain extraneous argon. Excess argon is not commonly found in muscovite unless it is formed under high pressure (c.f., Arnaud and Kelley, 1995; Boundy et al., 1997). The application of SCTF is an efficient way to determine the distribution of single-crystal ages in a sample.

Single crystal incremental heating (SCIH) experiments are used to heat single crystals in a series of steps of increasing temperature, while the argon released from each step is measured. In this case, an age for each step is calculated, and the pattern of different ages may indicate the timing of multiple events or resolve extraneous argon. This approach was used for K-feldspar, since this mineral commonly contains extraneous argon in defects of the crystals or fluid inclusions. The age spectra of SCIH provide additional information that can be useful to evaluating the overall thermal history.

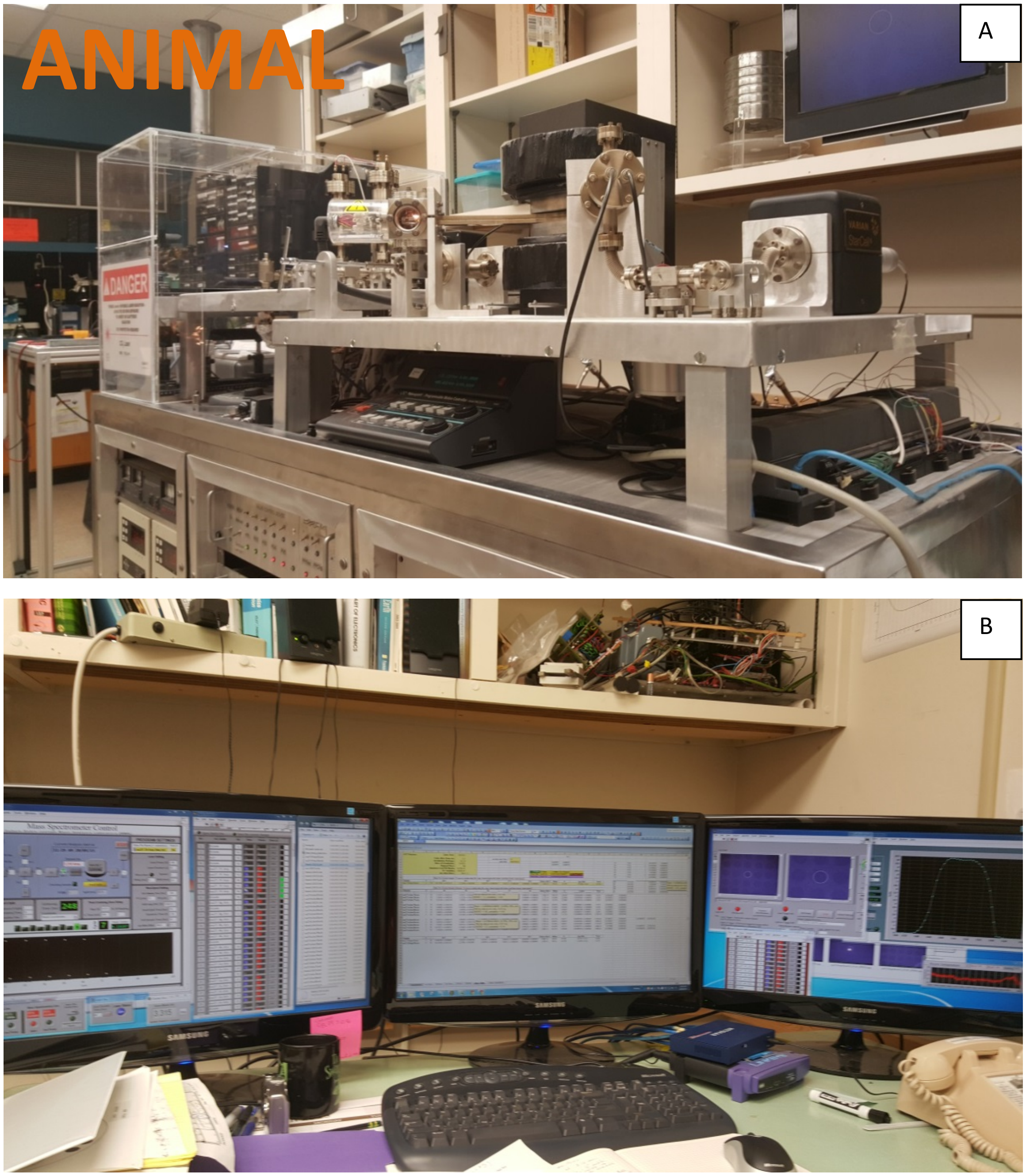

Figure 13. (A) Argon extraction system and the mass spectrometer in the lab ANIMAL. (B) The system is fully automated and under computer control.

5.2 Basement Rocks

5.2.1 Muscovite in the basement rock samples

Muscovite crystals from six basement rock samples have been dated (Fig. 14). All of these samples are from the Ashe Metamorphic Suite, eastern Blue Ridge. The crystal size is mainly between 400 μm to 800 μm. For samples KV-3-14, KV-4-14, KV-5-14, KV-6-14, and KV-7-14, twenty-five crystals of muscovite from each sample were selected to be analyzed by SCTF experiment. For sample KV-2-14, ten crystals were analyzed.

Two samples, KV-2-14 and KV-3-14 yield age distributions with single modes, and average ages for all crystals analyzed of 316.73±0.43 Ma and 321.70±0.45 Ma respectively (at the 95% confidence level). For these results, both the MSWD values are less than 5. The low MSWD values for data of these samples are consistent with age dispersion due to closure temperature variations for crystals of differing size that experienced cooling following a single metamorphic event. The age distributions for other muscovite samples are complex, with multiple modes and ranges of age that tend to increase to the northwest, suggestive of pre-Alleghanian events in the western Blue Ridge. Of these samples, KV-4-14 is farthest to the southeast. This sample yields ages clustered at ca. 325 Ma, but with a distribution that is skewed to ages as old as ~340 Ma. Proceeding a few kilometers to the northwest, sample KV-5-14 yields one of the most complex age distributions observed, without a clear mode, and ages ranging from ca. 320 Ma to 400 Ma. Although it was collected close to sample KV-5-14, sample KV-6-14 yields relative narrow age range from ca. 320 Ma to 345 Ma and lacks a prominent mode.

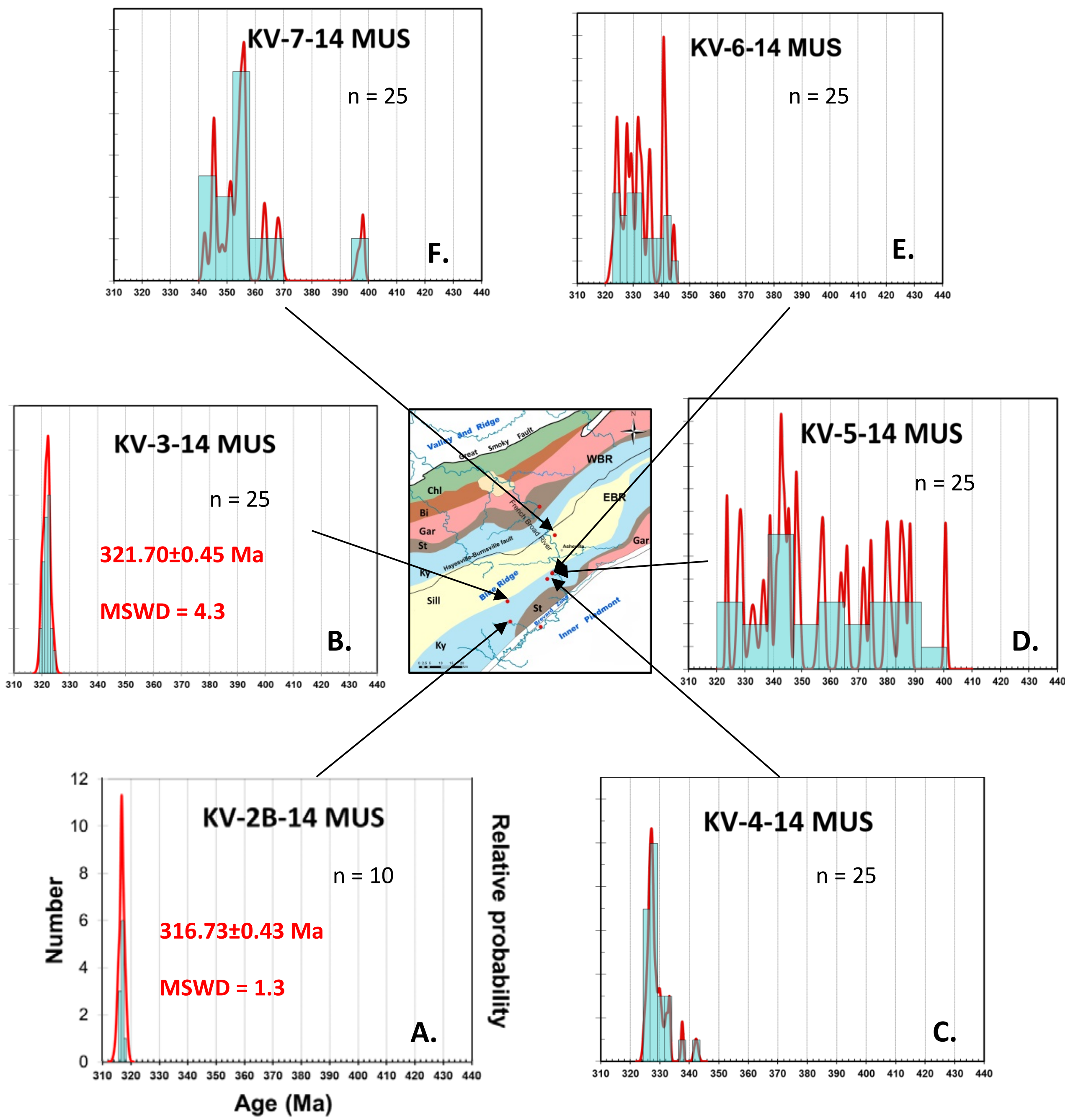

Figure 14. Age distribution of muscovite crystals from the basement rock samples. The horizontal and vertical axes for all the samples are in the same scale. Samples closed to the Brevard zone and Inner Piedmont are simple (A and B). The age distribution pattern is more complex to the north (C-F). Sample locations are marked in the small inset map with red dots.

Sample KV-7-14 was collected near the WBR-EBR boundary (Hayesville – Burnsville fault; Fig. 8). This sample yields ages clustered at ca. 355 Ma, but also yields a number of isolated ages as old as ca. 400 Ma. This northwesternmost sample is the only one in the present study that does not record any muscovite with ages younger than 340 Ma.

5.2.2 K-feldspar in the basement rock samples

Sample KV-1-14, from the Henderson Gneiss, was collected close to the eastern boundary of the Brevard fault zone. A total of ten crystals were analyzed for sample KV-1-14 (Fig. 15). The Henderson Gneiss consists of biotite- or microcline-augen gneiss, and the K-feldspar crystals from this sample represent porphyroclasts in the rock (see Fig. 9). In the age spectra for incremental heating experiments (Fig. 15), the ages of the five feldspar crystals begin at about 190 – 200 Ma and tend to rise through successive steps to ~290 – 370 Ma. The younger ages in each crystal can be interpreted to reflect cooling through minimum temperatures to permit argon diffusion in K-feldspar, or argon loss due to hydrothermal activity or the development of turbidity (Parsons et al., 1988; Villa, 2014). (Initial steps with very low $^{39}Ar_K$ and anomalously old ages with high uncertainty are interpreted to reflect decrepitation of fluid inclusions with unsupported ^{40}Ar, and are omitted from Figure 15; see full data in Appendix C.) The age spectra of two crystals show ages that decrease with the final (fusion) steps. This may be because the crystals are not evenly heated by the laser (with the bottom portion staying at lower temperature until fusion). Five K-feldspar crystals were also dated by SCTF, and yield total gas ages ranging from 273 Ma to 343 Ma (Fig. 15, histogram). The histogram represents recalculated ‘total gas’ ages for the 10 crystals analyzed, that vary between 270 Ma to 350 Ma.

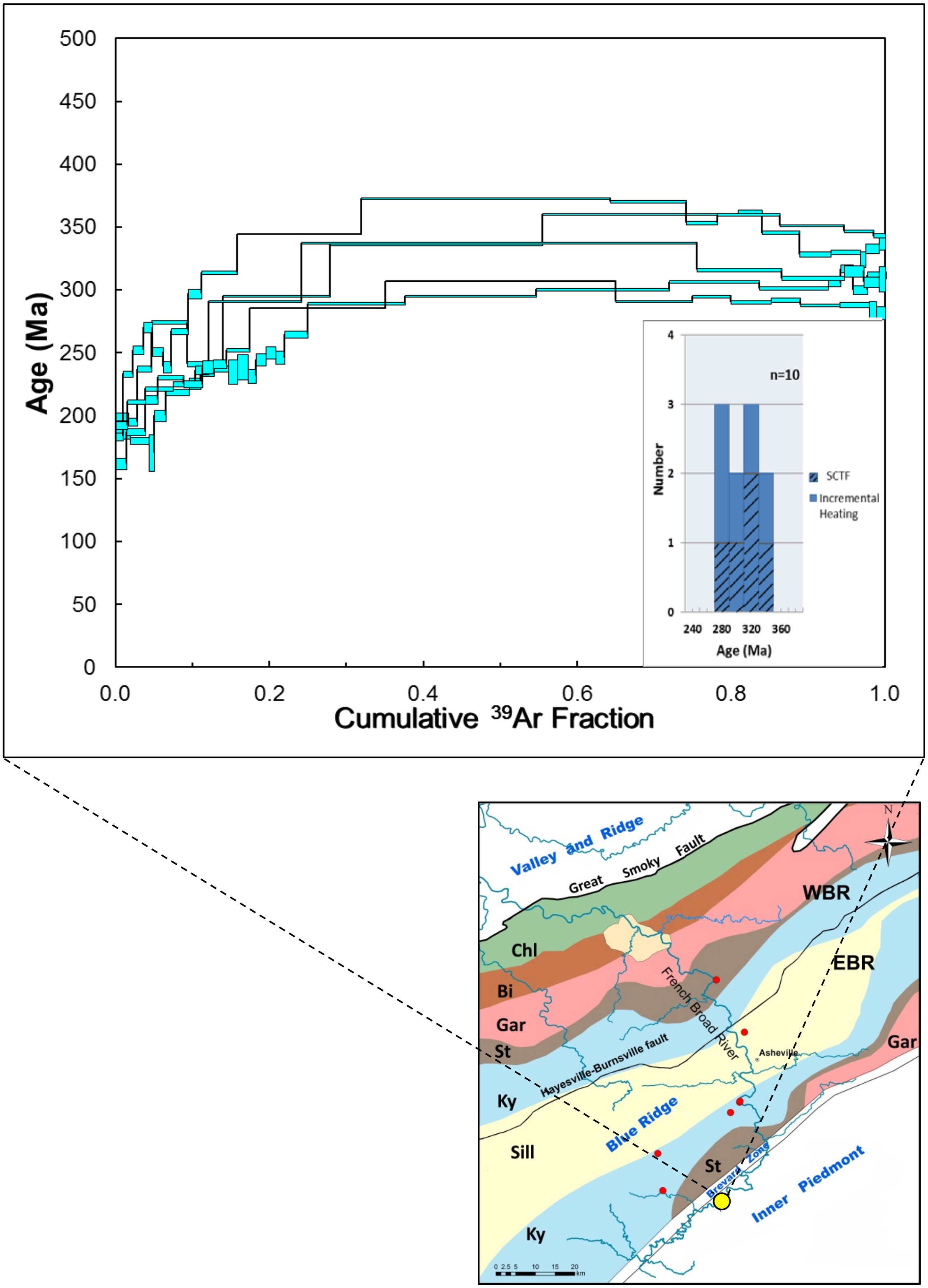

Figure 15. Age spectra of five K-feldspar crystals from sample KV-1-14 (Henderson gneiss) determined by $^{40}Ar/^{39}Ar$ incremental heating, with a histogram to represent the total-gas ages of those five and an additional five single-crystal fusion ages (10 total).

Sample KV-3-14 is biotite gneiss from the Ashe Metamorphic Suite, eastern Blue Ridge, which has no direct stratigraphic contact with the Precambrian basement rocks (Hatcher, 2005). A total of eight feldspar crystals were analyzed for this sample. Figure 16 shows the step heating results for four K-feldspar crystals. Dates are younger in the low-temperature heating steps, about 240 – 260 Ma, and then increase to maxima of 330 – 370 Ma. The youngest crystal has little discordance in the spectra, and its maximum age is close to the minimum ages of the other crystals. Four crystals were dated by SCTF measurements and yield age between 336 Ma to 357 Ma (Fig. 16).

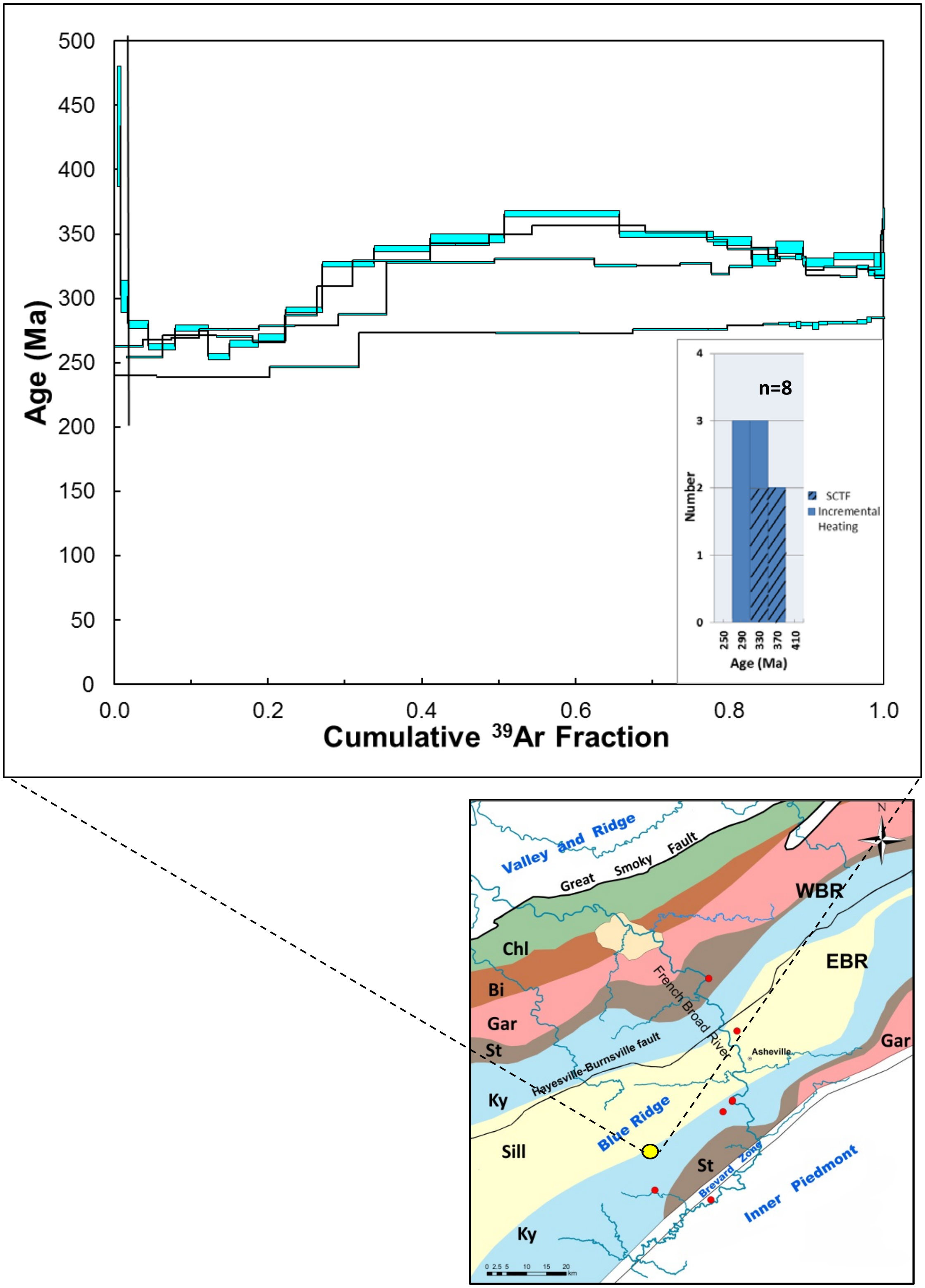

Figure 16. Age spectra of four K-feldspar crystals from sample KV-3-14 (Great Smoky Group) determined by $^{40}Ar/^{39}Ar$ incremental heating, with a histogram to represent the total-gas ages of those four and an additional four single-crystal fusion ages (8 total).

Sample KV-8-14 is biotite gneiss collected from the Precambrian Grenville basement, in rocks that Dallmeyer and Connelly (1993) correlated with the regional distribution of staurolite-grade metamorphic assemblages. During analysis of the single feldspar crystals from this sample, it became apparent that the amount of extraneous argon and overall discordance varied greatly from crystal to crystal. Thus, a larger number of crystals were selected for analysis in order to characterize the population. Nineteen crystals were analyzed through SCIH for sample KV-8-14, using five steps per analysis. The second and third incremental heating steps for all samples vary from ca. 270 Ma to ca. 400 Ma, with ages for subsequent steps that mostly vary within 800-1100 Ma. The minimum ages of each crystal are consistent with a record of cooling through final retention of $^{40}Ar^*$ in feldspar of this sample by ca. 270 Ma, among crystals that also contain varying amounts of unsupported 'excess' $^{40}Ar^*$. The older ages for the higher temperature steps and fusion increments are intriguing because they could be interpreted to result from retention of $^{40}Ar^*$ in feldspars that formed during the 1100 Ma Grenville event, but they also undoubtedly are affected by excess ^{40}Ar (note that a few feldspars with 5-10% of ^{39}Ar release in the fusion steps yield ages older than 1200 Ma). The most conservative interpretation of such 'saddle-shaped' release spectra is that the minimum ages (ca. 270 Ma in this case) provide a maximum estimate for the timing of final $^{40}Ar^*$ closure and retention in the sample.

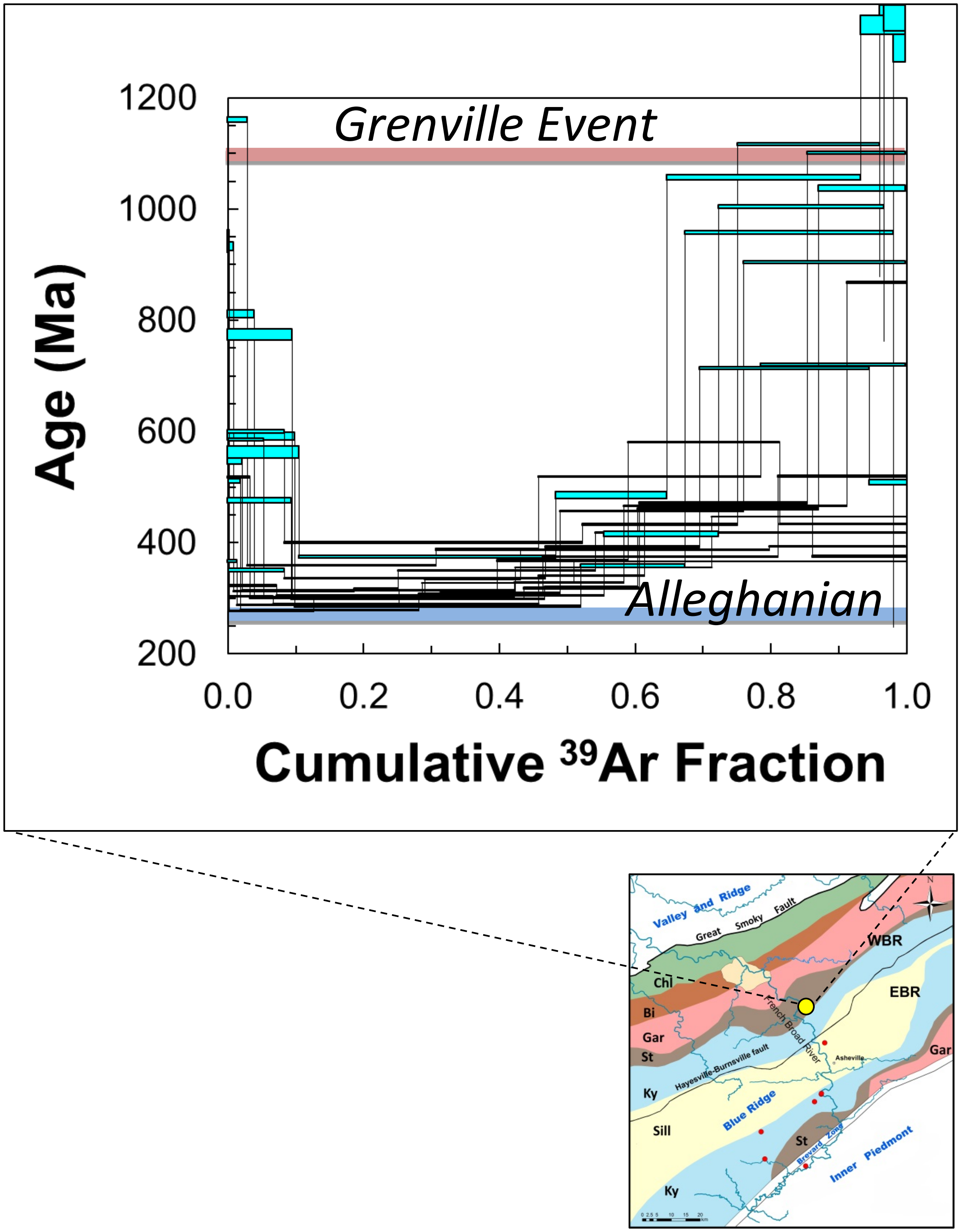

Figure 17. Incremental heating $^{40}Ar/^{39}Ar$ spectra (n=19) for single crystals of potassium feldspar from sample KV-8-14. Crystals were selected from the 420-840 µm sieve size range (20-40 mesh). The approximate timing of the Alleghanian (~320 Ma) and Grenville (~1100 Ma) events are indicated. Further discussion is provided in the text.

5.3 Detrital Sediments

Coarse sand samples were collected from the point bars in the catchments of the main ‘trunk’ stream and major tributaries of the French Broad River. We did not find very fresh detrital feldspar in the stream sediments, so in this section, only the muscovite sample ages are reported.

5.3.1 Muscovite in the detrital samples

The detrital muscovite samples from the main stream of the French Broad River are from the same sediment samples used in the study of Hietpas et al. (2010). These results were first presented by Dr. Willis Hames on the GSA conference talk in 2012. Three representative samples from the trunk stream of the French Broad River are selected to be reported here.

For each sample, more than one hundred crystals were analyzed to get reliable age distributions. The age distribution diagrams of sample FBR-2, FBR-5, and FBR-10 are shown in Figure 18. Sample FBR-2 was collected upstream near the source of the French Broad River. The age distribution has a single mode with an age of 315.06±0.50 Ma (MSWD = 13). The result indicates that all muscovite in the catchment for FBR-2 are around 315 Ma. In the same sample, detrital zircon and monazite record older events. A range of zircon ages from Grenvillian age to ca. 350 Ma is reported in Hietpas et al. (2010). For monazite, in addition to a record of Taconian age signature (~420 – 470 Ma), two monazite crystals yield Alleghanian ages at ~310 – 320 Ma (Hietpas et al., 2010; Fig. 18).

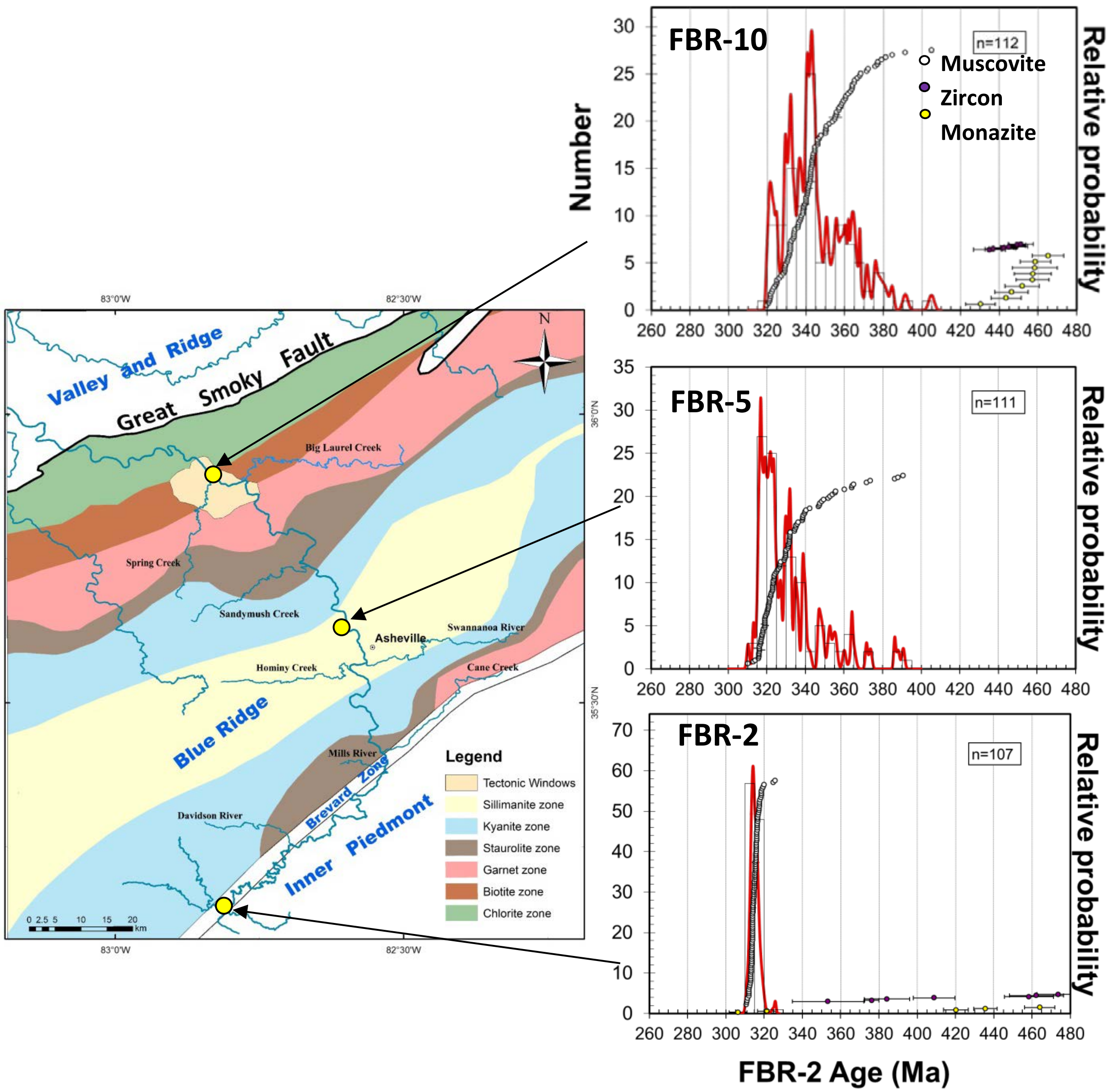

Figure 18. Age distribution of detrital minerals from the main stream of the French Broad River (Hietpas et al., 2010; Hames et al., 2012).

As the basement samples, the detrital muscovite samples also show increasing age complexity to the northwest. FBR-5 and FBR-10 have much more complex age distributions of muscovite than found in FBR-2. Sample FBR-5 yields ages in a range from 310 to 390 Ma with a prominent mode at ca. 320 Ma. Generally, the frequency of ages gradually decreases with increasing age. Sample FBR-10 yields a prominent mode at ca. 340 Ma, but many are also in the age range ~320 – 330 Ma. The frequency dramatically drops down at ages prior to 340 Ma and as old as ca. 400 Ma. The detrital monazite and zircon in this sample have ages more closely reflecting ~440 – 460 Ma crystallization in a Taconian event. Sample FBR-2 has detrital zircon ages as young as ~350 Ma, and detrital monazite ages as young as ~310 Ma, however, no post-Ordovician ages are recorded by zircon and monazite in sample FBR-10.

6 DISCUSSION

Muscovite in the basement samples

The age data from the muscovite samples indicate that muscovite crystals in one hand sample can preserve the record of a single event, and also can preserve record of multiple geologic events throughout the tectonothermal history. Basement samples near the Brevard zone, KV-2B-14 and KV-3-14, show simple muscovite age distributions compared with the muscovite samples to the north. These simple results indicate a small age variation within these single samples. The age variation from the crystals of these two samples is interpreted to result from the variation on closure temperature of muscovite (ca. 350 ºC – 400 ºC), but following a single metamorphic and deformational event. In KV-2B-14, minerals show obvious deformation textures (Fig. 10A). The early Pennsylvanian muscovite age (316.73±0.43 Ma) is interpreted to record cooling through muscovite closure temperatures following deformation. Sample KV-3-14, which is to the north of KV-2B-14, yields an older early Pennsylvanian age (321.70±0.45 Ma). The age of KV-3-14 is also interpreted to reflect cooling following a tectonothermal event, though it more closely approximates the timing of the event than sample KV-2B-14. The muscovite samples in Dallmeyer’s work (1988) collected from the eastern Blue Ridge in Georgia are similar and also support the interpretation. The age data of these eastern Blue Ridge samples are consistent with the muscovite chrontours shown in Figure 1 and are collectively interpreted to record progressive cooling following Alleghanian thrusting and peak metamorphism.

For the muscovite samples of rocks collected to the northwest with complex results, the ages ranging from 320 Ma to 400 Ma cannot be correlated to one single event. This complexity is interpreted to result from the polymetamorphism and superimposed pre-Alleghanian deformation events in rocks of the region northwest of the Brevard fault zone.

Sample KV-4-14 (Fig. 14C), with ages that range from ca. 324 – 342 Ma, shows a prominent mode at ca. 327 Ma. This muscovite sample is interpreted to have age components reflecting earlier events, and to be strongly overprinted by the Alleghanian event. The 25 analyses for sample KV-5-14 yield an age range of ca. 80 m.y. and have the highest age complexity compared with other muscovite samples. The ages are almost uniformly distributed between 320 – 400 Ma, with the highest frequency (n=6) at ca. 340 Ma. The result is consistent with the petrographic analysis that this sample is characterized by multiple-generations of muscovite (see Fig. 11C, D). Sample KV-6-14 yields age from ca. 325 to 345 Ma. This sample was collected within two kilometers of sample KV-5-14. No prominent mode is recorded in these two samples. (The ‘peak’ in probability shown in red line but with low frequency in the histogram, see Figure 14 D, E, is controlled by only a few analyses.) The lack of ages older than ~345 Ma in sample KV-6-14 is an indication that it experienced more thorough recrystallization and generation of new muscovite in the Alleghanian event. KV-7-14 is the northernmost sample collected from the eastern Blue Ridge and it yielded two muscovite crystals with ages of ~400 Ma. Moreover, in contrast to the other five basement samples of muscovite with ages as young as ca. 320 Ma, this sample does not yield any muscovite age younger than ca. 340 Ma. The results for sample KV-7-14 are consistent with early Alleghanian overprint of pre-existing metamorphic assemblages in the Mississippian (Visean, ca. 335 Ma). For the muscovite samples dated in the basement rocks, only sample KV-5-14 yields ages in Middle Devonian (370 – 390 Ma). This age distribution pattern is also reflected in the detrital samples.

Muscovite in the detrital sediments

The pattern of detrital muscovite age complexity in the French Broad River (Fig. 18) corresponds to that observed for the age distributions within basement samples. The sample from the upstream headwaters of the French Broad River shows a single mode, while the two samples collected downstream have a wide age range. Sample FBR-2 was collected from the headstream of the French Broad River. This sample shows a very simple pattern with a single mode with average ages of 315.06±0.50 Ma. The age is slightly younger and comparable to the muscovite ages of the two nearby basement samples (KV-2B-14 and KV-3-14). The complexity of detrital muscovite ages in the northwestern trunk stream samples (FBR-5 and FBR-10) seems due to increased input from polymetamorphic rocks of the Blue Ridge. The prominent modes of these three samples show a younging trend to the upstream (southeast) from middle Mississippian to early Pennsylvanian. This age distribution pattern is consistent with the result of the basement samples. The principal mode of FBR-10 is ~340 – 345 Ma, and this detrital sample was collected downstream of basement sample KV-7-14 that lacks muscovite younger than ~340 Ma. The principal mode of FBR-5 is ~315 – 325 Ma, and the basement samples (KV-2B-14, KV-3-14 and KV-4-14) in the upstream area of this detrital sample all show prominent modes within this age range. These results are interpreted to indicate that the detrital age signature most closely reflects the local sediment sources. The samples from the eastern Blue Ridge have abundant muscovite, while muscovite is generally sparse in the samples collected from the western Blue Ridge.

Detrital samples comprising more than 100 analyses have an approximate 95% probability of detecting any age component that constitutes at least 5% of the total population (Vermeesch, 2004). Considering the youngest detrital ages recorded, approximately 98% of the muscovite in sample FBR-2 is younger than 320 Ma. In contrast, 80% of the muscovite in sample FBR-5, and 99% of the detrital muscovite in sample FBR-10, is older than 320 Ma. This result indicates the age mode of prominent populations is modified by the influences of local sources along the course of the river, and that the most abundant muscovite in the headwaters of the river source may become a minor component downstream.

For comparison, the age data of the detrital zircon and detrital monazite are also plotted in the age distribution graph (Fig. 18). Hietpas et al. (2010) found that detrital monazite has an enhanced ability to record younger events in FBR sediment relative to detrital zircon. The sample with the most intense Alleghanian effects (FBR-2) has two monazite ages of ~310 – 320 Ma (Fig. 18), and a range of zircon ages from Grenvillian age to ca. 360 Ma (Hietpas et al., 2010). In contrast, their detrital sample FBR-10 does not show any Alleghanian age signature in zircon or monazite, but has crystallization ages at ~440 – 460 Ma. The results of the detrital zircon and monazite are consistent with the muscovite results of this study in that they can be interpreted to indicate a strong, local lithologic control on detrital mineral age.

K-feldspar in the basement samples

Potassium feldspar crystals from all three basement rocks sampled are characterized by discordant age spectra (Fig. 15, 16, and 17). The age spectra of KV-1-14 and KV-3-14 increase monotonically with progressive ^{39}Ar release over the majority of the heating steps. Based on volume diffusion theory, ^{40}Ar tends to concentrate more in the more retentive sites or in central portions of diffusion domains (e.g., McDougall and Harrison, 1999). A sample can lose ^{40}Ar from the less retentive sites during slow cooling or superimposed reheating event (McDougall and Harrison, 1999). In the age spectra of KV-1-14, the initial ages at ca. 200 Ma mark the final feldspar closure, consistent with cooling long after the Alleghanian event. Such cooling may have been accelerated by extension accompanying the breakup of Pangea and regional magmatism of the ca. 200 Ma Circum-Atlantic Magmatic Province (e.g., Hames et al., 2000). In the age spectra of KV-3-14, the initial ages at ca. 250 Ma indicate protracted slow cooling following Alleghanian orogeny. These minimum ages become progressively older for samples to the northwest, with ages beginning at ca. 250 Ma for KV-3-14 and minimum ages of ca. 280 Ma for sample KV-8-14. This pattern is interpreted to reflect cooling and final argon retention in feldspar occurring earlier in rocks to the northwest with a lower grade Alleghanian overprint.

Sample KV-1-14 and sample KV-3-14 yield maximum K-feldspar age of ca. 370 Ma. Considering the low closure temperature of K-feldspar, the ages are interpreted to record cooling following pre-Alleghanian events. Sample KV-8-14 shows very complex age distribution pattern with maximum ages up to ca. 1100 Ma. This result for feldspar is consistent with the age complexity of muscovite in the basement samples. The result of this sample indicates an ability of K-feldspar to retain record of earlier histories through multiple reheating events. This is due to the structural stability of the K-feldspar under high temperature (Foland, 1974). The age data cover the history from the Alleghanian event back to the Grenville event. Fullagar and Bartholomew (1983) reported the age of the basement rocks is ca. 1200 Ma to ca. 1150 Ma.

^{40}Ar/ ^{39}Ar Age distribution pattern

The muscovite ‘chrontours’ (Fig. 1) of the Blue Ridge and Inner Piedmont were constructed based on the ^{40}Ar/^{39}Ar ages of previous geochronology studies along with considerations of metamorphic facies distributions. The muscovite samples with simple age results in the present study confirm the placement of chrontours of 310 Ma and 320 Ma in the study region (Fig. 19). The age complexity of the other samples to the northwest makes it difficult to correlate any ages older than 320 Ma with the simple ‘chrontours’. Goldberg and Dallmeyer (1997) reported muscovite ages in the Blue Ridge from the northern North Carolina that were determined using bulk-sample (multigrain) techniques to derive ‘plateau ages’. Incremental heating and bulk sample preparation can homogenize samples, leading to geologically meaningless results, and it is difficult to

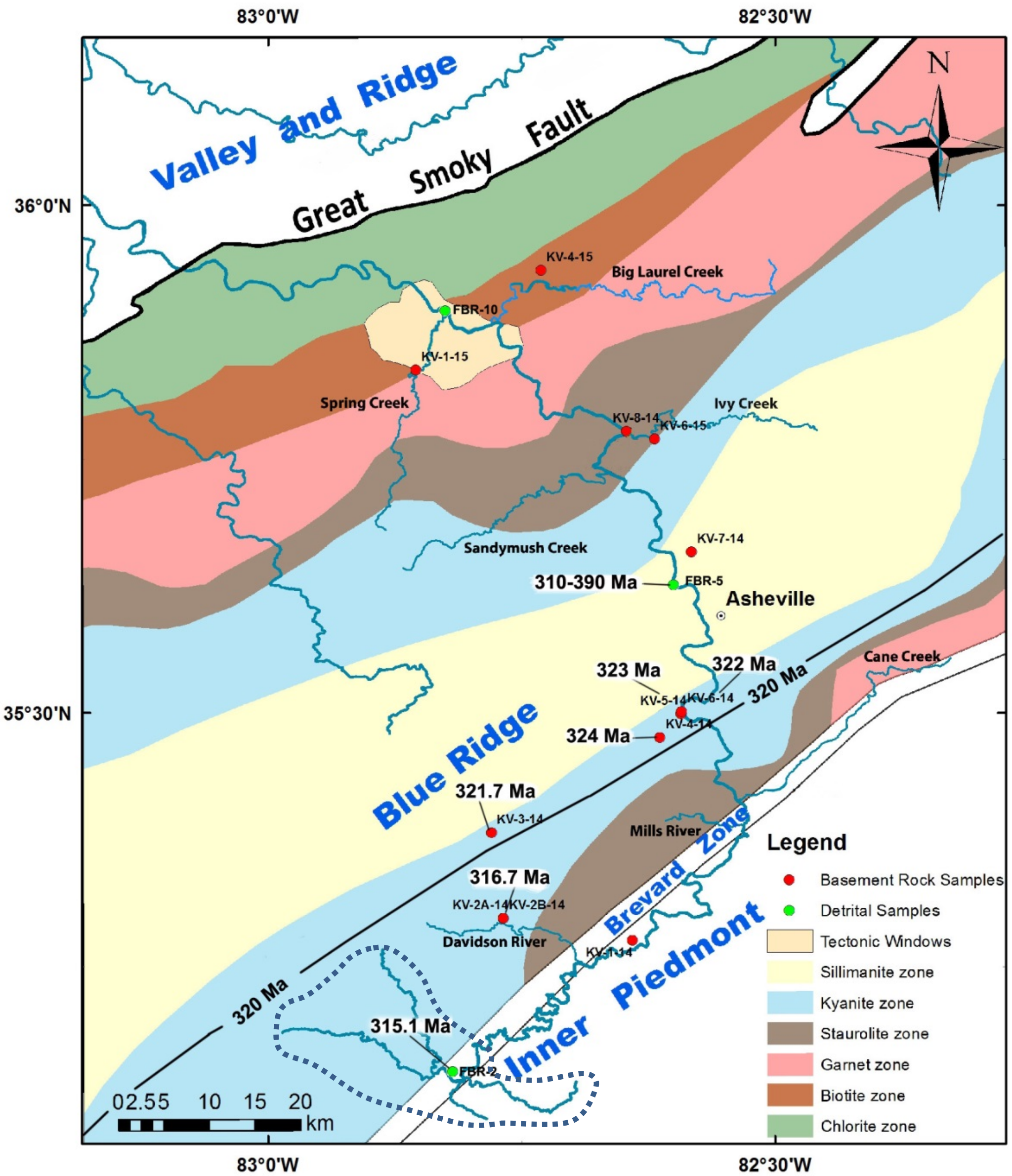

Figure 19. Map of study area showing the muscovite age distribution near the 320 Ma age ‘chrontour’. The ages of sample KV-4-14, KV-5-14, and KV-6-14 shown on the map are the youngest ages. The area surrounded by the dotted polygon represents the catchment of the headwaters.

evaluate the complexity that may exist in the samples studied by Goldberg and Dallmeyer (1997). But if we only consider the youngest single crystal ages of each sample, the age distribution of the muscovite samples in this present project can be interpreted to extend the 'chrontours' to the northwest to ca. 340 Ma. By using minimum single crystal muscovite ages, or the minimum closure ages of feldspars, one might, therefore, be able to extend the record of events in the western Blue Ridge.

The age results from both muscovite and K-feldspar are interpreted to record widespread Alleghanian metamorphic and deformational overprinting in the eastern Blue Ridge. Alleghanian effects appear to be significant but have less intensity in rocks throughout the western Blue Ridge. The northernmost muscovite sample KV-7-14 at medium-high grade yields ages older than ~340 Ma, so it is not likely the result of a single Alleghanian event, and instead is interpreted to record earlier polymetamorphism. The oldest muscovite ages observed in this study, from basement or detrital samples, are ~400 Ma. This could reflect slow cooling following Ordovician Taconian metamorphism, but it seems more likely that most of the pre-Carboniferous muscovite in the FBR catchment grew or recrystallized during a Devonian Acadian event.

Source of muscovite in the detrital sediments

The western Blue Ridge (WBR) and the eastern Blue Ridge (EBR) are two different lithostratigraphic terranes separated by the Haysville fault (Dallmeyer, 1988). To the northwest of the fault, WBR consists of basement complex covered by metasedimentary sequences; to the southeast of the fault, EBR is characterized by distinct thrust sheets (Williams and Hatcher, 1982). In the FBR region, the WBR is predominantly mafic and calc-alkaline migmatite gneiss and various biotite-, hornblende-, or garnet-bearing gneisses (Connelly and Dallmeyer, 1993). The EBR largely consists of feldspathic metasandstone with interbeds of feldspathic quartz-mica schist or gray phyllite and Grenville basement (Dallmeyer, 1975a; Miller et al., 2000). The felsic intrusions are mainly peraluminous, and intermediate and mafic intrusions are not common (Miller et al., 2006). In the present study, muscovite is abundant in the basement samples collected from the EBR; however, the samples in the WBR generally lack muscovite. This may result from the peralkaline character of intrusions in the WBR of the FBR region. Considering the availability of muscovite in the sources, one would expect the basement samples from the EBR to be dominant as the source of the muscovite downstream. However, muscovite ages younger than 320 Ma only predominate the upstream source of the FBR (detrital sample FBR-2), yet all of the muscovite collected in samples FBR-5 and FBR-10 downstream is dominated by ages older than 320 Ma. This observation is most consistent with a strong, local control on detrital sediment composition. Even though there is less muscovite in the low-grade, calc-alkaline basement of the WBR, the muscovite that is contributed locally (and perhaps from small, local tributaries) is proportionally much greater than derived from the EBR.

Detrital mineral age bias

All the detrital geochronometers have their own shortcomings. Hietpas et al. (2010) compared the crystallization ages recorded in detrital zircon to that in the detrital monazite from the FBR stream sediments. Alleghanian ages are only present in the ages of the detrital monazite, and detrital zircon records older crystallization ages. They interpreted that the abundance of older ages in detrital zircon results from the super-refractory nature of early-formed zircon and proposed that detrital monazite is a more effective proxy to record moderate to low grade metamorphic events. The muscovite data for detrital sample FBR-10, the farthest downstream and the closest to the Great Smoky fault, yields Devonian to Mississippian ages (ca. 400 – 320 ma), but the detrital zircon and detrital monazite from this sample (Hietpas et al., 2010) only record the Ordovician Taconian and the Mesoproterozoic Grenville events (Fig. 20). Post-Ordovician monazite or zircon ages are only present in detrital monazite from the upstream samples. The distributions for the U-Pb monazite and zircon ages and the $^{40}Ar/^{39}Ar$ muscovite ages all indicate strong, local control by the source, but they tend to record different events. As shown in Figure 20, muscovite $^{40}Ar/^{39}Ar$ ages tend to record younger ages corresponding to cooling or recrystallization events in the middle crust (Hames et al., 2012), whereas monazite and zircon reflect mobility of phosphorous and zirconium, respectively, during fluid flow or higher temperature events (Hietpas et al., 2010).

Although the age distribution of muscovite from the samples becomes more complex toward the lower grade metamorphic rocks, the data show no pre-Paleozoic signature either in the basement samples or detrital samples. However, the age data of the K-feldspar from sample KV-8-14 records a history that includes the Grenville event. The data of the present study, therefore, document that K-feldspar incremental ages have the potential to discriminate the Grenville and superimposed Paleozoic events in the western Blue Ridge. K-feldspar also has great potential as a detrital chronometer, though that was

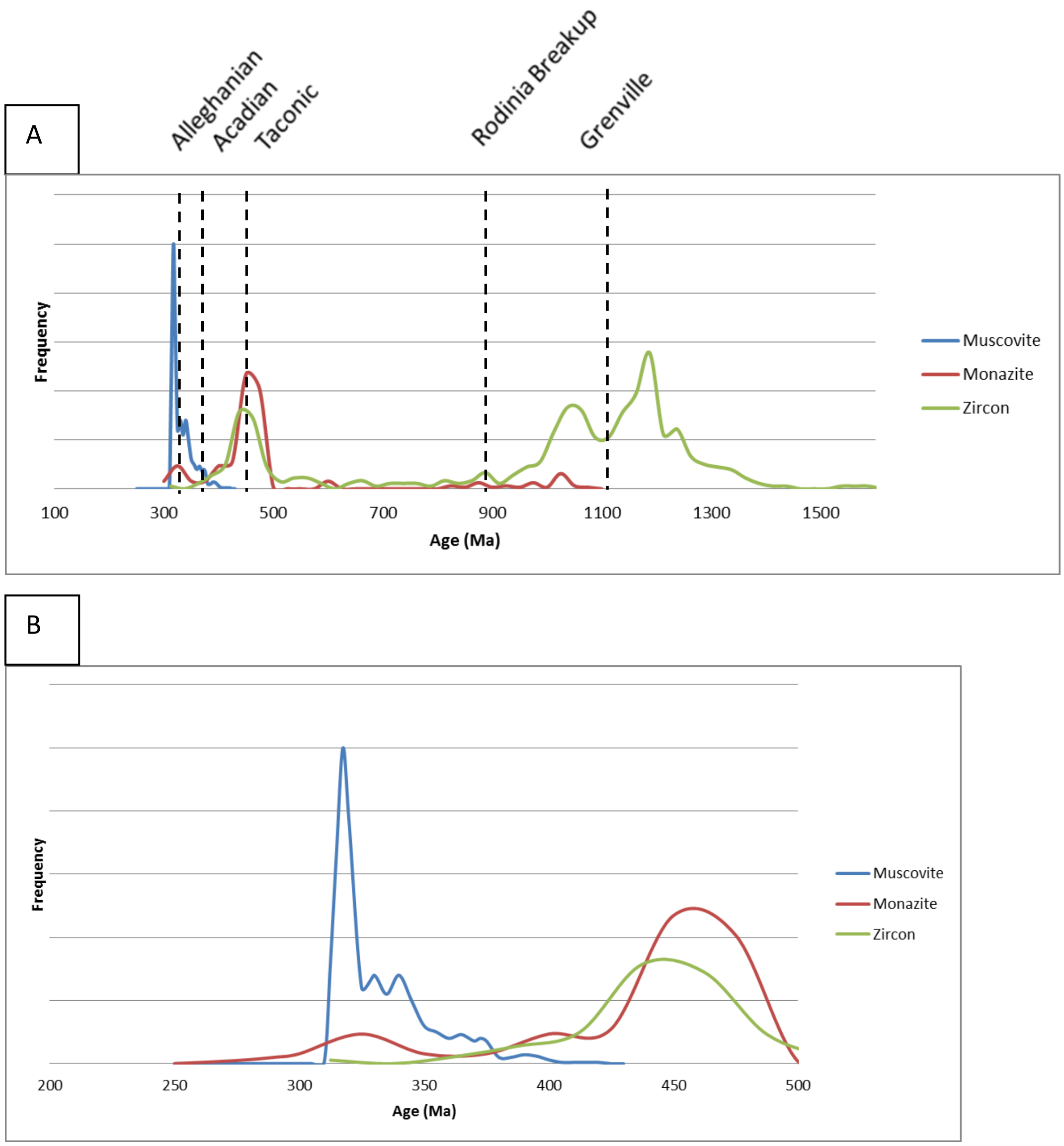

Figure 20. Age distribution of detrital minerals (with data from Hietpas, 2010 and Hames et al., 2012). (A) Zircon records the Precambrian events, while muscovite and monazite record the younger events in the Paleozoic. (B) Age signal of the three minerals in Paleozoic. The total number of muscovite analyses from eight samples is 876.

not determinant during the current study because detrital K-feldspar was too weathered for analysis. Future work could focus on the preservation of detrital K-feldspar during weathering and erosion in the French Broad River catchment, with age determinations to evaluate its use as a detrital geochronometer.

7 CONCLUSIONS

The $^{40}Ar/^{39}Ar$ ages for muscovite and K-feldspar in this study are simpler in the Inner Piedmont and the eastern Blue Ridge and become more complex in the western Blue Ridge to the northwest. The increasing $^{40}Ar/^{39}Ar$ age complexity of the basement rocks samples to the northwest is interpreted to results from the multiple reheating events, reflecting polymetamorphism. The 'muscovite chrontours' based on the previous geochronology data are consistent with the eastern Blue Ridge samples but are difficult to extrapolate to the region with the metamorphic rocks disturbed by the reheating events. However, the youngest ages recorded in these samples are consistent with previous $^{40}Ar/^{39}Ar$ studies and allow correlations to the 'muscovite chrontours'.

The results from the basement samples in the catchment documents the complexity of the detrital samples' signal is not only due to the increasing sediment input of local tributaries from heterogeneous sources (as discussed by Brewer et al., 2006, for streams in the Nepalese Himalaya), but also to the complexity of polymetamorphism in the Barrovian metamorphic rocks west of the Brevard fault zone. The basement samples collected from the western Blue Ridge generally lack muscovite. For the detrital samples in the western Blue Ridge, the source of muscovite could be dominated by the rocks upstream in the eastern Blue Ridge that contain abundant muscovite. Instead, the detrital samples tend to reflect the ages of the rock samples near the sampling sites more strongly.

The age results of the detrital samples examined in this study emphasize that the detrital age distribution is not simply the sum of all the rock samples in the catchment area.

Based on observations for basement samples in this study, K-feldspar, as a low-temperature geochronometer, tends to record more (especially older) events through a long history as compared to muscovite, especially in the metamorphic rocks at low grade. This is not only restricted to a single crystal which is reflected from the age spectra, but also for a single sample when the age range of single crystals is considered. Substantial differences exist in the distribution of single-crystal K-feldspar ages among rocks that provide detritus to the French Broad River. Thus, future studies could explore the use of K-feldspar as a detrital chronometer in this river catchment system. Further study could also focus on the basement samples in the western Blue Ridge to decipher Alleghanian, Acadian and Taconian overprinting effects in this region.

REFERENCES

Arnaud, N.O. and Kelley, S.P., 1995, Evidence for excess argon during high pressure metamorphism in the Dora Maira Massif (western Alps, Italy), using an ultra-violet laser ablation microprobe ^{40}Ar-^{39}Ar technique: Contributions to Mineralogy and Petrology, v. 121, no. 1, p. 1-11.

Boundy, T.M., Hall, C.M., Li, G., Essene, E.J. and Halliday, A.N., 1997, Fine-scale isotopic heterogeneities and fluids in the deep crust: a $^{40}Ar/^{39}Ar$ laser ablation and TEM study of muscovites from a granulite-eclogite transition zone: Earth and Planetary Science Letters, v. 148, no. 1, p. 223-242.

Brewer I.D., Burbank D.W., and Hodges K.V., 2006, Downstream development of a detrital cooling-age signal: Insights from $^{40}Ar/^{39}Ar$ muscovite thermochronology in the Nepalese Himalaya: Geological Society of America Special Papers, v. 398, p. 321-338.

Carpenter R.H., 1970, Metamorphic history of the Blue Ridge province of Tennessee and North Carolina: Geological Society of America Bulletin, v. 81, no. 3, p. 749-762.

*Connelly J.B. and Dallmeyer R.D., 1993, Polymetamorphic evolution of the western Blue Ridge: evidence from $^{40}Ar/^{39}Ar$ whole-rock slate/phyllite and muscovite ages: American Journal of Science, v. 293, p. 322-322.

Copeland P. and Harrison T.M., 1990, Episodic rapid uplift in the Himalaya revealed by $^{40}Ar/^{39}Ar$ analysis of detrital K-feldspar and muscovite, Bengal fan: Geology, v. 18, no. 4, p. 354-357.

Publications used as sources of age data for compilation of Figure 1, that were not otherwise cited in the text, are marked with an asterisk mark '*'.

Corrie S.L. and Kohn M.J., 2007, Resolving the timing of orogenesis in the Western Blue Ridge, southern Appalachians, via in situ ID-TIMS monazite geochronology: Geology, v. 35, no. 7, p. 627-630.

Dallmeyer R.D., 1975a, $^{40}Ar/^{39}Ar$ ages of biotite and hornblende from a progressively remetamorphosed basement terrane: their bearing on interpretation of release spectra: Geochimica et Cosmochimica Acta, v. 39, no. 12, p. 1655-1669.

Dallmeyer, R. D., 1975b, Incremental $^{40}Ar/^{39}Ar$ ages of biotite and hornblende from retrograded basement gneisses of the southern Blue Ridge; their bearing on the age of Paleozoic metamorphism: American Journal of Science, v. 275, no. 4, p. 444-460.

*Dallmeyer, R.D., 1978, $^{40}Ar/^{39}Ar$ incremental-release ages of hornblende and biotite across the Georgia Inner Piedmont; their bearing on late Paleozoic-early Mesozoic tectonothermal history: American Journal of Science, v. 278, p. 124-149.

*Dallmeyer, R. D., Wright, J. E., Secor, D. T., and Snoke, A. W., 1986, Character of the Alleghanian orogeny in the southern Appalachians: Part II. Geochronological constraints on the tectonothermal evolution of the eastern Piedmont in South Carolina: Geological Society of America Bulletin, v. 97, p. 1329-1344.

*Dallmeyer R.D., 1988, Late Paleozoic tectonothermal evolution of the western Piedmont and eastern Blue Ridge, Georgia: Controls on the chronology of terrane accretion and transport in the southern Appalachian orogen: Geological Society of America Bulletin, v. 100, p. 702-713.

Davis, T.L., 1993, Lithostratigraphy, structure, and metamorphism of a crystalline thrust terrane, western Inner Piedmont, North Carolina [PhD dissertation]: Knoxville, University of Tennessee, Knoxville, 245 p.

Fan, D., Hames, W.E., Steltenpohl, M.G., and Tull, J.F., 2015, Distributions of $^{40}Ar/^{39}Ar$ mineral ages and metamorphic isograds in regionally metamorphosed lithologies of the Western Blue Ridge and Talladega Slate Belt, Southern Appalachians: Geological Society of America Abstracts with Programs, v. 47, no. 2, p. 14.

Foland, K. A., 1974, Ar 40 diffusion in homogenous orthoclase and an interpretation of Ar diffusion in K-feldspars: Geochimica et Cosmochimica Acta,v. 38, no. 1, p. 151-166.

Fullagar, P.D. and Bartholomew, M.J., 1983, Rubidium¡/Strontium ages of the Watauga River, Cranberry, and Crossing Knob gneisses, northwestern North Carolina. Geological Investigations in the Blue Ridge of Northwestern North Carolina: Carolina Geological Society Field Trip Guidebook, Virginia Polytechnic Institute and State University, Blacksburg, VA, p.17.

Gastaldo, R. A., Guthrie, G. M., Steltenpohl, M. G., 1993, Mississippian fossils from southern Appalachian metamorphic rocks and their implications for late Paleozoic tectonic evolution: Science, v. 262, no. 5134, p. 732-734

*Goldberg S.A. and Dallmeyer R.D., 1997, Chronology of Paleozoic metamorphism and deformation in the Blue Ridge thrust complex, North Carolina and Tennessee: American Journal of Science, v. 297, p. 488-526.

Hames, W. E., and Bowring, S. A., 1994, An empirical evaluation of the argon diffusion geometry in muscovite: Earth and Planetary Science Letters, v. 124, no. 1, p. 161-169.

Hames, W.E., Renne, P.R. and Ruppel, C., 2000, New evidence for geologically instantaneous emplacement of earliest Jurassic Central Atlantic magmatic province basalts on the North American margin: Geology, v. 28, no. 9, p. 859-862.

Hames W.E., Moore M, Priester C, Samson S.D. and Hietpas J, 2012, Diversity is a beautiful thing: A test of combined $^{40}Ar/^{39}Ar$ muscovite, Th/Pb monazite and U/Pb zircon ages in modern stream sediment to characterize the Southwestern Blue Ridge: Geological Society of America Abstracts with Programs, v. 44, no. 7, p. 71.

Harper, S.B. and Fullagar, P.D., 1981, Rb-Sr ages of granitic gneisses of the Inner Piedmont belt of northwestern North Carolina and southwestern South Carolina: Geological Society of America Bulletin, v. 92, no. 11, p. 864-872.

Harris, A. G., Harris, L. D., and Epstein, J. B., 1978, Oil and gas data from Paleozoic rocks in the Appalachian Basin: maps for assessing hydrocarbon potential and thermal maturity (conodont color-alteration isograds and overburden isopachs) (No. DOE/ET/10136-T2): Geological Survey, Washington, DC (USA).

Hatcher Jr, R.D., 2005, Southern and central Appalachians: Encyclopedia of Geology, p. 72-81.

Hatcher Jr R.D. and Goldberg S. A., 1991, The Blue Ridge Province , in Horton, J.W., Jr., and Zullo, V.A., editors: The Geology of the Carolinas --- Carolina Geological Society 50th Anniversary Volume: Knoxville, University of Tennessee Press, p. 11-35.

*Hibbard, J. P., Miller, B. V., Hames, W. E., Standard, I. D., Allen, J. S., Lavallee, S. B., and Boland, I. B., 2012, Kinematics, U-Pb geochronology, and $^{40}Ar/^{39}Ar$ thermochronology of the Gold Hill shear zone, North Carolina: The Cherokee orogeny in Carolina, southern Appalachians: Geological Society of America Bulletin, v. 124, p. 643-656.

Hietpas J, Samson S, Moecher D and Schmitt AK, 2010, Recovering tectonic events from the sedimentary record: Detrital monazite plays in high fidelity: Geology, v. 38, no. 2, p. 167-170.

Hodges, K.V., 1991, Pressure-Temperature Paths. Annual Review of Earth and Planetary: Sciences, v. 19, p. 207.

*Layfield N. T., 2009, Permian to Cretaceous evolution of the Piedmont along the Alabama – Georgia Coastal Plain unconformity [M.S. Thesis]: Auburn, Auburn University, 145 p.

Lovera, O. M., Richter, F. M., and Harrison, T. M., 1989, The $^{40}Ar/^{39}Ar$ thermochronometry for slowly cooled samples having a distribution of diffusion domain sizes: Journal of Geophysical Research: Solid Earth (1978–2012), v. 94, no. B12, p. 17917-17935.

*Maher, H. D., Dallmeyer, R. D., Secor, D. T., and Sacks, P. E., 1994, $^{40}Ar/^{39}Ar$ constraints on chronology of Augusta fault zone movement and late Alleghanian extension, Southern Appalachian Piedmont, South Carolina and Georgia: American Journal of Science, v. 294, no. 4, p. 428-448.

*McClellan, E.A., Steltenpohl, M.G., Thomas, C., and Miller, C.F., 2007, Isotopic age constraints and metamorphic history of the Talladega belt: New evidence for timing of arc magmatism and terrane emplacement along the southern Laurentian margin: The Journal of Geology, v. 115, p. 541–561.

McDougall I. and Harrison M.T., 1999, Geochronology and thermochronology by the $^{40}Ar/^{39}Ar$ method: New York, Oxford University Press, 271 p.

*McDonald W. M., 2008. $^{40}Ar/^{39}Ar$ ages of muscovite from the western Blue Ridge and Talladega Belt, Georgia and North Carolina [M.S. Thesis]: Auburn, Auburn University, 114 p.

Merrihue, C. and Turner, G., 1966, Potassium - argon dating by activation with fast neutrons: Journal of Geophysical Research, v. 71, no. 11, p.2852-2857.

Miller, B.V., Fetter, A.H. and Stewart, K.G., 2006, Plutonism in three orogenic pulses, eastern Blue Ridge Province, southern Appalachians: Geological Society of America Bulletin, v. 118, p. 171-184.

Miller, C.F., Hatcher Jr., R.D., Ayers, J.C., Coath, C.D., Harrison, T.M., 2000, Age and zircon inheritance of eastern Blue Ridge plutons, southwestern North Carolina and northeastern Georgia, with implications for magma history and evolution of the southern Appalachian orogeny: American Journal of Science, v. 300, p. 142-172.

Najman Y.M.R, Pringle M.S., Johnson M.R.W, Robertson A.H.F and Wijbrans JR, 1997, Laser ^{40}Ar/^{39}Ar dating of single detrital muscovite grains from early foreland-basin sedimentary deposits in India: Implications for early Himalayan evolution: Geology, v. 25, no. 6, p. 535-538.

Odom, A. L., and Fullagar, P. D., 1973, Geochronologic and tectonic relationships between the Inner Piedmont, Brevard zone, and Blue Ridge belts, North Carolina: American Journal of Science, v. 273-A, p. 133-149.

Parsons, I., Rex, D.C., Guise, P. and Halliday, A.N., 1988, Argon-loss by alkali feldspars: Geochimica et Cosmochimica Acta, v. 52, no. 5, p.1097-1112.

Passchier, C.W. and Trouw, R.A., 1996, Microtectonics (Vol. 2). Berlin: Springer, 366 p.

Rejebian, V. A., Harris, A. G., and Huebner, J. S., 1987, Conodont color and textural alteration: An index to regional metamorphism, contact metamorphism, and hydrothermal alteration: Geological Society of America Bulletin, v. 99, no. 4, p. 471-479.

*Steltenpohl, M. G., and Kunk, M. J., 1993, ^{40}Ar/^{39}Ar thermochronology and Alleghanian development of the southernmost Appalachian Piedmont, Alabama and southwest Georgia: Geological Society of America Bulletin, v. 105, no. 6, p. 819-833.

Steltenpohl, M. G., Hatcher, R. D., Mueller, P. A., Heatherington, A. L., and Wooden, J. L., 2010, Geologic history of the Pine Mountain window, Alabama and Georgia: Insights from a new geologic map and U-Pb isotopic dates: Geological Society of America Memoirs, v. 206, p. 837-857.

Steltenpohl, M. G., Schwartz, J. J., and Miller, B. V., 2013, Late to post-Appalachian strain partitioning and extension in the Blue Ridge of Alabama and Georgia: Geosphere, v. 9, no. 3, p. 647-666.

Trupe, C.H., Stewart, K.G., Adams, M.G., Waters, C.L., Miller, B.V. and Hewitt, L.K., 2003, The Burnsville fault: Evidence for the timing and kinematics of southern

Appalachian Acadian dextral transform tectonics: Geological Society of America Bulletin, v. 115, no. 11, p. 1365-1376.

Tull, J. F., Harris, A. G., Repetski, J. E., McKinney, F. K., Garrett, C. B., and Bearce, D. N., 1988, New paleontologic evidence constraining the age and paleotectonic setting of the Talladega slate belt, southern Appalachians: Geological Society of America Bulletin, v. 100, p. 1291-1299.

Tull, J. F., and Holm, C. S., 2005, Structural evolution of a major Appalachian salient-recess junction: Consequences of oblique collisional convergence across a continental margin transform fault: Geological Society of America Bulletin, v. 117, p. 482-499.

Tull J.F., Baggazi H. and Groszos M.S., 2012, Evolution of the Murphy synclinorium, southern Appalachian Blue Ridge, USA: Journal of Structural Geology, v. 44, p. 151-166.

Unrug, R., and Unrug, S., 1990, Paleontological evidence of Paleozoic age for the Walden Creek Group, Ocoee Supergroup, Tennessee: Geology, v. 18, p. 1041-1045.

Vermeesch, P., 2004, How many grains are needed for a provenance study? : Earth and Planetary Science Letters, v. 224, no. 3, p. 441-451.

Villa, I., 2014, Diffusion of Ar in K-feldspar: Present and absent: Special Publication – Geological Society of London, v. 378, p. 107-116.

Williams, H. and Hatcher, R.D., 1982, Suspect terranes and accretionary history of the Appalachian orogeny: Geology, v. 10, no. 10, p. 530-536.

Zeitler, P.K., Herczeg, A.L., McDougall, I. and Honda, M., 1987, U-Th-He dating of apatite: A potential thermochronometer: Geochimica et Cosmochimica Acta, v. 51, no. 10, p. 2865-2868.

APPENDICES

Appendix A. Sample Information

Rock Sample

Name	Longitude	Latitude	Lithology	Unit Name and Terrane	Phases Picked and Irradiated
KV-1-14	W 82.64223	N 35.27439	Biotite augen gneiss with kfs porphyroblasts	Henderson Gneiss - Inner Piedmont	Biotite ~20 gr #18/40; K-spar ~50 gr #18/40
KV-2A-14	W 82.76948	N 35.29653	Granitic pegmatite with garnet	Ashe Metamorphic Suite- EBR	Muscovite ~50 gr #18/20; Biotite ~50 gr #18/40; K-spar ~50 gr #18/20
KV-2B-14	W 82.76948	N 35.29653	Muscovite-biotite-graphite schist	Ashe Metamorphic Suite - EBR	Muscovite ~50 gr #18/20; Biotite ~50 gr #20/40
KV-3-14	W 82.78100	N 35.38103	Biotite gneiss	Ashe Metamorphic Suite - EBR	Muscovite ~50 gr #18/40; Biotite ~50 gr #18/40; K-spar ~50 gr #18/20
KV-4-14	W 82.6147	N 35.47472	Biotite gneiss	Ashe Metamorphic Suite - EBR	Muscovite ~30 gr #18/40; Biotite ~50 gr #18/40
KV-5-14	W 82.59388	N 35.49802	Biotite gneiss with granite dikes	Ashe Metamorphic Suite - EBR	Muscovite ~50 gr #18/20; Biotite ~50 gr #18/20
KV-6-14	W 82.59321	N 35.50028	Garnet-muscovite-biotite schist	Ashe Metamorphic Suite - EBR	Muscovite ~50 gr #20/40; Biotite ~50 gr #20/40
KV-7-14	W 82.58306	N 35.65792	garnet-biotite-muscovite schist with quartz/feldsapr aggregates	Ashe Metamorphic Suite - EBR	Muscovite ~50 gr #18/20; Biotite ~50 gr #20/40
KV-8-14	W 82.64734	N 35.77713	Biotite gneiss in exposure with amphibolite	Grenville basement - WBR	Biotite ~60 gr #18/40; K-spar ~60 gr #20/40
KV-1-15	W 82.85475	N 35.83782	Mottled migmatitic granite from the Max Patch Granite	Max Patch Granite - WBR	K-spar ~50 gr #40/60
KV-4-15	W 82.73247	N 35.93606	Quarzite	Ocoee Supergroup - WBR	
KV-6-15	W 82.61926	N 35.76915	Biotite granitic gneiss	Grenville basement - WBR	K-spar ~50 gr #40/60

Stream Sample

Name	Longitude	Latitude	Location	Phases Picked and Irradiated
FBR-2	W 82.8265	N 35.14553	French Broad River (trunk)	Hietpas et al., 2010
FBR-5	W 82.5985	N 35.62443	French Broad River (trunk)	Hietpas et al., 2010
FBR-10	W 82.8226	N 35.89382	French Broad River (trunk)	Hietpas et al., 2010
KV-2-15	W 82.84356	N 35.8649	Spring Creek (tributary)	Muscovite 100 gr #20/60; Kspar 40 gr #40/60
KV-3-15	W 82.75193	N 35.92274	Big Laurel Creek (tributary)	Muscovite 30 gr #20/40, ~60 gr #40/60; Kspar 45 gr #20/60
KV-5-15	W 82.69545	N 35.7349	Sandymush Creek (tributary)	Muscovite 100 gr #20/40, 50 gr #40/60; Kspar ~35 gr #40/60
KV-7-15	W 82.64505	N 35.77571	Ivy Creek (tributary)	Muscovite ~90 gr #20/40, ~60 gr #40/60; Kspar 30 gr #40/60
KV-8-15	W 82.82417	N 35.8974	French Broad River (trunk)	Muscovite 50 gr #20/40, ~100 gr #40/60; Kspar 40 gr #40/60
KV-9-15	W 82.56719	N 35.39251	Mills River (tributary)	Muscovite 80 gr #20/40, ~70 gr #40/60; Kspar 25 gr #40/60
KV-10-15	W 82.49736	N 35.42385	Cane Creek (tributary)	Muscovite 50 gr #20/40, ~100 gr #40/60; Kspar 25 gr #40/60

Appendix B. Petrographic Descriptions

Sample KV-1-14: (Henderson gneiss; Inner Piedmont)

Mineral assemblage: microcline, quartz, biotite, plagioclase, sericite.

The sample is a biotite augen gneiss with pink K-feldspar porphyroblasts. Very clear gneissosity with biotite layers ~100 μm wide and feldspar-quartz layers ~200-500 μm wide. The texture of the sample in the thin section is inequigranular. Biotite defines the continuous foliation of the sample. Some K-feldspar crystals show kinking and fractures, indicating deformed twins and grain size reduction with dynamic recrystallization. Myrmekite forms where the plagioclase has been replaced by the K-feldspar due to metasomatism. Myrmekite is very common in this sample, and it is a texture interpreted to reflect deformation and hydrothermal effects. Quartz crystals are anhedral and show undulose extinction and grain-boundary bulging.

Sample KV-2A-14: (Ashe Metamorphic Suite; EBR)

Mineral assemblage: microcline, quartz, muscovite, biotite, plagioclase, garnet, epidote.

The sample is a deformed pegmatitic quartz diorite with garnet. Subeuhedral muscovite is medium-grained, and interspersed with quartz and plagioclase crystals. Plagioclase is abundant, and the crystal size is up to ~2 mm in diameter. Quartz shows undulose extinction and suture grain boundaries, with subgrains formed by the recrystallization of quartz. The metamorphic grade seems compatible with lower amphibolites facies.

Sample KV-2B-14: (Ashe Metamorphic Suite; EBR)

Mineral assemblage: biotite, plagioclase, orthocloase, quartz, muscovite, garnet, graphite, kyanite, staurolite

The sample is muscovite-biotite-graphite schist, collected from the same stop with KV-2A-14. It has lower amphibolites-facies assemblage. The foliation is along the preferred orientation of the platy minerals like mica. Muscovite and biotite define the single generation fabric. Plagioclase is present as stretched elongate lenses raging from 1mm to 3 mm. Biotite inclusions in the plagioclase porphyroclasts grow along the cleavage, and they follow the same direction with the external foliation.

Sample KV-3-14: (Ashe Metamorphic Suite; EBR)

Mineral assemblage: biotite, quartz, muscovite, K-feldspar, plagioclase

This sample is a biotite gneiss. Mica and quartz define the foliation. The quartz layers have width usually of one single crystal (~200 – 600 μm). The sample contains quartz, feldspar, and muscovite porphyroclasts. The fabrics are folded, and 'mica fish' are present. Porphyroclasts have mica tails. Recrystallization of quartz and feldspar (overgrowth) can be observed. Some single grains of quartz bulge into plagioclase, and some occur as inclusions in the feldspar. The mica inclusions in the plagioclase show different fabric orientation compared to the mica in the matrix. The rock sample has experienced medium-grade conditions (lower amphibolites facies).

Sample KV-4-14: (Ashe Metamorphic Suite; EBR)

Mineral assemblage: biotite, quartz, garnet, plagioclase (0.5-3mm), staurolite, sillimanite, K-feldspar, myrmekite

This sample is a biotite gneiss with feldspar porphyroblasts, containing an amphibolites-facies assemblage. Myrmekite (intergrowth of quartz set in plagioclase) is common in this sample. Mica envelopes microcline porphyroclasts, showing ‘Z’ folds. K-feldspar crystals have poikiloblastic texture with finer grained quartz and muscovite inclusions. Quartz has undulose extinction and polycrystalline quartz aggregates developed by subgrain rotation recrystallization.

Sample KV-5-14: (Ashe Metamorphic Suite; EBR)

Mineral assemblage: biotite, muscovite, quartz, feldspar, calcite

This sample is a muscovite-biotite gneiss. It is very rich in biotite (>70%), and it has different fabric orientation deformed by biotite. Biotite has grain size ~1 mm. Muscovite is not as abundant as biotite in the sample. Some fine-grained muscovite shows the preferred orientation and is interlayered with biotite. Some isolated large muscovite grains (~800 μm) cut across the fabrics, but they do not define any foliation. Calcite is present in clusters of crystals, and it is in contact with quartz aggregates. This may suggest hydrothermal effects on this sample.

Sample KV-6-14: (Ashe Metamorphic Suite; EBR)

Mineral assemblage: muscovite, biotite, garnet, quartz, plagioclase, rutile

This sample is a garnet-muscovite-biotite schist. The size of the garnet porphyroblasts is about 0.5 – 1 mm. Biotite inclusions in garnet show the direction of the first fabric generation which is different from the external foliation. Garnet is abundant. Muscovite that was recrystallized subsequent to the porphyroblast growth shows undulose extinction and the birefringence color is abnormal. Anhedral quartz has evidence for subgrain rotation recrystallization. Quartz also has undulose extinction. Feldspar porphyroblasts have many fractures.

Sample KV-7-14: (Ashe Metamorphic Suite; EBR)

Mineral assemblage: quartz, plagioclase, biotite, garnet, muscovite

The sample is a garnet-biotite-muscovite schist. Muscovite crystals surround garnet porphyroblasts and are folded with undulatory extinction. Garnet has quartz and biotite inclusions. Mica defines foliation. The biotite layers of the principle foliation cut cross some large plagioclase crystals (~800 µm). Subgrain rotation recrystallization occurs in quartz based on examining the extinction positions of quartz subgrains.

Sample KV-8-14: (Grenville basement; WBR)

Mineral assemblage: quartz, plagioclase, biotite, K-feldspar, sphene

The sample is a biotite granitic gneiss. Biotite defines the foliation of the sample. Biotite occurs in two forms: brown colored and green colored. Brown colored biotite has strong pleochroic. Quartz and K-feldspar show granoblastic interlobate texture. Quartz crystals bulge into K-feldspar. Large quartz grains typically have undulose extinction. Bulging and subgrain rotation recrystallization occur in quartz. Plagioclase is medium to coarse grained subhedral in shape.

Sample KV-1-15: (Max Patch Granite; WBR)

Mineral assemblage: quartz, K-feldspar, plagioclase, myrmekite, biotite, epidote

This sample is a mottled migmatitic granite from the Max Patch Granite. It was collected near a tectonic window. The main minerals, like feldspar and quartz, are medium to coarse grained. K-feldspar occurs in pink color in the hand sample, and is partly altered into yellow-green colored epidote. Quartz shows undulose extinction. Myrmekite grows next to the k-feldspar grains. Some grains are surrounded by ‘bright rims’ under cross polarized light. The ‘rims’ may be late-formed quartz due to hydrothermal event.

Sample KV-4-15: (Ocoee Supergroup; WBR)

Mineral assemblage: plagioclase, quartz, biotite

The sample is a metasedimentary rock (quartzite) at lower metamorphic grade. Quartz shows undulose extinction, indicating the rock was under high strain. There are strong fractures on large quartz crystals and plagioclase crystals, filled with mica groundmass and fine-grained feldspar. The sample is matrix-supported rock. Large grains are not commonly in contact.

Sample KV-6-15: (Grenville basement; WBR)

Mineral assemblage: microcline, plagioclase, biotite, quartz, garnet, sericite, sphene

This sample is a biotite granitic gneiss. Quartz shows bulging and undulose extinction. Recrystallization of quartz occurs as grain boundary. Feldspar shows granoblastic texture. Myrmekite is observed at grain boundaries of K-feldspar crystals. Myrmekite forms from the intergrowth of plagioclase and quartz. It is actually the incomplete replacement of K-feldspar. The myrmekite in this sample is present in two different types: wartlike myrmekite and ghost myrmekite.

Appendix C. $^{40}Ar/^{39}Ar$ Data

Muscovite of basement rock samples (SCTF)

Sensitivity (Moles/volt):	1.62E-14	2E-16
Measured 40/36 of Air:	291.0	1.5
(36/37)Ca:	0.0003005	0.0000044
(39/37)Ca:	0.0008200	0.0000820
GA1550 Biotite Monitor Age:	9.879E+07	
FC Sanidine Monitor Age:	2.802E+07	

Incremental heating and fusion analyses were accomplished with a CO2 laser.
Data are corrected for interfeering nuclear reactions, blank, and mass discrimination.
Data are in volts and errors are the standard deviation unless indicated otherwise.
Plateau ages include errors arising from precision of measurement and in estimating the J-value.
All samples were analyzed within 250 days of irradiation.

n	^{40}Ar(*+atm)	^{39}Ar (K)	^{38}Ar (Cl+atm)	^{37}Ar (Ca)	^{36}Ar (Atm)	Moles^{40}Ar	%Rad	R	Age(Ma)
KV-2B-14 (au27.3c.mus)		**316.73±0.43 Ma**		MSWD= 1.3					
1	17.89104 ± 0.022161	1.81409 ± 0.002853	0.02336 ± 0.000160	0.01201 ± 0.000819	0.0012416 ± 0.00002151	4.12E-13	97.9%	9.6600	318.09 ± 0.660
2	20.84668 ± 0.021444	2.16325 ± 0.001703	0.02775 ± 0.000110	0.01127 ± 0.001257	0.0001558 ± 0.00002468	4.80E-13	99.8%	9.6154	316.74 ± 0.426
3	16.78280 ± 0.026275	1.73255 ± 0.002988	0.02224 ± 0.000150	0.00804 ± 0.001169	0.0003437 ± 0.00002870	3.87E-13	99.4%	9.6281	317.12 ± 0.760
4	13.10901 ± 0.005382	1.35511 ± 0.001883	0.01762 ± 0.000112	0.01392 ± 0.000774	0.0002061 ± 0.00001195	3.02E-13	99.5%	9.6288	317.14 ± 0.469
5	19.22625 ± 0.006622	1.99211 ± 0.001553	0.02576 ± 0.000100	0.00505 ± 0.001307	0.0002641 ± 0.00001307	4.43E-13	99.6%	9.6120	316.64 ± 0.278
6	22.29479 ± 0.024991	2.31468 ± 0.002688	0.02958 ± 0.000130	0.00801 ± 0.001181	0.0003957 ± 0.00001391	5.14E-13	99.5%	9.5814	315.71 ± 0.516
7	18.00058 ± 0.033213	1.86822 ± 0.004495	0.02388 ± 0.000149	0.01317 ± 0.001424	0.0003383 ± 0.00001388	4.15E-13	99.4%	9.5816	315.72 ± 0.965
8	16.98825 ± 0.043616	1.75709 ± 0.005208	0.02256 ± 0.000093	0.00672 ± 0.001117	0.0003203 ± 0.00001848	3.91E-13	99.4%	9.6145	316.71 ± 1.253
9	18.70804 ± 0.033837	1.89815 ± 0.003485	0.02499 ± 0.000130	0.01112 ± 0.001530	0.0014072 ± 0.00001717	4.31E-13	97.8%	9.6369	317.39 ± 0.841
10	13.16430 ± 0.026643	1.36352 ± 0.003725	0.01773 ± 0.000121	0.00976 ± 0.001464	0.0002941 ± 0.00002860	3.03E-13	99.3%	9.5909	316.00 ± 1.101
KV-3-14 (au27.2m.mus)		**321.70±0.45 Ma**		MSWD= 4.3					
1	18.57705 ± 0.008248	1.89234 ± 0.001903	0.02442 ± 0.000159	0.01175 ± 0.000873	0.0000575 ± 0.00002247	4.28E-13	99.9%	9.8086	322.57 ± 0.373
2	13.32374 ± 0.010235	1.35547 ± 0.001397	0.01763 ± 0.000111	0.01537 ± 0.000827	0.0003519 ± 0.00001400	3.07E-13	99.2%	9.7540	320.92 ± 0.428
3	19.37472 ± 0.021758	1.98043 ± 0.002513	0.02652 ± 0.000349	0.01575 ± 0.001138	0.0003795 ± 0.00001377	4.46E-13	99.4%	9.7273	320.11 ± 0.550
4	13.90658 ± 0.014808	1.41199 ± 0.001455	0.01854 ± 0.000145	0.01017 ± 0.001054	0.0003073 ± 0.00001376	3.20E-13	99.3%	9.7854	321.87 ± 0.489
5	15.60759 ± 0.019301	1.57540 ± 0.002688	0.02057 ± 0.000084	0.00975 ± 0.001263	0.0007925 ± 0.00001758	3.60E-13	98.5%	9.7590	321.07 ± 0.696
6	17.21748 ± 0.005245	1.74551 ± 0.002367	0.02327 ± 0.000125	0.01164 ± 0.001080	0.0005019 ± 0.00002011	3.97E-13	99.1%	9.7795	321.69 ± 0.465
7	23.79194 ± 0.025442	2.42426 ± 0.003006	0.03136 ± 0.000173	0.02842 ± 0.001017	0.0005077 ± 0.00001207	5.48E-13	99.4%	9.7534	320.90 ± 0.531
8	19.26528 ± 0.011891	1.95880 ± 0.001802	0.02573 ± 0.000131	0.01591 ± 0.001519	0.0004336 ± 0.00001074	4.44E-13	99.3%	9.7707	321.42 ± 0.362
9	13.86279 ± 0.014205	1.40352 ± 0.001784	0.01951 ± 0.000313	0.01206 ± 0.000888	0.0002618 ± 0.00001415	3.19E-13	99.4%	9.8229	323.00 ± 0.539
10	15.11245 ± 0.012181	1.53802 ± 0.002448	0.02017 ± 0.000104	0.02095 ± 0.001379	0.0003668 ± 0.00001531	3.48E-13	99.3%	9.7568	321.01 ± 0.585
11	21.87975 ± 0.007763	2.22191 ± 0.003747	0.02944 ± 0.000124	0.01373 ± 0.001950	0.0003459 ± 0.00001446	5.04E-13	99.5%	9.8013	322.35 ± 0.562
12	21.88993 ± 0.023167	2.24791 ± 0.002669	0.02890 ± 0.000164	0.01246 ± 0.001007	0.0001650 ± 0.00001239	5.04E-13	99.8%	9.7162	319.78 ± 0.513
13	17.44224 ± 0.025539	1.75968 ± 0.003401	0.02298 ± 0.000157	0.00911 ± 0.001315	0.0003697 ± 0.00001081	4.02E-13	99.4%	9.8501	323.81 ± 0.792
14	16.67471 ± 0.014423	1.68337 ± 0.002292	0.02225 ± 0.000218	0.01421 ± 0.001196	0.0009862 ± 0.00001682	3.84E-13	98.3%	9.7324	320.27 ± 0.535
15	15.61810 ± 0.012351	1.60101 ± 0.002419	0.02075 ± 0.000134	0.01287 ± 0.001389	0.0001625 ± 0.00001241	3.60E-13	99.7%	9.7252	320.05 ± 0.553
16	16.84867 ± 0.009072	1.71258 ± 0.001527	0.02213 ± 0.000157	0.01833 ± 0.001483	0.0002112 ± 0.00001437	3.88E-13	99.6%	9.8018	322.36 ± 0.347
17	12.80812 ± 0.010761	1.28526 ± 0.002096	0.01716 ± 0.000185	0.01301 ± 0.000998	0.0005410 ± 0.00001130	2.95E-13	98.8%	9.8410	323.54 ± 0.607
18	13.54914 ± 0.019632	1.37944 ± 0.002278	0.01814 ± 0.000153	0.01800 ± 0.001071	0.0001473 ± 0.00001331	3.12E-13	99.7%	9.7906	322.03 ± 0.716
19	18.62619 ± 0.030682	1.91101 ± 0.003538	0.02470 ± 0.000163	0.02090 ± 0.001407	0.0002637 ± 0.00001333	4.29E-13	99.6%	9.7060	319.48 ± 0.798
20	13.95739 ± 0.013337	1.41212 ± 0.002058	0.01842 ± 0.000086	0.01546 ± 0.001047	0.0003991 ± 0.00001136	3.22E-13	99.2%	9.8005	322.32 ± 0.572
21	17.30598 ± 0.023407	1.73751 ± 0.003548	0.02250 ± 0.000114	0.01679 ± 0.000808	0.0010248 ± 0.00001767	3.99E-13	98.3%	9.7859	321.88 ± 0.809
22	19.40371 ± 0.019643	1.94603 ± 0.002500	0.02578 ± 0.000100	0.01732 ± 0.001120	0.0012350 ± 0.00002107	4.47E-13	98.1%	9.7834	321.81 ± 0.547
23	8.32681 ± 0.010945	0.83268 ± 0.000719	0.01113 ± 0.000091	0.00087 ± 0.001093	0.0005416 ± 0.00001063	1.92E-13	98.1%	9.8078	322.54 ± 0.532
24	18.34067 ± 0.015703	1.85225 ± 0.003238	0.02391 ± 0.000124	0.01561 ± 0.000845	0.0006765 ± 0.00002820	4.23E-13	98.9%	9.7939	322.12 ± 0.651
25	9.97873 ± 0.015325	1.00231 ± 0.001577	0.01298 ± 0.000080	-0.00088 ± 0.001201	0.0003185 ± 0.00001444	2.30E-13	99.1%	9.8619	324.17 ± 0.733

n	^{40}Ar(*+atm)		^{39}Ar (K)		^{38}Ar (Cl+atm)		^{37}Ar (Ca)		^{36}Ar (Atm)		Moles^{40}Ar	%Rad	R	Age(Ma)	
KV-4-14 (au27.2f.mus)				**324 - 342 Ma**											
1	6.25630	± 0.005332	0.62321	± 0.001040	0.00875	± 0.000046	0.00258	± 0.001436	0.0002100	± 0.00000812	1.44E-13	99.0%	9.9397	326.51	± 0.631
2	11.60910	± 0.005415	1.14569	± 0.001800	0.01527	± 0.000097	0.01013	± 0.001076	0.0002837	± 0.00001171	2.68E-13	99.3%	10.0606	330.14	± 0.554
3	6.52387	± 0.006395	0.65131	± 0.000842	0.00862	± 0.000052	0.00169	± 0.001150	0.0001902	± 0.00001541	1.50E-13	99.1%	9.9305	326.23	± 0.581
4	5.58746	± 0.004793	0.56010	± 0.000944	0.00746	± 0.000041	-0.00032	± 0.000962	0.0001357	± 0.00000817	1.29E-13	99.3%	9.9042	325.44	± 0.636
5	2.65606	± 0.002295	0.26501	± 0.000326	0.00360	± 0.000042	0.00059	± 0.000751	0.0000512	± 0.00000746	6.12E-14	99.4%	9.9657	327.29	± 0.566
6	12.19774	± 0.007130	1.21440	± 0.001550	0.01582	± 0.000143	0.01131	± 0.000976	0.0001535	± 0.00001009	2.81E-13	99.6%	10.0078	328.56	± 0.470
7	10.52340	± 0.007670	1.04918	± 0.000678	0.01440	± 0.000104	0.01218	± 0.001068	0.0002022	± 0.00001106	2.42E-13	99.4%	9.9743	327.55	± 0.337
8	10.24420	± 0.011412	1.01739	± 0.001645	0.01376	± 0.000122	0.00038	± 0.001169	0.0001463	± 0.00000761	2.36E-13	99.6%	10.0266	329.12	± 0.653
9	22.41945	± 0.023224	2.24092	± 0.003933	0.03016	± 0.000164	0.03660	± 0.001243	0.0004029	± 0.00001182	5.17E-13	99.5%	9.9531	326.91	± 0.672
10	19.99276	± 0.016916	1.96924	± 0.003006	0.02650	± 0.000232	0.02293	± 0.001374	0.0001460	± 0.00002667	4.61E-13	99.8%	10.1318	332.27	± 0.596
11	14.12707	± 0.007196	1.39957	± 0.001824	0.01859	± 0.000092	0.01319	± 0.001107	0.0006363	± 0.00001244	3.26E-13	98.7%	9.9604	327.13	± 0.472
12	13.13417	± 0.009086	1.32030	± 0.002038	0.01779	± 0.000115	0.00680	± 0.001443	0.0002891	± 0.00002895	3.03E-13	99.3%	9.8837	324.82	± 0.593
13	17.65868	± 0.012205	1.75782	± 0.002998	0.02335	± 0.000107	0.01310	± 0.000802	0.0003397	± 0.00001234	4.07E-13	99.4%	9.9894	328.00	± 0.611
14	21.92385	± 0.017107	2.18495	± 0.002916	0.02918	± 0.000118	0.01656	± 0.001665	0.0006450	± 0.00001427	5.05E-13	99.1%	9.9476	326.75	± 0.514
15	10.01485	± 0.013684	0.99824	± 0.001983	0.01313	± 0.000050	0.00110	± 0.000933	0.0001315	± 0.00000942	2.31E-13	99.6%	9.9937	328.13	± 0.799
16	16.05821	± 0.007076	1.59030	± 0.002233	0.02145	± 0.000111	0.01439	± 0.001253	0.0006496	± 0.00001208	3.70E-13	98.8%	9.9778	327.65	± 0.494
17	22.67747	± 0.019130	2.26290	± 0.002666	0.03033	± 0.000176	0.01732	± 0.001583	0.0005200	± 0.00001367	5.23E-13	99.3%	9.9543	326.95	± 0.481
18	7.72505	± 0.007582	0.75804	± 0.001331	0.01001	± 0.000055	0.00179	± 0.000936	0.0001279	± 0.00000855	1.78E-13	99.5%	10.1412	332.55	± 0.681
19	8.59151	± 0.007999	0.86040	± 0.000988	0.01233	± 0.000066	0.00091	± 0.000647	0.0001170	± 0.00001401	1.98E-13	99.6%	9.9454	326.68	± 0.510
20	14.98842	± 0.008498	1.44317	± 0.001333	0.02258	± 0.000095	0.04990	± 0.001236	0.0003848	± 0.00001376	3.45E-13	99.2%	10.3104	337.61	± 0.380
21	13.72562	± 0.006273	1.35878	± 0.001914	0.01811	± 0.000134	0.01575	± 0.001462	0.0002470	± 0.00002635	3.16E-13	99.5%	10.0489	329.79	± 0.526
22	8.79978	± 0.008760	0.83521	± 0.001378	0.01292	± 0.000069	0.00266	± 0.001086	0.0001928	± 0.00000818	2.03E-13	99.4%	10.4681	342.32	± 0.671
23	18.26243	± 0.014392	1.78487	± 0.000903	0.02665	± 0.000131	0.01009	± 0.000721	0.0003956	± 0.00001402	4.21E-13	99.4%	10.1669	333.32	± 0.323
24	21.45723	± 0.019501	2.11737	± 0.003479	0.02751	± 0.000085	0.01309	± 0.001113	0.0003422	± 0.00001355	4.94E-13	99.5%	10.0868	330.92	± 0.627
25	15.59879	± 0.015340	1.56126	± 0.002331	0.02130	± 0.000262	0.01157	± 0.001030	0.0003905	± 0.00001648	3.59E-13	99.3%	9.9180	325.86	± 0.596
KV-5-14 (au27.2b.mus&au27.2d.mus)						**323 - 400 Ma**									
1	21.22693	± 0.019353	1.74161	± 0.001468	0.02366	± 0.000146	0.01203	± 0.000964	0.0009690	± 0.00001681	4.89E-13	98.7%	12.0244	388.09	± 0.497
2	22.30146	± 0.039560	2.15795	± 0.003437	0.02875	± 0.000147	0.01810	± 0.001308	0.0004656	± 0.00001384	5.14E-13	99.4%	10.2716	336.46	± 0.809
3	13.80240	± 0.013776	1.15981	± 0.001714	0.01606	± 0.000088	0.01019	± 0.001330	0.0006218	± 0.00001605	3.18E-13	98.7%	11.7430	379.90	± 0.699
4	21.53370	± 0.035078	2.14096	± 0.003114	0.02913	± 0.000239	0.02100	± 0.001356	0.0005735	± 0.00001829	4.96E-13	99.2%	9.9798	327.71	± 0.726
5	22.79157	± 0.059426	2.22175	± 0.004477	0.03003	± 0.000154	0.01721	± 0.001128	0.0008509	± 0.00003324	5.25E-13	98.9%	10.1460	332.70	± 1.118
6	16.89776	± 0.024151	1.46557	± 0.001725	0.02036	± 0.000088	0.02073	± 0.002249	0.0003383	± 0.00002241	3.89E-13	99.4%	11.4631	371.71	± 0.708
7	15.50633	± 0.029975	1.40321	± 0.002149	0.01990	± 0.000114	0.02165	± 0.001337	0.0005290	± 0.00001603	3.57E-13	99.0%	10.9408	356.34	± 0.895
8	16.96698	± 0.012938	1.70761	± 0.001653	0.02572	± 0.000207	0.02318	± 0.001343	0.0005508	± 0.00001647	3.91E-13	99.0%	9.8422	323.58	± 0.413
9	15.05423	± 0.017629	1.49829	± 0.002378	0.02026	± 0.000134	0.01618	± 0.001118	0.0001767	± 0.00001110	3.47E-13	99.7%	10.0139	328.74	± 0.655
10	22.47132	± 0.025384	2.03960	± 0.002866	0.02732	± 0.000087	0.01705	± 0.000758	0.0002692	± 0.00001292	5.18E-13	99.6%	10.9794	357.48	± 0.650
11	19.12467	± 0.012489	1.59708	± 0.002279	0.02144	± 0.000072	0.01331	± 0.000807	0.0003598	± 0.00001399	4.41E-13	99.4%	11.9090	384.73	± 0.613
12	22.88323	± 0.022131	2.12097	± 0.001406	0.02907	± 0.000132	0.01553	± 0.001310	0.0022523	± 0.00003537	5.27E-13	97.1%	10.4760	342.55	± 0.444
13	15.27427	± 0.011425	1.23410	± 0.001870	0.01665	± 0.000066	0.01197	± 0.001506	0.0017842	± 0.00002294	3.52E-13	96.5%	11.9506	385.94	± 0.699
14	21.86040	± 0.022980	2.09752	± 0.001715	0.02789	± 0.000173	0.01851	± 0.002177	0.0005205	± 0.00002801	5.04E-13	99.3%	10.3496	338.78	± 0.472
15	14.09397	± 0.019650	1.25203	± 0.001822	0.01723	± 0.000133	0.01337	± 0.001197	0.0002787	± 0.00001574	3.25E-13	99.4%	11.1922	363.76	± 0.747
16	18.02985	± 0.011262	1.59295	± 0.002343	0.02156	± 0.000138	0.02393	± 0.000975	0.0003073	± 0.00001307	4.15E-13	99.5%	11.2630	365.84	± 0.593
17	11.73960	± 0.004813	1.09271	± 0.001315	0.01474	± 0.000071	0.00975	± 0.001127	0.0003304	± 0.00001444	2.71E-13	99.2%	10.6551	347.88	± 0.464
18	10.15914	± 0.009345	0.93458	± 0.001472	0.01253	± 0.000039	0.00494	± 0.001555	0.0013897	± 0.00001438	2.34E-13	96.0%	10.4314	341.22	± 0.666
19	7.99225	± 0.010249	0.67730	± 0.001723	0.00887	± 0.000067	0.00063	± 0.001174	0.0000494	± 0.00000772	1.84E-13	99.8%	11.7786	380.94	± 1.093
20	11.75275	± 0.004905	1.10908	± 0.001466	0.01501	± 0.000089	0.01174	± 0.000932	0.0000978	± 0.00001787	2.71E-13	99.8%	10.5718	345.40	± 0.504
21	11.06171	± 0.006289	1.04975	± 0.002256	0.01402	± 0.000114	0.00939	± 0.001569	0.0000705	± 0.00000867	2.55E-13	99.8%	10.5185	343.82	± 0.770
22	17.90324	± 0.017080	1.65842	± 0.002678	0.02315	± 0.000242	0.00903	± 0.001200	0.0006065	± 0.00001463	4.13E-13	99.0%	10.6879	348.85	± 0.666
23	20.36823	± 0.021614	1.73810	± 0.001705	0.02383	± 0.000127	0.01351	± 0.001028	0.0009916	± 0.00001840	4.69E-13	98.6%	11.5509	374.28	± 0.558
24	18.50017	± 0.018889	1.75439	± 0.003801	0.02400	± 0.000130	0.00938	± 0.000827	0.0002415	± 0.00002136	4.26E-13	99.6%	10.5049	343.41	± 0.834
25	24.07520	± 0.021326	1.92411	± 0.001584	0.02607	± 0.000175	0.01026	± 0.001001	0.0003758	± 0.00001388	5.55E-13	99.5%	12.4552	400.55	± 0.491

KV-6-14 (au27.1m.mus)				322 - 344 Ma											
n	^{40}Ar(*+atm)		^{39}Ar (K)		^{38}Ar (Cl+atm)		^{37}Ar (Ca)		^{36}Ar (Atm)		Moles^{40}Ar	%Rad	R	Age(Ma)	
1	5.71862	± 0.003742	0.54301	± 0.000472	0.00758	± 0.000030	0.00066	± 0.001018	0.0000562	± 0.00000712	1.32E-13	99.7%	10.5009	340.88	± 0.393
2	4.98002	± 0.004053	0.48663	± 0.000661	0.00700	± 0.000042	0.00310	± 0.001117	0.0000879	± 0.00000680	1.15E-13	99.5%	10.1809	331.39	± 0.544
3	9.43850	± 0.005152	0.90961	± 0.001520	0.01243	± 0.000080	0.00563	± 0.001628	0.0001486	± 0.00000767	2.17E-13	99.5%	10.3287	335.78	± 0.599
4	8.19820	± 0.008714	0.82068	± 0.001021	0.01170	± 0.000066	0.00404	± 0.000939	0.0001465	± 0.00000823	1.89E-13	99.5%	9.9373	324.13	± 0.542
5	6.52290	± 0.005872	0.61799	± 0.000680	0.00817	± 0.000044	0.00108	± 0.001027	0.0000639	± 0.00000645	1.50E-13	99.7%	10.5247	341.58	± 0.497
6	16.14622	± 0.010522	1.59207	± 0.002097	0.02188	± 0.000222	0.01716	± 0.001497	0.0001610	± 0.00001327	3.72E-13	99.7%	10.1128	329.36	± 0.492
7	4.79117	± 0.003092	0.48149	± 0.001260	0.00643	± 0.000038	0.00250	± 0.001064	0.0001008	± 0.00001067	1.10E-13	99.4%	9.8894	322.70	± 0.901
8	4.25282	± 0.002725	0.41067	± 0.000700	0.00584	± 0.000051	0.00442	± 0.001328	0.0000255	± 0.00000715	9.80E-14	99.8%	10.3386	336.07	± 0.635
9	6.86920	± 0.005871	0.65354	± 0.001373	0.00857	± 0.000069	0.00124	± 0.001142	0.0000361	± 0.00000710	1.58E-13	99.8%	10.4946	340.69	± 0.781
10	7.05112	± 0.006988	0.70521	± 0.000943	0.00984	± 0.000107	0.00655	± 0.001003	0.0001409	± 0.00000793	1.62E-13	99.4%	9.9405	324.23	± 0.554
11	7.40407	± 0.006441	0.73541	± 0.000837	0.00957	± 0.000081	0.00557	± 0.001457	0.0000198	± 0.00000603	1.71E-13	99.9%	10.0608	327.82	± 0.477
12	9.67552	± 0.014264	0.93301	± 0.001292	0.01274	± 0.000074	0.00234	± 0.001399	0.0001691	± 0.00000863	2.23E-13	99.5%	10.3170	335.43	± 0.688
13	14.08958	± 0.013051	1.39534	± 0.001388	0.01939	± 0.000069	0.04520	± 0.001327	0.0002207	± 0.00001248	3.25E-13	99.5%	10.0541	327.62	± 0.455
14	15.23382	± 0.015227	1.48503	± 0.002309	0.02099	± 0.000193	0.01550	± 0.001377	0.0000937	± 0.00001800	3.51E-13	99.8%	10.2406	333.17	± 0.628
15	17.72637	± 0.006568	1.72239	± 0.002158	0.02320	± 0.000099	0.05093	± 0.001381	0.0006228	± 0.00001578	4.08E-13	99.0%	10.1879	331.60	± 0.447
16	11.74453	± 0.006703	1.14600	± 0.001895	0.01613	± 0.000136	0.01813	± 0.001389	0.0001566	± 0.00001254	2.71E-13	99.6%	10.2095	332.24	± 0.593
17	21.21256	± 0.012946	2.00787	± 0.001517	0.02925	± 0.000173	0.02217	± 0.000992	0.0005148	± 0.00001483	4.89E-13	99.3%	10.4900	340.56	± 0.341
18	13.65258	± 0.013469	1.32855	± 0.002210	0.01747	± 0.000145	0.01618	± 0.001128	0.0002142	± 0.00001294	3.15E-13	99.5%	10.2299	332.85	± 0.653
19	13.84365	± 0.012694	1.38522	± 0.002964	0.02012	± 0.000147	0.02064	± 0.001262	0.0002929	± 0.00002360	3.19E-13	99.4%	9.9328	324.00	± 0.776
20	18.03588	± 0.025824	1.70961	± 0.001879	0.02512	± 0.000194	0.01998	± 0.000932	0.0002381	± 0.00002278	4.16E-13	99.6%	10.5098	341.14	± 0.631
21	16.40661	± 0.016935	1.54089	± 0.001672	0.02205	± 0.000132	0.01373	± 0.000571	0.0001555	± 0.00001278	3.78E-13	99.7%	10.6185	344.36	± 0.523
22	16.99233	± 0.030169	1.68920	± 0.003164	0.02449	± 0.000122	0.04070	± 0.001303	0.0001826	± 0.00002884	3.92E-13	99.7%	10.0299	326.89	± 0.862
23	17.55030	± 0.028750	1.74957	± 0.002465	0.02449	± 0.000092	0.01818	± 0.001387	0.0002821	± 0.00001465	4.04E-13	99.5%	9.9846	325.54	± 0.711
24	13.42174	± 0.019200	1.31874	± 0.002536	0.02017	± 0.000104	0.01537	± 0.001360	0.0002022	± 0.00001342	3.09E-13	99.6%	10.1335	329.98	± 0.800
25	12.94683	± 0.015781	1.27363	± 0.001337	0.01872	± 0.000086	0.01231	± 0.000908	0.0003077	± 0.00001554	2.98E-13	99.3%	10.0949	328.83	± 0.546
KV-7-14 (au27.1q.mus)				342 - 398 Ma											
1	17.56340	± 0.015308	1.58894	± 0.001643	0.02087	± 0.000145	0.02188	± 0.001291	0.0001717	± 0.00001255	4.05E-13	99.7%	11.0230	356.26	± 0.489
2	24.07647	± 0.044052	2.18228	± 0.003809	0.02787	± 0.000120	0.03518	± 0.000697	0.0001443	± 0.00002457	5.55E-13	99.8%	11.0148	356.02	± 0.908
3	20.59949	± 0.041415	1.82226	± 0.002126	0.02359	± 0.000120	0.02305	± 0.001397	0.0002807	± 0.00001248	4.75E-13	99.6%	11.2601	363.20	± 0.850
4	19.78289	± 0.029375	1.80453	± 0.002232	0.02312	± 0.000152	0.02933	± 0.001446	0.0001950	± 0.00002107	4.56E-13	99.7%	10.9326	353.60	± 0.694
5	17.52201	± 0.024811	1.63408	± 0.002050	0.02104	± 0.000108	0.02875	± 0.001867	0.0003267	± 0.00001285	4.04E-13	99.4%	10.6655	345.74	± 0.662
6	18.95600	± 0.035663	1.71270	± 0.004233	0.02245	± 0.000148	0.01924	± 0.001794	0.0004100	± 0.00001009	4.37E-13	99.4%	10.9983	355.53	± 1.113
7	19.40029	± 0.021995	1.72046	± 0.002873	0.02271	± 0.000082	0.01923	± 0.001402	0.0000725	± 0.00002126	4.47E-13	99.9%	11.2649	363.34	± 0.744
8	17.09805	± 0.040355	1.60047	± 0.002790	0.02110	± 0.000236	0.03520	± 0.001902	0.0002390	± 0.00001178	3.94E-13	99.6%	10.6413	345.03	± 1.019
9	17.18327	± 0.033196	1.49204	± 0.002254	0.01964	± 0.000147	0.01953	± 0.001459	0.0003459	± 0.00001225	3.96E-13	99.4%	11.4494	368.72	± 0.913
10	18.83254	± 0.036966	1.70321	± 0.002645	0.02234	± 0.000105	0.02064	± 0.001332	0.0003774	± 0.00001366	4.34E-13	99.4%	10.9928	355.37	± 0.898
11	15.45701	± 0.028503	1.44385	± 0.002402	0.01982	± 0.000228	0.02048	± 0.001579	0.0002374	± 0.00002466	3.56E-13	99.5%	10.6582	345.53	± 0.877
12	16.29064	± 0.010155	1.50970	± 0.003657	0.01943	± 0.000094	0.02078	± 0.000978	0.0002058	± 0.00000989	3.75E-13	99.6%	10.7517	348.28	± 0.877
13	13.68760	± 0.026095	1.24510	± 0.001976	0.01626	± 0.000088	0.02608	± 0.000849	0.0001553	± 0.00001832	3.15E-13	99.7%	10.9584	354.36	± 0.893
14	21.70450	± 0.022181	1.73784	± 0.001648	0.02281	± 0.000178	0.00997	± 0.001467	0.0001335	± 0.00001058	5.00E-13	99.8%	12.4672	398.13	± 0.559
15	17.88783	± 0.023821	1.43656	± 0.002989	0.01921	± 0.000144	0.01200	± 0.001600	0.0001832	± 0.00002666	4.12E-13	99.7%	12.4150	396.63	± 0.998
16	15.80781	± 0.017867	1.47995	± 0.001331	0.01935	± 0.000114	0.02710	± 0.001712	0.0001729	± 0.00000994	3.64E-13	99.7%	10.6486	345.24	± 0.504
17	20.47570	± 0.019969	1.93392	± 0.003056	0.02534	± 0.000094	0.03260	± 0.001882	0.0003093	± 0.00002281	4.72E-13	99.6%	10.5421	342.10	± 0.648
18	16.95769	± 0.023638	1.53339	± 0.002047	0.02007	± 0.000116	0.02277	± 0.001011	0.0002023	± 0.00001627	3.91E-13	99.6%	11.0215	356.21	± 0.697
19	18.40016	± 0.027882	1.67057	± 0.003077	0.02241	± 0.000145	0.03475	± 0.001122	0.0004073	± 0.00002588	4.24E-13	99.3%	10.9444	353.95	± 0.862
20	13.52229	± 0.024401	1.24334	± 0.002276	0.01642	± 0.000105	0.02570	± 0.001105	0.0001498	± 0.00002081	3.12E-13	99.7%	10.8423	350.95	± 0.919
21	19.85222	± 0.020717	1.79623	± 0.002104	0.02423	± 0.000230	0.01604	± 0.001764	0.0004533	± 0.00001439	4.57E-13	99.3%	10.9785	354.95	± 0.566
22	13.68836	± 0.015351	1.19370	± 0.001999	0.01599	± 0.000112	0.02205	± 0.001657	0.0002135	± 0.00002481	3.15E-13	99.5%	11.4161	367.75	± 0.770
23	21.49851	± 0.040730	1.94794	± 0.002891	0.02516	± 0.000128	0.03662	± 0.001548	0.0001822	± 0.00001291	4.95E-13	99.7%	11.0108	355.90	± 0.861
24	23.64864	± 0.038825	2.17376	± 0.003734	0.02814	± 0.000057	0.02197	± 0.001110	0.0002222	± 0.00000975	5.45E-13	99.7%	10.8499	351.18	± 0.838
25	14.04116	± 0.016240	1.28804	± 0.003108	0.01652	± 0.000107	0.01869	± 0.001168	0.0001646	± 0.00001902	3.24E-13	99.7%	10.8649	351.61	± 0.955

K-feldspar of basement samples

KV-1-14 (au27.3f.ksp)			SCTF						
n	^{40}Ar(*+atm)	^{39}Ar (K)	^{38}Ar (Cl+atm)	^{37}Ar (Ca)	^{36}Ar (Atm)	Moles^{40}Ar	%Rad	R	Age(Ma)
1	18.55192 ± 0.015115	2.25188 ± 0.002481	0.02976 ± 0.000196	0.03157 ± 0.000249	0.0004864 ± 0.00004033	1.42E-13	99.2%	8.1759	272.86 ± 0.416
2	16.30593 ± 0.030511	1.72352 ± 0.003259	0.02362 ± 0.000179	0.01329 ± 0.000167	0.0005253 ± 0.00001858	1.25E-13	99.0%	9.3715	309.51 ± 0.838
3	20.22365 ± 0.029758	1.90426 ± 0.003577	0.02667 ± 0.000150	0.05480 ± 0.000361	0.0008542 ± 0.00002145	1.55E-13	98.8%	10.4906	343.16 ± 0.836
4	22.35878 ± 0.031646	2.34040 ± 0.003800	0.03114 ± 0.000172	0.01108 ± 0.000190	0.0006770 ± 0.00001921	1.72E-13	99.1%	9.4684	312.45 ± 0.684
5	12.60196 ± 0.006605	1.24534 ± 0.001836	0.01831 ± 0.000110	0.00510 ± 0.000193	0.0005959 ± 0.00001578	9.68E-14	98.6%	9.9783	327.83 ± 0.535
KV-1-14 (au27.3f.ksp.97)			**SCIH**	**Time duration**	20s				
p	^{40}Ar(*+atm)	^{39}Ar (K)	^{38}Ar (Cl+atm)	^{37}Ar (Ca)	^{36}Ar (Atm)	Moles^{40}Ar	%Rad	R	Age(Ma)
0.4	0.00062 ± 0.000093	0.00019 ± 0.000077	0.00001 ± 0.000030	0.00023 ± 0.000110	0.0000022 ± 0.00001259	1.44E-17	-2.0%	0.0439	1.58 ± 716.020
0.45	0.00588 ± 0.000130	0.00140 ± 0.000078	-0.00001 ± 0.000020	0.00016 ± 0.000060	0.0000117 ± 0.00001111	1.35E-16	41.1%	1.7393	61.60 ± 83.804
0.5	0.12466 ± 0.000323	0.02597 ± 0.000096	0.00032 ± 0.000035	0.00292 ± 0.000145	0.0000086 ± 0.00001112	2.87E-15	98.0%	4.7118	162.24 ± 4.419
0.53	0.26351 ± 0.000271	0.04810 ± 0.000168	0.00061 ± 0.000027	0.00037 ± 0.000124	-0.0000065 ± 0.00001239	6.07E-15	100.7%	5.4794	187.34 ± 2.691
0.56	0.45456 ± 0.000668	0.06934 ± 0.000135	0.00084 ± 0.000023	0.00029 ± 0.000108	-0.0000018 ± 0.00001116	1.05E-14	100.1%	6.5562	221.98 ± 1.699
0.59	0.36270 ± 0.000357	0.05435 ± 0.000152	0.00070 ± 0.000029	0.00008 ± 0.000076	-0.0000048 ± 0.00001102	8.36E-15	100.4%	6.6740	225.73 ± 2.134
0.62	0.23660 ± 0.000339	0.03371 ± 0.000100	0.00043 ± 0.000026	-0.00002 ± 0.000093	-0.0000128 ± 0.00001134	5.45E-15	101.6%	7.0185	236.65 ± 3.441
0.65	2.04677 ± 0.001789	0.23174 ± 0.000378	0.00321 ± 0.000031	0.00031 ± 0.000129	0.0000489 ± 0.00001270	4.72E-14	99.3%	8.7701	291.17 ± 0.764
0.7	10.30175 ± 0.003779	0.98850 ± 0.001528	0.01388 ± 0.000068	0.00057 ± 0.000088	0.0003856 ± 0.00001339	2.37E-13	98.9%	10.3064	337.66 ± 0.558
0.75	2.03893 ± 0.001543	0.21130 ± 0.000582	0.00292 ± 0.000045	-0.00001 ± 0.000166	0.0000362 ± 0.00001676	4.70E-14	99.5%	9.5986	316.39 ± 1.193
0.8	1.46332 ± 0.001440	0.15592 ± 0.000602	0.00209 ± 0.000044	-0.00018 ± 0.000109	0.0000051 ± 0.00001735	3.37E-14	99.9%	9.3753	309.63 ± 1.645
0.85	0.46478 ± 0.001077	0.04859 ± 0.000109	0.00065 ± 0.000021	-0.00014 ± 0.000118	-0.0000733 ± 0.00002190	1.07E-14	104.7%	9.5645	315.36 ± 4.508
0.9	0.36314 ± 0.000604	0.03914 ± 0.000136	0.00051 ± 0.000033	-0.00009 ± 0.000085	-0.0000265 ± 0.00001602	8.37E-15	102.2%	9.2769	306.64 ± 4.168
0.93	0.15185 ± 0.000440	0.01622 ± 0.000124	0.00020 ± 0.000023	-0.00019 ± 0.000127	-0.0000367 ± 0.00001643	3.50E-15	107.1%	9.3601	309.17 ± 10.205
0.96	0.02458 ± 0.000221	0.00254 ± 0.000091	0.00004 ± 0.000024	-0.00007 ± 0.000094	0.0000401 ± 0.00001663	5.66E-16	51.8%	5.0094	172.02 ± 67.755
1	0.03054 ± 0.000107	0.00342 ± 0.000124	0.00008 ± 0.000029	-0.00027 ± 0.000181	-0.0000030 ± 0.00002198	7.04E-16	102.9%	8.9247	295.90 ± 63.884
KV-1-14 (au27.3f.ksp.98)			**SCIH**	**Time duration**	20s				
0.45	0.05183 ± 0.000315	0.00938 ± 0.000073	0.00012 ± 0.000023	0.00183 ± 0.000114	0.0000303 ± 0.00001140	1.19E-15	82.7%	4.5918	158.29 ± 12.533
0.5	0.27560 ± 0.000698	0.04693 ± 0.000280	0.00059 ± 0.000025	0.00542 ± 0.000175	0.0000384 ± 0.00001228	6.35E-15	95.9%	5.6420	192.62 ± 2.942
0.53	0.47598 ± 0.000938	0.07510 ± 0.000240	0.00088 ± 0.000022	0.00053 ± 0.000129	0.0000274 ± 0.00001259	1.10E-14	98.3%	6.2311	211.59 ± 1.866
0.55	0.34004 ± 0.000433	0.05304 ± 0.000190	0.00068 ± 0.000021	0.00032 ± 0.000158	0.0000242 ± 0.00001895	7.84E-15	97.9%	6.2768	213.06 ± 3.677
0.57	0.75810 ± 0.000749	0.10924 ± 0.000305	0.00141 ± 0.000034	0.00076 ± 0.000146	0.0000369 ± 0.00001888	1.75E-14	98.6%	6.8403	231.01 ± 1.860
0.59	0.53929 ± 0.000788	0.07854 ± 0.000375	0.00103 ± 0.000016	0.00036 ± 0.000094	0.0000526 ± 0.00001806	1.24E-14	97.1%	6.6688	225.57 ± 2.574
0.61	0.31038 ± 0.000331	0.04367 ± 0.000184	0.00057 ± 0.000019	-0.00006 ± 0.000145	0.0000016 ± 0.00002328	7.15E-15	99.8%	7.0958	239.09 ± 5.409
0.63	0.41029 ± 0.000555	0.05598 ± 0.000157	0.00069 ± 0.000023	0.00014 ± 0.000085	0.0000280 ± 0.00001858	9.45E-15	98.0%	7.1822	241.81 ± 3.391
0.65	0.73201 ± 0.001378	0.09636 ± 0.000370	0.00128 ± 0.000028	0.00067 ± 0.000065	0.0000229 ± 0.00001253	1.69E-14	99.1%	7.5268	252.64 ± 1.689
0.67	4.91413 ± 0.003054	0.56590 ± 0.000813	0.00784 ± 0.000056	0.00220 ± 0.000093	0.0001434 ± 0.00001253	1.13E-13	99.1%	8.6093	286.23 ± 0.501
0.69	9.06615 ± 0.007273	0.96214 ± 0.001194	0.01308 ± 0.000083	0.00168 ± 0.000154	0.0003678 ± 0.00001470	2.09E-13	98.8%	9.3101	307.65 ± 0.484
0.71	2.86619 ± 0.001854	0.32253 ± 0.000558	0.00433 ± 0.000033	0.00070 ± 0.000125	0.0001117 ± 0.00001321	6.60E-14	98.8%	8.7843	291.60 ± 0.677
0.74	1.44778 ± 0.001047	0.16092 ± 0.000428	0.00208 ± 0.000028	0.00042 ± 0.000090	0.0000468 ± 0.00001260	3.34E-14	99.0%	8.9111	295.49 ± 1.124
0.79	1.46761 ± 0.001427	0.16509 ± 0.000149	0.00220 ± 0.000034	0.00015 ± 0.000113	0.0000743 ± 0.00001836	3.38E-14	98.5%	8.7567	290.76 ± 1.160
0.85	1.10016 ± 0.002123	0.12417 ± 0.000493	0.00163 ± 0.000029	0.00046 ± 0.000173	0.0000195 ± 0.00001195	2.54E-14	99.5%	8.8143	292.52 ± 1.605
0.79	1.46763 ± 0.001428	0.16513 ± 0.000153	0.00221 ± 0.000033	0.00019 ± 0.000113	0.0001152 ± 0.00001880	3.38E-14	97.7%	8.6817	288.46 ± 1.186
0.85	1.10017 ± 0.002123	0.12420 ± 0.000494	0.00164 ± 0.000028	0.00050 ± 0.000173	0.0000681 ± 0.00001907	2.54E-14	98.2%	8.6963	288.90 ± 1.991
0.9	0.25793 ± 0.000393	0.02829 ± 0.000100	0.00037 ± 0.000021	0.00030 ± 0.000211	0.0000551 ± 0.00002089	5.94E-15	93.7%	8.5433	284.20 ± 7.355
0.95	0.34612 ± 0.000734	0.03862 ± 0.000150	0.00053 ± 0.000025	0.00031 ± 0.000096	0.0000642 ± 0.00001920	7.98E-15	94.5%	8.4728	282.03 ± 5.065

KV-1-14 (au27.3f.ksp.99)					SCIH		Time duration		20s						
p	^{40}Ar(*+atm)		^{39}Ar (K)		^{38}Ar (Cl+atm)		^{37}Ar (Ca)		^{36}Ar (Atm)		Moles^{40}Ar	%Rad	R	Age(Ma)	
0.4	0.00885	± 0.000203	0.00052	± 0.000050	0.00001	± 0.000024	-0.00048	± 0.000137	-0.0000251	± 0.00001265	2.04E-16	183.9%	16.9875	527.00	± 234.213
0.44	0.03481	± 0.000226	0.00570	± 0.000084	0.00008	± 0.000029	0.00076	± 0.000145	-0.0000133	± 0.00001070	8.02E-16	111.3%	6.1192	208.00	± 19.159
0.47	0.06337	± 0.000230	0.01265	± 0.000062	0.00014	± 0.000022	0.00157	± 0.000157	-0.0000428	± 0.00001667	1.46E-15	120.0%	5.0215	172.41	± 13.415
0.5	0.18867	± 0.000254	0.03517	± 0.000096	0.00049	± 0.000031	0.00311	± 0.000110	-0.0000292	± 0.00001064	4.35E-15	104.6%	5.3729	183.88	± 3.110
0.53	0.37803	± 0.000697	0.05441	± 0.000309	0.00070	± 0.000027	0.00156	± 0.000149	0.0000049	± 0.00001059	8.71E-15	99.6%	6.9245	233.68	± 2.394
0.56	0.42519	± 0.000563	0.05291	± 0.000131	0.00078	± 0.000029	0.00160	± 0.000109	0.0000906	± 0.00001860	9.80E-15	93.7%	7.5327	252.82	± 3.567
0.59	0.39969	± 0.000594	0.04675	± 0.000153	0.00069	± 0.000032	0.00117	± 0.000100	0.0000708	± 0.00001936	9.21E-15	94.8%	8.1048	270.65	± 4.213
0.61	0.44510	± 0.000982	0.05509	± 0.000133	0.00078	± 0.000027	0.00047	± 0.000242	0.0001122	± 0.00001852	1.03E-14	92.6%	7.4791	251.14	± 3.454
0.63	0.32812	± 0.000758	0.04392	± 0.000264	0.00060	± 0.000032	0.00033	± 0.000093	0.0000544	± 0.00001810	7.56E-15	95.1%	7.1047	239.37	± 4.412
0.65	0.72441	± 0.000862	0.08797	± 0.000227	0.00134	± 0.000038	0.00038	± 0.000136	0.0000686	± 0.00001797	1.67E-14	97.2%	8.0049	267.55	± 2.163
0.66	0.61418	± 0.000975	0.06784	± 0.000185	0.00098	± 0.000021	0.00004	± 0.000085	0.0000179	± 0.00002434	1.42E-14	99.1%	8.9760	297.47	± 3.638
0.67	1.80109	± 0.001752	0.18866	± 0.000612	0.00271	± 0.000046	0.00034	± 0.000114	0.0000121	± 0.00001903	4.15E-14	99.8%	9.5280	314.25	± 1.450
0.68	6.81127	± 0.003811	0.64150	± 0.000617	0.00956	± 0.000085	0.00039	± 0.000133	0.0001378	± 0.00001969	1.57E-13	99.4%	10.5543	345.06	± 0.487
0.69	15.05354	± 0.006688	1.29912	± 0.001426	0.01870	± 0.000108	0.00156	± 0.000087	0.0003655	± 0.00002417	3.47E-13	99.3%	11.5045	373.11	± 0.479
0.7	4.53883	± 0.003737	0.39517	± 0.001023	0.00575	± 0.000053	0.00001	± 0.000142	0.0000877	± 0.00002041	1.05E-13	99.4%	11.4200	370.64	± 1.127
0.72	1.77293	± 0.002463	0.16238	± 0.000508	0.00231	± 0.000035	0.00002	± 0.000083	0.0000341	± 0.00001066	4.09E-14	99.4%	10.8565	354.03	± 1.373
0.75	3.61219	± 0.002315	0.32390	± 0.000869	0.00459	± 0.000031	0.00029	± 0.000100	0.0000948	± 0.00000844	8.32E-14	99.2%	11.0657	360.21	± 1.032
0.8	3.62687	± 0.002979	0.33484	± 0.000780	0.00472	± 0.000059	0.00011	± 0.000148	0.0000594	± 0.00001119	8.36E-14	99.5%	10.7793	351.74	± 0.930
0.85	1.62952	± 0.001948	0.15250	± 0.000428	0.00213	± 0.000031	0.00016	± 0.000112	0.0000306	± 0.00001164	3.75E-14	99.4%	10.6261	347.19	± 1.295
0.9	0.64419	± 0.001319	0.06121	± 0.000150	0.00086	± 0.000032	0.00009	± 0.000074	0.0000045	± 0.00000940	1.48E-14	99.8%	10.5026	343.52	± 1.848
KV-1-14 (au27.3f.ksp.100)					SCIH		Time duration		20s						
0.4	0.14487	± 0.000305	0.00074	± 0.000060	0.00005	± 0.000022	-0.00021	± 0.000166	-0.0000258	± 0.00001884	3.34E-15	105.3%	196.7206	2877.64	± 260.724
0.43	0.10167	± 0.000197	0.00129	± 0.000074	0.00007	± 0.000018	-0.00004	± 0.000084	0.0000179	± 0.00001063	2.34E-15	94.8%	74.7869	1648.41	± 113.598
0.46	0.29293	± 0.000286	0.01890	± 0.000110	0.00036	± 0.000027	0.00028	± 0.000096	0.0000226	± 0.00001111	6.75E-15	97.7%	15.1433	476.69	± 6.179
0.49	0.27313	± 0.000255	0.04545	± 0.000263	0.00060	± 0.000024	0.00126	± 0.000196	0.0000237	± 0.00001284	6.29E-15	97.4%	5.8579	199.59	± 3.088
0.52	0.19832	± 0.000223	0.03462	± 0.000093	0.00037	± 0.000036	0.00147	± 0.000091	-0.0000029	± 0.00001038	4.57E-15	100.4%	5.7322	195.54	± 3.075
0.57	0.37513	± 0.000779	0.05298	± 0.000170	0.00068	± 0.000024	0.00335	± 0.000148	0.0000075	± 0.00001227	8.64E-15	99.4%	7.0448	237.48	± 2.481
0.6	1.12295	± 0.001398	0.13314	± 0.000429	0.00174	± 0.000022	0.00351	± 0.000107	0.0000905	± 0.00001309	2.59E-14	97.6%	8.2361	274.72	± 1.372
0.63	0.42299	± 0.000528	0.05867	± 0.000132	0.00072	± 0.000028	0.00108	± 0.000099	0.0000073	± 0.00001246	9.75E-15	99.5%	7.1753	241.60	± 2.204
0.65	0.31091	± 0.000666	0.04288	± 0.000132	0.00059	± 0.000020	0.00066	± 0.000131	0.0000380	± 0.00001540	7.16E-15	96.4%	6.9908	235.77	± 3.695
0.66	0.24376	± 0.000327	0.03353	± 0.000134	0.00048	± 0.000028	0.00072	± 0.000177	0.0000113	± 0.00001191	5.62E-15	98.6%	7.1735	241.54	± 3.682
0.67	3.61561	± 0.003028	0.40170	± 0.000759	0.00539	± 0.000056	0.00337	± 0.000151	0.0001317	± 0.00001188	8.33E-14	98.9%	8.9047	295.29	± 0.682
0.68	8.24702	± 0.003863	0.79410	± 0.001105	0.01144	± 0.000116	0.00323	± 0.000154	0.0003225	± 0.00001456	1.90E-13	98.8%	10.2657	336.45	± 0.530
0.69	8.19872	± 0.009301	0.73262	± 0.000653	0.01022	± 0.000086	0.00136	± 0.000177	0.0002798	± 0.00001204	1.89E-13	99.0%	11.0783	360.58	± 0.549
0.7	1.00113	± 0.000932	0.09005	± 0.000455	0.00125	± 0.000037	0.00016	± 0.000117	0.0000000	± 0.00001236	2.31E-14	100.0%	11.1171	361.73	± 2.279
0.72	1.48026	± 0.001167	0.13869	± 0.000354	0.00181	± 0.000033	0.00022	± 0.000101	0.0000420	± 0.00001411	3.41E-14	99.2%	10.5843	345.95	± 1.354
0.75	1.20200	± 0.001250	0.11843	± 0.000474	0.00160	± 0.000028	0.00023	± 0.000108	0.0000590	± 0.00001957	2.77E-14	98.5%	10.0021	328.55	± 2.115
0.8	1.11237	± 0.000883	0.10990	± 0.000410	0.00146	± 0.000038	0.00044	± 0.000139	0.0000194	± 0.00001260	2.56E-14	99.5%	10.0700	330.59	± 1.687
0.85	0.19759	± 0.000267	0.02000	± 0.000115	0.00024	± 0.000031	0.00002	± 0.000166	-0.0000230	± 0.00001241	4.55E-15	103.4%	9.8788	324.84	± 6.327
0.9	0.49503	± 0.000627	0.04808	± 0.000102	0.00061	± 0.000029	-0.00005	± 0.000106	0.0000227	± 0.00001797	1.14E-14	98.6%	10.1558	333.16	± 3.717
0.95	0.27124	± 0.000776	0.02606	± 0.000147	0.00031	± 0.000021	0.00011	± 0.000124	0.0000088	± 0.00001319	6.25E-15	99.0%	10.3104	337.78	± 5.356

KV-1-14 (au27.3f.ksp.101)				SCIH				Time duration		20s					
p	^{40}Ar(*+atm)		^{39}Ar (K)		^{38}Ar (Cl+atm)		^{37}Ar (Ca)		^{36}Ar (Atm)		Moles ^{40}Ar	%Rad	R	Age(Ma)	
0.49	0.19827	± 0.000240	0.03551	± 0.000139	0.00039	± 0.000033	0.00104	± 0.000102	0.0000166	± 0.00001249	4.57E-15	97.5%	5.4479	186.32	± 3.641
0.52	0.25421	± 0.000445	0.04713	± 0.000167	0.00058	± 0.000029	0.00138	± 0.000127	0.0000185	± 0.00001262	5.86E-15	97.8%	5.2802	180.86	± 2.808
0.55	0.07260	± 0.000256	0.01270	± 0.000069	0.00014	± 0.000022	0.00045	± 0.000126	0.0000315	± 0.00001847	1.67E-15	87.2%	4.9898	171.37	± 14.823
0.57	0.16538	± 0.000283	0.02736	± 0.000122	0.00034	± 0.000026	0.00048	± 0.000164	0.0000133	± 0.00001187	3.81E-15	97.6%	5.9027	201.04	± 4.476
0.6	0.37889	± 0.000590	0.05798	± 0.000287	0.00072	± 0.000025	0.00058	± 0.000166	0.0000109	± 0.00001279	8.73E-15	99.1%	6.4804	219.56	± 2.489
0.62	0.19361	± 0.000349	0.02896	± 0.000137	0.00037	± 0.000029	0.00021	± 0.000094	-0.0000082	± 0.00001238	4.46E-15	101.2%	6.6862	226.12	± 4.423
0.65	0.49147	± 0.000856	0.06956	± 0.000252	0.00092	± 0.000027	0.00039	± 0.000090	-0.0000133	± 0.00001516	1.13E-14	100.8%	7.0659	238.14	± 2.374
0.66	0.15338	± 0.000238	0.02182	± 0.000084	0.00024	± 0.000025	0.00025	± 0.000148	0.0000033	± 0.00002133	3.53E-15	99.4%	6.9873	235.66	± 9.793
0.67	0.18609	± 0.000236	0.02616	± 0.000059	0.00029	± 0.000020	0.00015	± 0.000129	-0.0000096	± 0.00002636	4.29E-15	101.5%	7.1148	239.69	± 10.050
0.68	0.14109	± 0.000179	0.01959	± 0.000085	0.00026	± 0.000016	0.00005	± 0.000095	0.0000212	± 0.00001067	3.25E-15	95.6%	6.8841	232.40	± 5.546
0.69	0.18093	± 0.000211	0.02451	± 0.000085	0.00035	± 0.000018	0.00034	± 0.000119	0.0000077	± 0.00001140	4.17E-15	98.7%	7.2914	245.25	± 4.711
0.7	0.19724	± 0.000257	0.02619	± 0.000122	0.00040	± 0.000020	0.00026	± 0.000103	0.0000054	± 0.00001166	4.54E-15	99.2%	7.4713	250.90	± 4.583
0.72	0.16961	± 0.000180	0.02210	± 0.000107	0.00036	± 0.000020	0.00027	± 0.000125	0.0000250	± 0.00001124	3.91E-15	95.6%	7.3402	246.79	± 5.213
0.75	0.45239	± 0.000915	0.05599	± 0.000224	0.00082	± 0.000027	0.00024	± 0.000062	0.0000277	± 0.00001260	1.04E-14	98.2%	7.9340	265.35	± 2.532
0.8	2.12744	± 0.001310	0.24111	± 0.000699	0.00335	± 0.000036	0.00088	± 0.000075	0.0000821	± 0.00001055	4.90E-14	98.9%	8.7233	289.73	± 0.969
0.85	2.94740	± 0.004252	0.32681	± 0.000674	0.00448	± 0.000027	0.00114	± 0.000191	0.0001123	± 0.00001173	6.79E-14	98.9%	8.9175	295.68	± 0.831
0.9	3.02306	± 0.003014	0.33031	± 0.000787	0.00453	± 0.000045	0.00124	± 0.000136	0.0000650	± 0.00001794	6.97E-14	99.4%	9.0944	301.08	± 0.946
0.93	2.08940	± 0.001216	0.22279	± 0.000590	0.00304	± 0.000035	0.00091	± 0.000115	0.0000624	± 0.00000960	4.81E-14	99.1%	9.2959	307.22	± 0.940
0.95	1.56804	± 0.001021	0.17114	± 0.000414	0.00232	± 0.000039	0.00052	± 0.000094	0.0000211	± 0.00001786	3.61E-14	99.6%	9.1264	302.06	± 1.272
1	0.29491	± 0.000494	0.03168	± 0.000091	0.00044	± 0.000027	0.00043	± 0.000130	0.0000044	± 0.00000961	6.80E-15	99.6%	9.2684	306.38	± 3.136
1.05	0.30656	± 0.000706	0.03163	± 0.000094	0.00041	± 0.000020	0.00031	± 0.000181	0.0000059	± 0.00000940	7.06E-15	99.4%	9.6371	317.55	± 3.135
1.1	0.32220	± 0.000649	0.03508	± 0.000166	0.00049	± 0.000031	0.00016	± 0.000138	0.0000116	± 0.00001099	7.42E-15	98.9%	9.0872	300.86	± 3.440
1.13	0.43398	± 0.000916	0.04553	± 0.000146	0.00068	± 0.000040	0.00017	± 0.000102	0.0000116	± 0.00001001	1.00E-14	99.3%	9.4667	312.40	± 2.953
1.15	0.05841	± 0.000316	0.00667	± 0.000032	0.00011	± 0.000025	0.00047	± 0.000117	0.0000116	± 0.00000244	1.35E-15	98.8%	8.6591	287.76	± 16.316
KV-3-14 (au27.2h.ksp)				SCTF											
n	^{40}Ar(*+atm)		^{39}Ar (K)		^{38}Ar (Cl+atm)		^{37}Ar (Ca)		^{36}Ar (Atm)		Moles ^{40}Ar	%Rad	R	Age(Ma)	
1	77.16049	± 0.125190	7.00177	± 0.021330	0.09175	± 0.000578	0.08972	± 0.001063	0.0016271	± 0.00009288	5.93E-13	99.4%	10.9528	356.87	± 1.246
2	14.99321	± 0.011646	1.45380	± 0.001566	0.01905	± 0.000148	0.01512	± 0.000162	0.0002923	± 0.00001719	3.45E-13	99.4%	10.2548	336.12	± 0.463
3	15.41017	± 0.023585	1.45866	± 0.002171	0.01886	± 0.000156	0.01844	± 0.000125	0.0003872	± 0.00002199	3.55E-13	99.3%	10.4874	343.07	± 0.752
4	21.62376	± 0.041478	1.96436	± 0.002735	0.02543	± 0.000158	0.01961	± 0.000146	0.0005297	± 0.00001962	4.98E-13	99.3%	10.9294	356.18	± 0.856
KV-3-14 (au27.2h.ksp.110)				SCIH				Time duration		20s					
p	^{40}Ar(*+atm)		^{39}Ar (K)		^{38}Ar (Cl+atm)		^{37}Ar (Ca)		^{36}Ar (Atm)		Moles ^{40}Ar	%Rad	R	Age(Ma)	
0.45	1.43383	± 0.001329	0.00200	± 0.000076	0.00030	± 0.000024	0.00014	± 0.000136	0.0001669	± 0.00002598	3.30E-14	96.6%	690.6548	4860.47	± 191.894
0.47	0.33083	± 0.000241	0.00231	± 0.000095	0.00011	± 0.000032	0.00045	± 0.000219	0.0000982	± 0.00002092	7.62E-15	91.2%	130.8855	2317.86	± 115.253
0.49	0.52828	± 0.000981	0.01092	± 0.000072	0.00023	± 0.000024	0.00126	± 0.000110	0.0000620	± 0.00002685	1.22E-14	96.5%	46.7271	1189.19	± 20.324
0.51	0.09628	± 0.000261	0.00561	± 0.000042	0.00007	± 0.000026	0.00117	± 0.000121	0.0000699	± 0.00002021	2.22E-15	78.6%	13.5002	430.65	± 34.238
0.53	0.30507	± 0.000416	0.02156	± 0.000086	0.00032	± 0.000023	0.00678	± 0.000178	0.0000401	± 0.00002422	7.03E-15	96.1%	13.6311	434.36	± 10.746
0.55	0.50509	± 0.001065	0.05214	± 0.000164	0.00070	± 0.000031	0.01989	± 0.000183	0.0001055	± 0.00002070	1.16E-14	93.8%	9.1279	302.10	± 4.069
0.58	1.26466	± 0.001119	0.14888	± 0.000482	0.00195	± 0.000040	0.04458	± 0.000495	0.0000519	± 0.00001113	2.91E-14	98.8%	8.4210	280.43	± 1.201
0.6	1.55389	± 0.001623	0.19586	± 0.000454	0.00254	± 0.000038	0.00987	± 0.000217	0.0000534	± 0.00001222	3.58E-14	99.0%	7.8581	262.99	± 0.914
0.63	2.04670	± 0.001996	0.24469	± 0.000637	0.00321	± 0.000034	0.00785	± 0.000252	0.0000385	± 0.00001154	4.72E-14	99.4%	8.3211	277.35	± 0.904
0.66	1.19066	± 0.001339	0.15499	± 0.000313	0.00199	± 0.000028	0.00529	± 0.000100	0.0000392	± 0.00001089	2.74E-14	99.0%	7.6109	255.27	± 0.917
0.68	1.67215	± 0.001614	0.20880	± 0.000531	0.00271	± 0.000044	0.00873	± 0.000192	0.0000521	± 0.00001328	3.85E-14	99.1%	7.9390	265.50	± 0.963
0.7	1.63337	± 0.000966	0.20138	± 0.000473	0.00258	± 0.000040	0.00816	± 0.000318	0.0000168	± 0.00001395	3.76E-14	99.7%	8.0902	270.20	± 0.947
0.73	2.37177	± 0.001309	0.26843	± 0.000416	0.00352	± 0.000031	0.01027	± 0.000247	0.0000409	± 0.00001364	5.47E-14	99.5%	8.7944	291.91	± 0.694
0.75	3.75359	± 0.001983	0.37557	± 0.000543	0.00524	± 0.000081	0.01158	± 0.000145	0.0000604	± 0.00001233	8.65E-14	99.5%	9.9501	326.99	± 0.597
0.78	4.31414	± 0.002988	0.41409	± 0.000828	0.00553	± 0.000042	0.01023	± 0.000144	0.0000820	± 0.00001343	9.94E-14	99.4%	10.3623	339.33	± 0.787
0.8	5.75080	± 0.005009	0.53871	± 0.001485	0.00718	± 0.000052	0.01105	± 0.000230	0.0000865	± 0.00001387	1.33E-13	99.6%	10.6298	347.30	± 1.038
0.84	9.47452	± 0.008540	0.83758	± 0.001101	0.01116	± 0.000055	0.01018	± 0.000158	0.0001179	± 0.00001136	2.18E-13	99.6%	11.2715	366.27	± 0.600
0.88	7.40226	± 0.008276	0.68825	± 0.001276	0.00914	± 0.000055	0.00675	± 0.000315	0.0000526	± 0.00001251	1.71E-13	99.8%	10.7335	350.38	± 0.780
0.93	2.93999	± 0.002210	0.27807	± 0.000745	0.00362	± 0.000051	0.00256	± 0.000089	0.0000142	± 0.00001060	6.77E-14	99.9%	10.5586	345.18	± 1.030
0.98	1.78478	± 0.001698	0.17716	± 0.000387	0.00230	± 0.000021	0.00150	± 0.000150	0.0000090	± 0.00001871	4.11E-14	99.9%	10.0604	330.30	± 1.293
1.03	2.09617	± 0.002938	0.20126	± 0.000609	0.00259	± 0.000040	0.00170	± 0.000093	0.0000174	± 0.00001808	4.83E-14	99.8%	10.3903	340.17	± 1.431
1.08	2.25304	± 0.001903	0.22303	± 0.000310	0.00290	± 0.000036	0.00230	± 0.000168	0.0000723	± 0.00002141	5.19E-14	99.1%	10.0073	328.70	± 1.077
1.15	2.97794	± 0.001669	0.29095	± 0.000440	0.00371	± 0.000041	0.00414	± 0.000122	0.0000739	± 0.00002060	6.86E-14	99.3%	10.1615	333.33	± 0.874
1.25	0.77814	± 0.001070	0.07574	± 0.000192	0.00099	± 0.000036	0.00140	± 0.000183	0.0000802	± 0.00001937	1.79E-14	97.0%	9.9635	327.39	± 2.668

KV-3-14 (au27.2h.ksp.115)		SCIH		Time duration	20s				
p	^{40}Ar(*+atm)	^{39}Ar (K)	^{38}Ar (Cl+atm)	^{37}Ar (Ca)	^{36}Ar (Atm)	Moles^{40}Ar	%Rad	R	Age(Ma)
0.5	1.70362 ± 0.001289	0.03773 ± 0.000144	0.00055 ± 0.000034	0.00054 ± 0.000086	0.0002837 ± 0.00002010	3.93E-14	95.1%	42.9272	1116.95 ± 6.134
0.6	3.76399 ± 0.003983	0.51464 ± 0.000737	0.00661 ± 0.000059	0.01054 ± 0.000207	0.0002673 ± 0.00001482	8.67E-14	97.9%	7.1623	241.19 ± 0.524
0.7	9.93492 ± 0.007893	1.37385 ± 0.001438	0.01745 ± 0.000098	0.00883 ± 0.000261	0.0005058 ± 0.00001549	2.29E-13	98.5%	7.1233	239.96 ± 0.339
0.75	8.06639 ± 0.006581	1.08906 ± 0.002055	0.01400 ± 0.000054	0.00634 ± 0.000260	0.0001517 ± 0.00001480	1.86E-13	99.4%	7.3661	247.60 ± 0.529
0.79	13.91384 ± 0.004724	1.67609 ± 0.001127	0.02180 ± 0.000111	0.01079 ± 0.000174	0.0004390 ± 0.00002093	3.21E-13	99.1%	8.2246	274.36 ± 0.242
0.83	8.47183 ± 0.007121	1.01950 ± 0.002114	0.01308 ± 0.000074	0.00591 ± 0.000168	0.0003533 ± 0.00001442	1.95E-13	98.8%	8.2080	273.85 ± 0.636
0.87	5.46595 ± 0.005699	0.65913 ± 0.001289	0.00849 ± 0.000045	0.00394 ± 0.000114	0.0001991 ± 0.00001252	1.26E-13	98.9%	8.2040	273.73 ± 0.641
0.91	7.59046 ± 0.003581	0.90727 ± 0.001949	0.01145 ± 0.000077	0.00515 ± 0.000153	0.0002070 ± 0.00001203	1.75E-13	99.2%	8.2994	276.68 ± 0.627
0.94	2.03110 ± 0.001740	0.24289 ± 0.000735	0.00311 ± 0.000033	0.00112 ± 0.000134	0.0000488 ± 0.00001160	4.68E-14	99.3%	8.3034	276.80 ± 0.995
0.96	3.64609 ± 0.001900	0.43142 ± 0.000660	0.00556 ± 0.000057	0.00239 ± 0.000145	0.0000663 ± 0.00001310	8.40E-14	99.5%	8.4064	279.98 ± 0.544
0.98	1.64928 ± 0.001462	0.19442 ± 0.000252	0.00244 ± 0.000039	0.00085 ± 0.000076	0.0000229 ± 0.00001019	3.80E-14	99.6%	8.4487	281.28 ± 0.680
1.01	1.10035 ± 0.001044	0.12973 ± 0.000318	0.00165 ± 0.000041	0.00071 ± 0.000126	0.0000125 ± 0.00001084	2.54E-14	99.7%	8.4542	281.45 ± 1.107
1.05	0.74549 ± 0.001337	0.08784 ± 0.000273	0.00112 ± 0.000028	0.00049 ± 0.000120	0.0000169 ± 0.00001462	1.72E-14	99.3%	8.4304	280.72 ± 1.926
1.1	0.42758 ± 0.000984	0.05078 ± 0.000112	0.00069 ± 0.000026	0.00039 ± 0.000141	0.0000019 ± 0.00001369	9.85E-15	99.9%	8.4100	280.09 ± 2.799
1.15	1.15651 ± 0.001398	0.13615 ± 0.000293	0.00178 ± 0.000038	0.00054 ± 0.000101	0.0000278 ± 0.00001529	2.66E-14	99.3%	8.4344	280.85 ± 1.307
1.2	0.65167 ± 0.000926	0.07756 ± 0.000325	0.00107 ± 0.000024	0.00046 ± 0.000132	0.0000045 ± 0.00001949	1.50E-14	99.8%	8.3857	279.34 ± 2.766
1.25	0.97110 ± 0.001157	0.11411 ± 0.000325	0.00148 ± 0.000036	0.00053 ± 0.000097	0.0000171 ± 0.00000972	2.24E-14	99.5%	8.4664	281.83 ± 1.212
1.3	1.50682 ± 0.001550	0.17758 ± 0.000512	0.00232 ± 0.000040	0.00052 ± 0.000154	0.0000116 ± 0.00001160	3.47E-14	99.8%	8.4662	281.82 ± 1.077
1.36	1.49362 ± 0.001360	0.17582 ± 0.000263	0.00227 ± 0.000043	0.00075 ± 0.000141	0.0000146 ± 0.00001158	3.44E-14	99.7%	8.4710	281.97 ± 0.816
1.42	1.06749 ± 0.001248	0.12473 ± 0.000513	0.00159 ± 0.000038	0.00039 ± 0.000150	0.0000260 ± 0.00001175	2.46E-14	99.3%	8.4973	282.78 ± 1.530
1.5	0.43893 ± 0.001221	0.05052 ± 0.000153	0.00066 ± 0.000027	0.00018 ± 0.000100	0.0000233 ± 0.00001015	1.01E-14	98.4%	8.5529	284.49 ± 2.305
1.6	1.42483 ± 0.001124	0.16562 ± 0.000307	0.00216 ± 0.000031	0.00045 ± 0.000103	0.0000064 ± 0.00001120	3.28E-14	99.9%	8.5917	285.69 ± 0.879
KV-3-14 (au27.2h.ksp.116)		SCIH		Time duration	20s				
0.5	3.21619 ± 0.002066	0.00467 ± 0.000087	0.00046 ± 0.000014	0.00025 ± 0.000111	0.0003565 ± 0.00001930	7.41E-14	96.7%	666.0513	4799.53 ± 93.372
0.6	5.12021 ± 0.003179	0.17280 ± 0.000363	0.00285 ± 0.000028	0.00316 ± 0.000089	0.0004615 ± 0.00001045	1.18E-13	97.3%	28.8442	820.71 ± 1.914
0.7	4.19444 ± 0.002694	0.54758 ± 0.000590	0.00770 ± 0.000040	0.00884 ± 0.000179	0.0000879 ± 0.00001177	9.67E-14	99.4%	7.6140	255.37 ± 0.386
0.8	6.64789 ± 0.002818	0.81001 ± 0.000835	0.01064 ± 0.000064	0.00974 ± 0.000458	0.0001603 ± 0.00000988	1.53E-13	99.3%	8.1498	272.05 ± 0.328
0.85	4.61736 ± 0.002647	0.56486 ± 0.000983	0.00735 ± 0.000062	0.00528 ± 0.000128	0.0000947 ± 0.00001030	1.06E-13	99.4%	8.1257	271.30 ± 0.532
0.89	3.86522 ± 0.002616	0.48094 ± 0.000893	0.00615 ± 0.000032	0.00609 ± 0.000204	0.0000936 ± 0.00001008	8.91E-14	99.3%	7.9805	266.79 ± 0.570
0.92	4.24871 ± 0.003613	0.48842 ± 0.001191	0.00633 ± 0.000059	0.00747 ± 0.000174	0.0000555 ± 0.00001593	9.79E-14	99.6%	8.6668	288.00 ± 0.813
0.95	5.07075 ± 0.003210	0.53636 ± 0.000670	0.00707 ± 0.000042	0.00853 ± 0.000215	0.0001115 ± 0.00001035	1.17E-13	99.4%	9.3941	310.20 ± 0.476
0.97	11.79418 ± 0.010486	1.16873 ± 0.000616	0.01540 ± 0.000101	0.01311 ± 0.000272	0.0001418 ± 0.00003637	2.72E-13	99.6%	10.0567	330.19 ± 0.457
0.98	4.03741 ± 0.002224	0.38411 ± 0.000586	0.00509 ± 0.000042	0.00304 ± 0.000140	0.0000650 ± 0.00001558	9.30E-14	99.5%	10.4619	342.30 ± 0.682
1	5.34017 ± 0.004869	0.50807 ± 0.000660	0.00665 ± 0.000039	0.00424 ± 0.000120	0.0000748 ± 0.00002407	1.23E-13	99.6%	10.4681	342.49 ± 0.712
1.02	7.07779 ± 0.006452	0.65635 ± 0.000461	0.00865 ± 0.000047	0.00464 ± 0.000250	0.0000886 ± 0.00001403	1.63E-13	99.6%	10.7444	350.70 ± 0.454
1.04	18.80142 ± 0.014470	1.70822 ± 0.001399	0.02226 ± 0.000118	0.01151 ± 0.000142	0.0002397 ± 0.00001827	4.33E-13	99.6%	10.9657	357.26 ± 0.416
1.06	10.17327 ± 0.012290	0.93965 ± 0.001057	0.01249 ± 0.000100	0.00679 ± 0.000327	0.0001036 ± 0.00001214	2.34E-13	99.7%	10.7948	352.20 ± 0.596
1.1	3.24507 ± 0.002996	0.30601 ± 0.000734	0.00395 ± 0.000046	0.00292 ± 0.000137	0.0000338 ± 0.00001146	7.48E-14	99.7%	10.5727	345.60 ± 0.961
1.15	6.49284 ± 0.002722	0.62531 ± 0.001363	0.00806 ± 0.000055	0.00592 ± 0.000213	0.0000502 ± 0.00001313	1.50E-13	99.8%	10.3606	339.28 ± 0.781
1.2	1.71768 ± 0.002286	0.17052 ± 0.000329	0.00219 ± 0.000050	0.00094 ± 0.000138	0.0000080 ± 0.00001095	3.96E-14	99.9%	10.0599	330.28 ± 0.995
1.25	2.36580 ± 0.001252	0.23258 ± 0.000507	0.00297 ± 0.000043	0.00191 ± 0.000101	0.0000242 ± 0.00001337	5.45E-14	99.7%	10.1422	332.75 ± 0.933
1.3	0.87222 ± 0.000832	0.08592 ± 0.000341	0.00112 ± 0.000039	0.00037 ± 0.000140	0.0000033 ± 0.00001249	2.01E-14	99.9%	10.1405	332.70 ± 1.959
1.35	0.18144 ± 0.000347	0.01561 ± 0.000089	0.00015 ± 0.000046	0.00018 ± 0.000125	0.0000140 ± 0.00001245	4.18E-15	97.7%	11.3570	368.79 ± 7.976
1.4	0.58346 ± 0.001042	0.05815 ± 0.000114	0.00072 ± 0.000018	0.00051 ± 0.000100	0.0000018 ± 0.00001675	1.34E-14	99.9%	10.0263	329.28 ± 2.929
1.5	4.98068 ± 0.001774	0.51415 ± 0.000682	0.00657 ± 0.000039	0.00295 ± 0.000238	0.0000330 ± 0.00001030	1.15E-13	99.8%	9.6688	318.51 ± 0.480
1.6	2.51968 ± 0.002004	0.26063 ± 0.000591	0.00345 ± 0.000088	0.00119 ± 0.000134	0.0000229 ± 0.00000987	5.81E-14	99.7%	9.6420	317.70 ± 0.850
1.7	1.67111 ± 0.001490	0.16661 ± 0.000382	0.00214 ± 0.000032	0.00121 ± 0.000098	0.0000765 ± 0.00001994	3.85E-14	98.6%	9.8951	325.33 ± 1.417
1.8	0.93217 ± 0.000773	0.09542 ± 0.000482	0.00120 ± 0.000035	0.00044 ± 0.000152	0.0000088 ± 0.00001130	2.15E-14	99.7%	9.7421	320.72 ± 2.009
1.9	1.45154 ± 0.001433	0.14990 ± 0.000377	0.00189 ± 0.000027	0.00059 ± 0.000131	0.0000217 ± 0.00000870	3.34E-14	99.6%	9.6410	317.67 ± 1.031
2	0.42663 ± 0.000608	0.04167 ± 0.000157	0.00042 ± 0.000034	0.00039 ± 0.000167	0.0000097 ± 0.00000956	9.83E-15	99.3%	10.1707	333.61 ± 2.602
2.1	0.14914 ± 0.000398	0.01349 ± 0.000114	0.00017 ± 0.000023	0.00023 ± 0.000100	0.0000019 ± 0.00002133	3.44E-15	99.6%	11.0175	358.79 ± 15.551

KV-3-14 (au27.2h.ksp.118)		SCIH		Time duration	20s				
p	^{40}Ar(*+atm)	^{39}Ar (K)	^{38}Ar (Cl+atm)	^{37}Ar (Ca)	^{36}Ar (Atm)	Moles^{40}Ar	%Rad	R	Age(Ma)
0.5	3.60914 ± 0.002137	0.00905 ± 0.000198	0.00107 ± 0.000028	0.00073 ± 0.000087	0.0003464 ± 0.00001781	8.32E-14	97.2%	387.5394	3910.98 ± 88.119
0.6	2.89309 ± 0.001941	0.14070 ± 0.000557	0.00247 ± 0.000054	0.00853 ± 0.000102	0.0002968 ± 0.00001735	6.67E-14	97.0%	19.9452	604.86 ± 2.739
0.7	3.10464 ± 0.002190	0.38837 ± 0.000261	0.00518 ± 0.000069	0.01967 ± 0.000139	0.0001521 ± 0.00002637	7.15E-14	98.6%	7.8832	263.77 ± 0.720
0.8	3.27577 ± 0.002577	0.40357 ± 0.000508	0.00532 ± 0.000041	0.00739 ± 0.000196	0.0000964 ± 0.00001963	7.55E-14	99.1%	8.0482	268.90 ± 0.627
0.85	3.07822 ± 0.002376	0.37850 ± 0.000586	0.00494 ± 0.000056	0.00555 ± 0.000153	0.0000512 ± 0.00001411	7.09E-14	99.5%	8.0941	270.32 ± 0.597
0.89	3.37103 ± 0.003190	0.40563 ± 0.000468	0.00531 ± 0.000038	0.00608 ± 0.000143	0.0000208 ± 0.00002632	7.77E-14	99.8%	8.2970	276.60 ± 0.761
0.92	3.56290 ± 0.002198	0.42792 ± 0.001065	0.00556 ± 0.000061	0.00732 ± 0.000147	0.0000452 ± 0.00001118	8.21E-14	99.6%	8.2965	276.59 ± 0.757
0.95	4.25778 ± 0.005038	0.50483 ± 0.001082	0.00663 ± 0.000055	0.00803 ± 0.000245	0.0000633 ± 0.00001267	9.81E-14	99.6%	8.3986	279.74 ± 0.731
0.97	5.11118 ± 0.003556	0.60602 ± 0.000927	0.00797 ± 0.000052	0.01066 ± 0.000275	0.0000641 ± 0.00001042	1.18E-13	99.6%	8.4045	279.92 ± 0.501
1	5.78225 ± 0.003078	0.66328 ± 0.001493	0.00881 ± 0.000064	0.01120 ± 0.000200	0.0000645 ± 0.00001372	1.33E-13	99.7%	8.6906	288.73 ± 0.700
1.05	15.07729 ± 0.008625	1.50123 ± 0.002580	0.02015 ± 0.000062	0.02452 ± 0.000260	0.0002157 ± 0.00001563	3.47E-13	99.6%	10.0024	328.56 ± 0.606
1.15	14.15754 ± 0.005487	1.39450 ± 0.001928	0.01840 ± 0.000145	0.01828 ± 0.000254	0.0002358 ± 0.00001973	3.26E-13	99.5%	10.1037	331.60 ± 0.498
1.21	5.81964 ± 0.006734	0.58366 ± 0.001333	0.00766 ± 0.000045	0.00567 ± 0.000146	0.0000889 ± 0.00001266	1.34E-13	99.5%	9.9270	326.29 ± 0.865
1.28	6.04278 ± 0.006003	0.60536 ± 0.000815	0.00791 ± 0.000061	0.00512 ± 0.000197	0.0001140 ± 0.00001266	1.39E-13	99.4%	9.9274	326.30 ± 0.585
1.36	4.33167 ± 0.002011	0.43377 ± 0.000691	0.00564 ± 0.000063	0.00330 ± 0.000162	0.0000162 ± 0.00002084	9.98E-14	99.9%	9.9757	327.76 ± 0.717
1.45	2.37570 ± 0.002685	0.24437 ± 0.000629	0.00313 ± 0.000027	0.00141 ± 0.000064	0.0000101 ± 0.00001077	5.47E-14	99.9%	9.7100	319.76 ± 0.997
1.55	3.26980 ± 0.003381	0.32920 ± 0.000864	0.00432 ± 0.000059	0.00273 ± 0.000130	0.0000344 ± 0.00001115	7.53E-14	99.7%	9.9024	325.55 ± 0.978
1.65	3.62286 ± 0.001739	0.34730 ± 0.000557	0.00462 ± 0.000057	0.00326 ± 0.000174	0.0000506 ± 0.00001326	8.35E-14	99.6%	10.3894	340.14 ± 0.680
1.75	4.07938 ± 0.002616	0.39964 ± 0.000779	0.00530 ± 0.000052	0.00473 ± 0.000139	0.0000712 ± 0.00001286	9.40E-14	99.5%	10.1562	333.17 ± 0.754
1.85	2.37388 ± 0.001815	0.24102 ± 0.000269	0.00317 ± 0.000034	0.00330 ± 0.000185	0.0000292 ± 0.00000958	5.47E-14	99.6%	9.8147	322.91 ± 0.584
1.95	4.81300 ± 0.003831	0.48554 ± 0.000836	0.00638 ± 0.000042	0.00635 ± 0.000232	0.0000173 ± 0.00001628	1.11E-13	99.9%	9.9035	325.59 ± 0.699
2.05	3.01060 ± 0.002931	0.30466 ± 0.000546	0.00398 ± 0.000048	0.00301 ± 0.000116	0.0000220 ± 0.00001142	6.94E-14	99.8%	9.8614	324.32 ± 0.756
2.15	0.37337 ± 0.000628	0.03456 ± 0.000085	0.00046 ± 0.000028	0.00058 ± 0.000091	0.0000103 ± 0.00001310	8.60E-15	99.2%	10.7172	349.90 ± 3.806
2.25	0.21422 ± 0.000337	0.01897 ± 0.000139	0.00024 ± 0.000023	0.00019 ± 0.000121	0.0000092 ± 0.00001488	4.94E-15	98.7%	11.1493	362.68 ± 8.025
KV-8-14 (au27.1o.ksp.70)		**SCIH**		**Time duration**	30s;10s (only the last step)				
0.6	4.79502 ± 0.002974	0.44981 ± 0.000715	0.00644 ± 0.000031	0.02629 ± 0.001341	0.0001479 ± 0.00000656	1.10E-13	99.1%	10.5629	345.14 ± 0.611
0.8	7.85105 ± 0.006263	0.83476 ± 0.001134	0.01139 ± 0.000139	0.08819 ± 0.001196	0.0000651 ± 0.00000660	1.81E-13	99.8%	9.3823	309.68 ± 0.495
1	12.50709 ± 0.005305	1.09540 ± 0.001673	0.01488 ± 0.000089	0.07499 ± 0.001047	0.0002013 ± 0.00001038	2.88E-13	99.5%	11.3636	368.79 ± 0.594
1.6	7.69481 ± 0.005905	0.65480 ± 0.001251	0.00893 ± 0.000048	0.03735 ± 0.001639	0.0001362 ± 0.00001403	1.77E-13	99.5%	11.6899	378.35 ± 0.809
2	1.67443 ± 0.001902	0.15706 ± 0.000368	0.00206 ± 0.000028	0.00098 ± 0.001165	0.0000101 ± 0.00000617	3.86E-14	99.8%	10.6419	347.49 ± 0.983
KV-8-14 (au27.1o.ksp.71)		**SCIH**		**Time duration**	30s;10s (only the last step)				
0.5	0.52835 ± 0.000371	0.03419 ± 0.000269	0.00059 ± 0.000030	0.01068 ± 0.001267	0.0000496 ± 0.00000770	1.22E-14	97.2%	15.0245	473.17 ± 4.382
0.7	1.23056 ± 0.001813	0.13607 ± 0.000467	0.00183 ± 0.000024	0.08020 ± 0.001852	0.0000548 ± 0.00000722	2.84E-14	98.7%	8.9251	295.76 ± 1.234
0.8	0.49177 ± 0.000301	0.05014 ± 0.000201	0.00068 ± 0.000020	0.06933 ± 0.001511	0.0000365 ± 0.00000725	1.13E-14	97.8%	9.5939	316.09 ± 1.924
1	1.42855 ± 0.001082	0.09726 ± 0.000258	0.00146 ± 0.000023	0.09006 ± 0.002005	0.0000745 ± 0.00000806	3.29E-14	98.5%	14.4632	457.55 ± 1.496
2	1.85878 ± 0.001680	0.04686 ± 0.000225	0.00106 ± 0.000030	0.09501 ± 0.002925	0.0001196 ± 0.00000824	4.28E-14	98.1%	38.9114	1036.88 ± 5.340
KV-8-14 (au27.1o.ksp.72)		**SCIH**		**Time duration**	30s;10s (only the last step)				
0.5	0.20050 ± 0.000698	0.00569 ± 0.000101	0.00013 ± 0.000018	0.00004 ± 0.001059	0.0000171 ± 0.00000609	4.62E-15	97.5%	34.3320	941.59 ± 19.462
0.7	2.28513 ± 0.002222	0.27786 ± 0.000623	0.00358 ± 0.000032	0.01905 ± 0.001205	0.0000357 ± 0.00000553	5.27E-14	99.5%	8.1862	273.04 ± 0.699
0.8	3.21892 ± 0.003345	0.36012 ± 0.000540	0.00463 ± 0.000042	0.03338 ± 0.001231	0.0000193 ± 0.00000679	7.42E-14	99.8%	8.9227	295.69 ± 0.571
1	4.94672 ± 0.002729	0.50110 ± 0.000913	0.00654 ± 0.000051	0.05681 ± 0.001729	0.0000126 ± 0.00001088	1.14E-13	99.9%	9.8644	324.25 ± 0.653
2	12.33040 ± 0.005230	1.09794 ± 0.001243	0.01462 ± 0.000105	0.09892 ± 0.001676	0.0001744 ± 0.00000906	2.84E-13	99.6%	11.1837	363.51 ± 0.448
KV-8-14 (au27.1o.ksp.73)		**SCIH**		**Time duration**	30s;10s (only the last step)				
0.5	0.66194 ± 0.000857	0.01894 ± 0.000148	0.00037 ± 0.000024	0.00453 ± 0.001219	0.0000668 ± 0.00000560	1.53E-14	97.0%	33.9078	932.50 ± 7.970
0.7	3.93965 ± 0.002694	0.41832 ± 0.000899	0.00548 ± 0.000044	0.06362 ± 0.001600	0.0000587 ± 0.00000758	9.08E-14	99.6%	9.3764	309.50 ± 0.723
0.8	1.45377 ± 0.000892	0.15207 ± 0.000396	0.00197 ± 0.000027	0.02818 ± 0.001680	-0.0000035 ± 0.00001062	3.35E-14	100.1%	9.5601	315.07 ± 1.084
1	7.28185 ± 0.006648	0.68442 ± 0.001391	0.00913 ± 0.000066	0.12096 ± 0.001996	0.0000809 ± 0.00001205	1.68E-13	99.7%	10.6047	346.38 ± 0.793
2	14.02626 ± 0.008296	1.07577 ± 0.001231	0.01433 ± 0.000066	0.09649 ± 0.001188	0.0002864 ± 0.00000945	3.23E-13	99.4%	12.9597	415.05 ± 0.544
KV-8-14 (au27.1o.ksp.76)		**SCIH**		**Time duration**	30s;10s (only the last step)				
0.5	1.58070 ± 0.001967	0.05291 ± 0.000134	0.00130 ± 0.000023	0.00887 ± 0.001327	0.0001548 ± 0.00000689	3.64E-14	97.1%	29.0112	824.16 ± 2.640
0.7	4.79399 ± 0.003192	0.52281 ± 0.000939	0.00723 ± 0.000052	0.10166 ± 0.002387	0.0001005 ± 0.00000588	1.10E-13	99.4%	9.1130	301.50 ± 0.592
0.8	2.77271 ± 0.001516	0.28428 ± 0.000783	0.00402 ± 0.000034	0.10553 ± 0.001301	0.0000181 ± 0.00001233	6.39E-14	99.8%	9.7350	320.35 ± 0.995
1	7.85648 ± 0.006102	0.61655 ± 0.001206	0.00940 ± 0.000111	0.13304 ± 0.001813	0.0002132 ± 0.00000765	1.81E-13	99.2%	12.6407	405.90 ± 0.869
2	7.04906 ± 0.008250	0.40044 ± 0.000931	0.00616 ± 0.000044	0.11732 ± 0.001878	0.0002768 ± 0.00000857	1.62E-13	98.8%	17.3994	537.79 ± 1.430

KV-8-14 (au27.1o.ksp.77)					SCIH		Time duration		30s;10s (only the last step)						
p	^{40}Ar(*+atm)		^{39}Ar (K)		^{38}Ar (Cl+atm)		^{37}Ar (Ca)		^{36}Ar (Atm)		Moles^{40}Ar	%Rad	R	Age(Ma)	
0.5	0.63361	± 0.000845	0.02116	± 0.000160	0.00058	± 0.000024	0.00766	± 0.001095	0.0001101	± 0.00000714	1.46E-14	94.9%	28.4089	810.37	± 7.160
0.7	1.94704	± 0.002271	0.21443	± 0.000472	0.00312	± 0.000021	0.11691	± 0.005457	0.0001046	± 0.00000595	4.49E-14	98.4%	8.9364	296.11	± 0.798
0.8	0.90079	± 0.001520	0.09190	± 0.000354	0.00144	± 0.000035	0.12223	± 0.002073	0.0000739	± 0.00000593	2.08E-14	97.6%	9.5652	315.22	± 1.496
1	2.01660	± 0.002014	0.13335	± 0.000382	0.00240	± 0.000036	0.10850	± 0.002161	0.0001083	± 0.00000747	4.65E-14	98.4%	14.8830	469.25	± 1.539
2	3.37943	± 0.002306	0.07822	± 0.000164	0.00239	± 0.000033	0.18051	± 0.002320	0.0002863	± 0.00001062	7.79E-14	97.5%	42.1278	1100.92	± 2.699
KV-8-14 (au27.1o.ksp.78)					SCIH		Time duration		30s;10s (only the last step)						
0.5	1.32619	± 0.002007	0.07812	± 0.000219	0.00121	± 0.000031	0.00559	± 0.000915	0.0001023	± 0.00000712	3.06E-14	97.7%	16.5904	516.04	± 1.879
0.7	5.62896	± 0.004650	0.62437	± 0.001270	0.00812	± 0.000086	0.07804	± 0.001251	0.0000520	± 0.00001232	1.30E-13	99.7%	8.9910	297.78	± 0.684
0.8	3.45983	± 0.001637	0.34154	± 0.000705	0.00450	± 0.000036	0.06231	± 0.001935	0.0000450	± 0.00000689	7.97E-14	99.6%	10.0913	331.06	± 0.731
1	10.65492	± 0.005658	0.89151	± 0.001659	0.01235	± 0.000115	0.06034	± 0.002181	0.0002512	± 0.00001293	2.46E-13	99.3%	11.8684	383.55	± 0.760
2	5.91800	± 0.004359	0.48657	± 0.000713	0.00645	± 0.000051	0.01939	± 0.001769	0.0001022	± 0.00001374	1.36E-13	99.5%	12.1006	390.30	± 0.697
KV-8-14 (au27.1o.ksp.79)					SCIH		Time duration		30s;10s (only the last step)						
0.5	0.37921	± 0.000516	0.01861	± 0.000177	0.00040	± 0.000017	0.00567	± 0.001208	0.0000628	± 0.00000600	8.74E-15	95.1%	19.3755	589.85	± 6.641
0.7	0.69289	± 0.000980	0.08006	± 0.000254	0.00112	± 0.000034	0.05846	± 0.001147	0.0000488	± 0.00000683	1.60E-14	97.9%	8.4757	281.97	± 1.304
0.8	0.32890	± 0.000489	0.02938	± 0.000199	0.00044	± 0.000019	0.05418	± 0.002324	0.0000282	± 0.00000631	7.58E-15	97.5%	10.9135	355.53	± 3.268
1	2.09488	± 0.001872	0.05831	± 0.000153	0.00161	± 0.000031	0.10045	± 0.001813	0.0001703	± 0.00000651	4.83E-14	97.6%	35.0677	957.24	± 2.860
2	0.38462	± 0.000417	0.00353	± 0.000081	0.00022	± 0.000021	0.00871	± 0.000837	0.0000252	± 0.00000636	8.86E-15	98.1%	106.8799	2060.43	± 49.617
KV-8-14 (au27.1o.ksp.80)					SCIH		Time duration		30s;10s (only the last step)						
0.5	0.51809	± 0.000816	0.02539	± 0.000106	0.00051	± 0.000026	0.00782	± 0.000939	0.0000614	± 0.00000626	1.19E-14	96.5%	19.6879	597.94	± 3.536
0.7	1.69391	± 0.001376	0.13406	± 0.000339	0.00228	± 0.000045	0.12407	± 0.001831	0.0001374	± 0.00000683	3.90E-14	97.6%	12.3338	397.05	± 1.184
0.8	0.95345	± 0.001229	0.06924	± 0.000141	0.00123	± 0.000022	0.09833	± 0.001602	0.0000711	± 0.00000672	2.20E-14	97.8%	13.4683	429.54	± 1.399
1	2.79681	± 0.001976	0.06426	± 0.000156	0.00141	± 0.000029	0.08391	± 0.001539	0.0001294	± 0.00001441	6.44E-14	98.6%	42.9292	1116.53	± 3.342
2	0.83569	± 0.001364	0.01162	± 0.000126	0.00032	± 0.000023	0.04273	± 0.002220	0.0000278	± 0.00001139	1.93E-14	99.0%	71.2336	1595.74	± 18.855
KV-8-14 (au27.1o.ksp.81)					SCIH		Time duration		30s;10s (only the last step)						
0.5	0.15110	± 0.000493	0.00807	± 0.000117	0.00020	± 0.000015	0.00216	± 0.001002	0.0000230	± 0.00000720	3.48E-15	95.5%	17.8771	550.51	± 11.787
0.7	1.04048	± 0.000590	0.10908	± 0.000509	0.00154	± 0.000028	0.03211	± 0.001889	0.0000403	± 0.00000743	2.40E-14	98.9%	9.4301	311.13	± 1.622
0.8	0.65574	± 0.001550	0.06553	± 0.000135	0.00094	± 0.000020	0.04072	± 0.001287	0.0001748	± 0.00000836	1.51E-14	92.1%	9.2196	304.74	± 1.624
1	1.46348	± 0.001380	0.10077	± 0.000210	0.00178	± 0.000028	0.07309	± 0.001374	0.0000630	± 0.00000702	3.37E-14	98.7%	14.3397	454.10	± 1.237
2	2.94495	± 0.001949	0.08906	± 0.000182	0.00209	± 0.000030	0.07719	± 0.001952	0.0001474	± 0.00001465	6.79E-14	98.5%	32.5796	903.75	± 2.385
KV-8-14 (au27.1o.ksp.82)					SCIH		Time duration		30s;10s (only the last step)						
0.5	0.37112	± 0.000336	0.03208	± 0.000122	0.00048	± 0.000015	0.00405	± 0.001299	0.0000408	± 0.00000594	8.55E-15	96.8%	11.1923	363.76	± 2.304
0.7	4.95328	± 0.002464	0.57677	± 0.000810	0.00766	± 0.000073	0.05055	± 0.001467	0.0000502	± 0.00000660	1.14E-13	99.7%	8.5624	284.64	± 0.440
0.8	3.87996	± 0.002938	0.41261	± 0.001044	0.00537	± 0.000054	0.06278	± 0.002836	-0.0000033	± 0.00001273	8.94E-14	100.0%	9.4035	310.33	± 0.873
1	7.55378	± 0.006285	0.69712	± 0.000686	0.00932	± 0.000083	0.09440	± 0.001374	0.0000694	± 0.00001123	1.74E-13	99.7%	10.8065	352.37	± 0.481
2	9.71176	± 0.009630	0.68976	± 0.000795	0.00944	± 0.000089	0.06972	± 0.001656	0.0002294	± 0.00000864	2.24E-13	99.3%	13.9818	444.05	± 0.690
KV-8-14 (au27.1o.ksp.83)					SCIH		Time duration		30s;10s (only the last step)						
0.5	0.43666	± 0.000542	0.04726	± 0.000108	0.00064	± 0.000017	0.00280	± 0.000713	0.0000210	± 0.00000659	1.01E-14	98.6%	9.1083	301.35	± 1.578
0.7	6.35032	± 0.002854	0.69563	± 0.001111	0.00893	± 0.000056	0.02404	± 0.001601	0.0000461	± 0.00000702	1.46E-13	99.8%	9.1093	301.38	± 0.511
0.8	4.95719	± 0.006055	0.49937	± 0.000453	0.00653	± 0.000050	0.02652	± 0.000925	0.0000301	± 0.00000720	1.14E-13	99.8%	9.9092	325.59	± 0.516
1	11.40695	± 0.004600	0.98862	± 0.001263	0.01366	± 0.000094	0.03692	± 0.001002	0.0001896	± 0.00001084	2.63E-13	99.5%	11.4816	372.26	± 0.512
2	7.00142	± 0.003872	0.62846	± 0.001018	0.00827	± 0.000063	0.00378	± 0.000929	0.0000879	± 0.00000762	1.61E-13	99.6%	11.0992	361.02	± 0.631
KV-8-14 (au27.1o.ksp.84)					SCIH		Time duration		30s;10s (only the last step)						
0.5	0.19917	± 0.000524	0.01257	± 0.000121	0.00025	± 0.000021	0.00810	± 0.000923	0.0000116	± 0.00001045	4.59E-15	98.3%	15.5785	488.45	± 9.167
0.7	0.46477	± 0.000453	0.04450	± 0.000117	0.00062	± 0.000015	0.04745	± 0.001481	0.0000200	± 0.00000769	1.07E-14	98.7%	10.3126	337.68	± 1.928
0.8	0.26415	± 0.000450	0.01951	± 0.000184	0.00031	± 0.000016	0.03771	± 0.002257	0.0000124	± 0.00000615	6.09E-15	98.6%	13.3534	426.28	± 5.089
1	1.08856	± 0.001382	0.03364	± 0.000123	0.00067	± 0.000027	0.04691	± 0.001477	0.0000692	± 0.00000798	2.51E-14	98.1%	31.7491	885.54	± 3.997
2	0.34259	± 0.000255	0.00798	± 0.000083	0.00023	± 0.000015	0.01062	± 0.001299	0.0000197	± 0.00000667	7.89E-15	98.3%	42.2209	1102.74	± 13.396
KV-8-14 (au27.1o.ksp.85)					SCIH		Time duration		30s;10s (only the last step)						
0.5	0.41831	± 0.000291	0.01468	± 0.000152	0.00058	± 0.000019	0.00213	± 0.000967	0.0000839	± 0.00000722	9.64E-15	94.1%	26.8042	773.12	± 9.538
0.7	0.65958	± 0.000629	0.07186	± 0.000172	0.00110	± 0.000020	0.03462	± 0.001442	0.0000169	± 0.00000674	1.52E-14	99.2%	9.1103	301.41	± 1.206
0.8	0.34154	± 0.000413	0.02653	± 0.000082	0.00052	± 0.000016	0.02436	± 0.001761	-0.0000139	± 0.00001320	7.87E-15	101.2%	12.8723	412.54	± 4.907
1	1.46397	± 0.001733	0.03814	± 0.000100	0.00138	± 0.000020	0.05145	± 0.002443	0.0001395	± 0.00000740	3.37E-14	97.2%	37.3034	1003.99	± 3.339
2	0.36986	± 0.000378	0.00501	± 0.000061	0.00033	± 0.000012	0.01201	± 0.000951	0.0000376	± 0.00000782	8.52E-15	97.0%	71.5651	1600.67	± 22.560
KV-8-14 (au27.1o.ksp.86)					SCIH		Time duration		30s;10s (only the last step)						
0.5	0.29653	± 0.000297	0.01768	± 0.000094	0.00023	± 0.000017	0.00233	± 0.001181	0.0000266	± 0.00000628	6.83E-15	97.3%	16.3263	508.88	± 4.321
0.7	2.29047	± 0.001828	0.27708	± 0.000512	0.00360	± 0.000028	0.02580	± 0.001165	0.0000279	± 0.00000699	5.28E-14	99.6%	8.2369	274.60	± 0.608
0.8	1.78588	± 0.001267	0.19300	± 0.000450	0.00256	± 0.000029	0.04198	± 0.001814	0.0000196	± 0.00000700	4.12E-14	99.7%	9.2233	304.85	± 0.825
1	4.19073	± 0.002819	0.36368	± 0.000837	0.00498	± 0.000059	0.05156	± 0.001382	0.0000839	± 0.00000754	9.66E-14	99.4%	11.4550	371.48	± 0.918
2	3.36025	± 0.002459	0.19986	± 0.000372	0.00295	± 0.000038	0.02480	± 0.001836	0.0001222	± 0.00000760	7.74E-14	98.9%	16.6326	517.18	± 1.103

KV-8-14 (au27.1o.ksp.87)		SCIH		Time duration	30s;10s (only the last step)				
p	^{40}Ar(*+atm)	^{39}Ar (K)	^{38}Ar (Cl+atm)	^{37}Ar (Ca)	^{36}Ar (Atm)	Moles^{40}Ar	%Rad	R	Age(Ma)
0.5	0.44174 ± 0.000903	0.04470 ± 0.000156	0.00067 ± 0.000015	0.00594 ± 0.000557	0.0000248 ± 0.00000648	1.02E-14	98.3%	9.7186	319.85 ± 1.927
0.7	1.87822 ± 0.001993	0.20592 ± 0.000635	0.00277 ± 0.000042	0.05794 ± 0.002243	0.0000072 ± 0.00001187	4.33E-14	99.9%	9.1112	301.44 ± 1.134
0.8	1.38227 ± 0.001290	0.12236 ± 0.000385	0.00167 ± 0.000031	0.02812 ± 0.001190	0.0000239 ± 0.00000729	3.19E-14	99.5%	11.2390	365.14 ± 1.334
1	2.71842 ± 0.001962	0.14195 ± 0.000243	0.00228 ± 0.000037	0.04603 ± 0.001679	0.0000931 ± 0.00000780	6.26E-14	99.0%	18.9571	578.95 ± 1.195
2	1.61631 ± 0.001661	0.11863 ± 0.000289	0.00169 ± 0.000026	0.00629 ± 0.001041	0.0000470 ± 0.00000766	3.72E-14	99.1%	13.5079	430.66 ± 1.301
KV-8-14 (au27.1o.ksp.88)		SCIH		Time duration	30s;10s (only the last step)				
0.5	0.89624 ± 0.001007	0.09747 ± 0.000359	0.00138 ± 0.000029	0.01363 ± 0.001527	0.0000438 ± 0.00000685	2.07E-14	98.6%	9.0619	299.94 ± 1.359
0.7	5.06249 ± 0.003509	0.58406 ± 0.001101	0.00753 ± 0.000073	0.12879 ± 0.001330	0.0000722 ± 0.00000851	1.17E-13	99.6%	8.6315	286.77 ± 0.596
0.8	2.39803 ± 0.001762	0.23191 ± 0.000424	0.00306 ± 0.000044	0.06502 ± 0.002332	0.0000414 ± 0.00000729	5.53E-14	99.5%	10.2881	336.95 ± 0.734
1	5.44611 ± 0.005584	0.37030 ± 0.000860	0.00579 ± 0.000100	0.08321 ± 0.001912	0.0001713 ± 0.00000793	1.25E-13	99.1%	14.5709	460.56 ± 1.197
2	2.40219 ± 0.001648	0.20808 ± 0.000530	0.00277 ± 0.000032	0.02073 ± 0.001222	0.0000471 ± 0.00000759	5.54E-14	99.4%	11.4778	372.14 ± 1.048
KV-8-14 (au27.1o.ksp.89)		SCIH		Time duration	30s;10s (only the last step)				
0.5	1.10416 ± 0.001003	0.05599 ± 0.000150	0.00118 ± 0.000023	0.01074 ± 0.000751	0.0001156 ± 0.00000732	2.54E-14	96.9%	19.1107	582.96 ± 2.071
0.7	3.63910 ± 0.001267	0.40020 ± 0.000942	0.00545 ± 0.000029	0.12285 ± 0.002500	0.0001323 ± 0.00000826	8.39E-14	98.9%	8.9958	297.92 ± 0.744
0.8	1.71886 ± 0.001109	0.17199 ± 0.000473	0.00242 ± 0.000029	0.09479 ± 0.002348	0.0000627 ± 0.00000614	3.96E-14	98.9%	9.8865	324.91 ± 0.991
1	5.29993 ± 0.002682	0.35648 ± 0.000766	0.00595 ± 0.000036	0.10030 ± 0.002335	0.0002325 ± 0.00000842	1.22E-13	98.7%	14.6750	463.46 ± 1.060
2	3.03111 ± 0.001621	0.09609 ± 0.000128	0.00231 ± 0.000030	0.10947 ± 0.002245	0.0002099 ± 0.00000911	6.98E-14	98.0%	30.8993	866.71 ± 1.492
KV-8-14 (au27.1o.ksp.90)		SCIH		Time duration	30s;10s (only the last step)				
0.5	0.31983 ± 0.000479	0.02936 ± 0.000105	0.00046 ± 0.000014	0.00709 ± 0.001146	0.0000249 ± 0.00000655	7.37E-15	97.7%	10.6420	347.49 ± 2.560
0.7	1.44078 ± 0.001264	0.14025 ± 0.000426	0.00190 ± 0.000038	0.06358 ± 0.001518	0.0000624 ± 0.00000673	3.32E-14	98.7%	10.1419	332.57 ± 1.161
0.8	1.00908 ± 0.001103	0.08277 ± 0.000261	0.00115 ± 0.000019	0.03634 ± 0.001638	0.0000335 ± 0.00000654	2.33E-14	99.0%	12.0725	389.48 ± 1.515
1	2.22177 ± 0.001731	0.09020 ± 0.000221	0.00152 ± 0.000025	0.05212 ± 0.001175	0.0001080 ± 0.00000780	5.12E-14	98.6%	24.2797	712.90 ± 2.002
2	0.33482 ± 0.000538	0.02045 ± 0.000120	0.00032 ± 0.000020	0.00734 ± 0.001482	0.0000093 ± 0.00000677	7.72E-15	99.2%	16.2385	506.49 ± 4.357

Muscovite in detrital samples

FBR-2 (au21.3f.mus)		310 - 325 Ma							
n	^{40}Ar(*+atm)	^{39}Ar (K)	^{38}Ar (Cl+atm)	^{37}Ar (Ca)	^{36}Ar (Atm)	Moles^{40}Ar	%Rad	R	Age(Ma)
1	8.32844 ± 0.009968	0.83876 ± 0.001559	0.01058 ± 0.000080	0.00046 ± 0.000078	0.0000113 ± 0.00001084	5.83E-14	100.0%	9.9255	317.75 ± 0.713
2	14.86904 ± 0.017924	1.51431 ± 0.002316	0.01988 ± 0.000273	0.00156 ± 0.000070	0.0001036 ± 0.00001755	1.04E-13	99.8%	9.7989	314.03 ± 0.622
3	4.40764 ± 0.006291	0.45100 ± 0.000681	0.00581 ± 0.000073	0.00024 ± 0.000055	0.0000927 ± 0.00001120	3.09E-14	99.4%	9.7124	311.49 ± 0.692
4	6.47887 ± 0.008742	0.65936 ± 0.001073	0.00861 ± 0.000085	0.00036 ± 0.000043	0.0000630 ± 0.00001153	4.54E-14	99.7%	9.7978	314.00 ± 0.686
5	10.13255 ± 0.006359	1.03593 ± 0.001398	0.01361 ± 0.000129	0.00108 ± 0.000070	0.0001551 ± 0.00001158	7.10E-14	99.5%	9.7369	312.21 ± 0.479
6	3.04066 ± 0.002846	0.30774 ± 0.000910	0.00411 ± 0.000035	0.00034 ± 0.000078	0.0000146 ± 0.00000959	2.13E-14	99.9%	9.8666	316.02 ± 1.025
7	3.58279 ± 0.003204	0.36005 ± 0.000841	0.00476 ± 0.000081	0.00031 ± 0.000054	0.0000297 ± 0.00001239	2.51E-14	99.8%	9.9266	317.79 ± 0.861
8	3.32300 ± 0.001787	0.33681 ± 0.000864	0.00435 ± 0.000037	0.00042 ± 0.000091	-0.0000113 ± 0.00001284	2.33E-14	100.1%	9.8664	316.02 ± 0.904
9	4.46063 ± 0.005772	0.45019 ± 0.000762	0.00571 ± 0.000045	0.00033 ± 0.000086	0.0000677 ± 0.00001372	3.12E-14	99.6%	9.8639	315.94 ± 0.735
10	3.48491 ± 0.003041	0.35273 ± 0.000689	0.00453 ± 0.000060	0.00039 ± 0.000057	0.0000215 ± 0.00001316	2.44E-14	99.8%	9.8620	315.89 ± 0.763
11	2.31961 ± 0.003056	0.23405 ± 0.000812	0.00303 ± 0.000037	0.00028 ± 0.000055	0.0000739 ± 0.00001411	1.62E-14	99.1%	9.8176	314.58 ± 1.309
12	4.37209 ± 0.004947	0.44593 ± 0.000844	0.00565 ± 0.000047	-0.00006 ± 0.000078	0.0000378 ± 0.00000994	3.06E-14	99.7%	9.7793	313.46 ± 0.724
13	6.75547 ± 0.007145	0.68023 ± 0.000791	0.00864 ± 0.000061	0.00005 ± 0.000054	0.0001373 ± 0.00001000	4.73E-14	99.4%	9.8715	316.17 ± 0.519
14	4.00134 ± 0.003827	0.40614 ± 0.001169	0.00516 ± 0.000051	0.00012 ± 0.000060	0.0000495 ± 0.00001088	2.80E-14	99.6%	9.8162	314.54 ± 0.991
15	5.27996 ± 0.004629	0.53732 ± 0.001651	0.00691 ± 0.000077	0.00027 ± 0.000084	0.0001534 ± 0.00001084	3.70E-14	99.1%	9.7421	312.36 ± 1.025
16	3.32191 ± 0.005383	0.33705 ± 0.001041	0.00437 ± 0.000061	-0.00008 ± 0.000066	0.0000088 ± 0.00001021	2.33E-14	99.9%	9.8481	315.48 ± 1.138
17	8.34888 ± 0.008243	0.85153 ± 0.001800	0.01079 ± 0.000095	0.00034 ± 0.000096	0.0000239 ± 0.00001524	5.85E-14	99.9%	9.7963	313.96 ± 0.753
18	2.56824 ± 0.003387	0.25907 ± 0.000675	0.00340 ± 0.000053	0.00023 ± 0.000059	-0.0000046 ± 0.00001210	1.80E-14	100.1%	9.9133	317.40 ± 1.027
19	6.95028 ± 0.007124	0.70907 ± 0.000717	0.00918 ± 0.000109	0.00023 ± 0.000086	0.0000051 ± 0.00001427	4.87E-14	100.0%	9.7999	314.06 ± 0.491
20	5.62315 ± 0.004051	0.56777 ± 0.001274	0.00729 ± 0.000060	0.00053 ± 0.000056	0.0000364 ± 0.00001304	3.94E-14	99.8%	9.8850	316.56 ± 0.778
21	4.07212 ± 0.004010	0.41437 ± 0.000636	0.00534 ± 0.000043	0.00029 ± 0.000074	0.0000353 ± 0.00001423	2.85E-14	99.7%	9.8021	314.13 ± 0.660
22	5.71781 ± 0.004609	0.57916 ± 0.000580	0.00744 ± 0.000083	0.00015 ± 0.000044	0.0000984 ± 0.00001127	4.00E-14	99.5%	9.8224	314.73 ± 0.446
23	6.40193 ± 0.002621	0.65213 ± 0.001333	0.00825 ± 0.000053	0.00019 ± 0.000064	0.0000651 ± 0.00001259	4.48E-14	99.7%	9.7875	313.70 ± 0.681
24	3.11715 ± 0.002788	0.31844 ± 0.000675	0.00394 ± 0.000044	0.00005 ± 0.000060	-0.0000037 ± 0.00001312	2.18E-14	100.0%	9.7889	313.74 ± 0.821
25	9.17664 ± 0.007316	0.92889 ± 0.001932	0.01189 ± 0.000092	0.00032 ± 0.000071	0.0000591 ± 0.00001175	6.43E-14	99.8%	9.8604	315.84 ± 0.715
26	6.80211 ± 0.008228	0.68138 ± 0.001969	0.00918 ± 0.000123	0.00024 ± 0.000079	0.0000633 ± 0.00001253	4.76E-14	99.7%	9.9554	318.63 ± 1.016
27	11.51751 ± 0.009572	1.17493 ± 0.001849	0.01529 ± 0.000195	0.00129 ± 0.000051	0.0000807 ± 0.00001775	8.07E-14	99.8%	9.7825	313.55 ± 0.577
28	5.40775 ± 0.003388	0.54748 ± 0.000894	0.00700 ± 0.000042	0.00075 ± 0.000061	0.0000121 ± 0.00001327	3.79E-14	99.9%	9.8711	316.16 ± 0.599
29	5.21144 ± 0.005241	0.53186 ± 0.001353	0.00670 ± 0.000062	0.00014 ± 0.000115	0.0000203 ± 0.00001322	3.65E-14	99.9%	9.7872	313.69 ± 0.891
30	16.61501 ± 0.016266	1.69674 ± 0.002708	0.02165 ± 0.000129	0.00130 ± 0.000059	0.0000741 ± 0.00001674	1.16E-13	99.9%	9.7795	313.46 ± 0.595
31	7.82382 ± 0.012303	0.80204 ± 0.001233	0.01019 ± 0.000062	0.00029 ± 0.000089	0.0000622 ± 0.00001300	5.48E-14	99.8%	9.7321	312.07 ± 0.705
32	3.88800 ± 0.003772	0.39200 ± 0.000857	0.00494 ± 0.000049	0.00013 ± 0.000077	-0.0000184 ± 0.00001249	2.72E-14	100.1%	9.9184	317.55 ± 0.817
33	7.77998 ± 0.006673	0.79485 ± 0.001434	0.01050 ± 0.000140	0.00021 ± 0.000071	0.0000175 ± 0.00000947	5.45E-14	99.9%	9.7816	313.52 ± 0.637
34	5.72932 ± 0.006202	0.56086 ± 0.001510	0.00723 ± 0.000064	0.00007 ± 0.000094	0.0004095 ± 0.00001425	4.01E-14	97.9%	9.9995	319.92 ± 0.979
35	5.00738 ± 0.005666	0.50601 ± 0.000665	0.00646 ± 0.000066	-0.00017 ± 0.000134	0.0000339 ± 0.00000968	3.51E-14	99.8%	9.8760	316.30 ± 0.579
36	3.35424 ± 0.003317	0.34074 ± 0.000972	0.00432 ± 0.000058	0.00028 ± 0.000080	0.0000203 ± 0.00001047	2.35E-14	99.8%	9.8266	314.85 ± 0.996
37	7.21848 ± 0.004021	0.73740 ± 0.001591	0.00961 ± 0.000071	0.00024 ± 0.000082	0.0000880 ± 0.00001312	5.06E-14	99.6%	9.7539	312.71 ± 0.719
38	6.19182 ± 0.004588	0.62647 ± 0.001155	0.00826 ± 0.000090	-0.00005 ± 0.000059	0.0000944 ± 0.00001286	4.34E-14	99.5%	9.8391	315.22 ± 0.658
39	5.99830 ± 0.004728	0.61062 ± 0.001348	0.00783 ± 0.000082	0.00020 ± 0.000068	0.0000086 ± 0.00001073	4.20E-14	100.0%	9.8191	314.63 ± 0.756
40	2.41705 ± 0.002543	0.24900 ± 0.000679	0.00317 ± 0.000036	0.00013 ± 0.000091	0.0000100 ± 0.00001073	1.69E-14	99.9%	9.6951	310.98 ± 0.998
41	5.87081 ± 0.007526	0.59568 ± 0.000904	0.00802 ± 0.000107	0.00004 ± 0.000077	0.0000299 ± 0.00001112	4.11E-14	99.8%	9.8407	315.26 ± 0.651
42	7.00767 ± 0.006568	0.71479 ± 0.001292	0.00942 ± 0.000128	0.00017 ± 0.000077	0.0000562 ± 0.00001306	4.91E-14	99.8%	9.7806	313.50 ± 0.663
43	2.78284 ± 0.002805	0.28180 ± 0.000734	0.00376 ± 0.000087	0.00009 ± 0.000073	0.0000253 ± 0.00001257	1.95E-14	99.7%	9.8488	315.50 ± 0.979
44	3.87787 ± 0.003588	0.38758 ± 0.001081	0.00497 ± 0.000047	0.00018 ± 0.000080	0.0000420 ± 0.00001177	2.72E-14	99.7%	9.9734	319.16 ± 0.984
45	3.07558 ± 0.004276	0.31095 ± 0.000778	0.00404 ± 0.000047	0.00002 ± 0.000041	0.0000130 ± 0.00001322	2.15E-14	99.9%	9.8786	316.38 ± 0.992
46	4.56901 ± 0.003274	0.46420 ± 0.000907	0.00584 ± 0.000031	0.00033 ± 0.000063	0.0000165 ± 0.00001139	3.20E-14	99.9%	9.8324	315.02 ± 0.696
47	5.80677 ± 0.005407	0.58751 ± 0.000725	0.00756 ± 0.000069	0.00048 ± 0.000055	0.0001437 ± 0.00001149	4.07E-14	99.3%	9.8116	314.41 ± 0.523
48	2.18663 ± 0.002313	0.22152 ± 0.000604	0.00277 ± 0.000018	0.00002 ± 0.000084	0.0000508 ± 0.00001126	1.53E-14	99.3%	9.8032	314.16 ± 1.042
49	5.49111 ± 0.004296	0.56134 ± 0.000997	0.00725 ± 0.000059	-0.00004 ± 0.000046	0.0000516 ± 0.00001118	3.85E-14	99.7%	9.7551	312.74 ± 0.637
50	2.76701 ± 0.002533	0.26974 ± 0.000601	0.00365 ± 0.000037	0.00033 ± 0.000100	0.0000869 ± 0.00000971	1.94E-14	99.1%	10.1629	324.71 ± 0.859
51	7.45229 ± 0.007500	0.75211 ± 0.001383	0.00961 ± 0.000070	0.00064 ± 0.000067	0.0002734 ± 0.00001107	5.22E-14	98.9%	9.8012	314.10 ± 0.680
52	5.66356 ± 0.005395	0.57158 ± 0.002263	0.00735 ± 0.000047	0.00006 ± 0.000077	0.0000963 ± 0.00001263	3.97E-14	99.5%	9.8589	315.80 ± 1.309
53	18.11979 ± 0.015833	1.81784 ± 0.001580	0.02472 ± 0.000133	0.00256 ± 0.000073	0.0003903 ± 0.00001547	1.27E-13	99.4%	9.9044	317.14 ± 0.401
54	8.04882 ± 0.006650	0.81156 ± 0.001469	0.01037 ± 0.000109	0.00074 ± 0.000079	0.0002444 ± 0.00001146	5.64E-14	99.1%	9.8288	314.91 ± 0.646
55	6.70560 ± 0.008934	0.67932 ± 0.001203	0.00869 ± 0.000049	0.00119 ± 0.000117	0.0002325 ± 0.00001352	4.70E-14	99.0%	9.7700	313.18 ± 0.726

FBR-2 (au21.3f.mus)			continued							
n	^{40}Ar(*+atm)	^{39}Ar (K)	^{38}Ar (Cl+atm)	^{37}Ar (Ca)	^{36}Ar (Atm)	Moles ^{40}Ar	%Rad	R	Age(Ma)
56	4.38117 ± 0.005039	0.44083 ± 0.000698	0.00588 ± 0.000099	0.00027 ± 0.000064	0.0000264 ± 0.00001017	3.07E-14	99.8%	9.9209	317.62 ± 0.660
57	5.87396 ± 0.005383	0.59249 ± 0.001051	0.00759 ± 0.000076	0.00034 ± 0.000118	0.0002763 ± 0.00001284	4.11E-14	98.6%	9.7762	313.37 ± 0.667
58	4.90139 ± 0.004923	0.49170 ± 0.000832	0.00628 ± 0.000036	0.00049 ± 0.000078	0.0001820 ± 0.00001358	3.43E-14	98.9%	9.8589	315.80 ± 0.680
59	6.40475 ± 0.005100	0.65432 ± 0.001188	0.00831 ± 0.000075	0.00042 ± 0.000119	0.0000442 ± 0.00001311	4.49E-14	99.8%	9.7686	313.14 ± 0.650
60	6.98156 ± 0.007327	0.70622 ± 0.001035	0.00900 ± 0.000073	0.00015 ± 0.000057	0.0000379 ± 0.00001293	4.89E-14	99.8%	9.8700	316.13 ± 0.597
61	3.91964 ± 0.005158	0.39329 ± 0.000879	0.00510 ± 0.000051	0.00026 ± 0.000094	0.0000139 ± 0.00001152	2.75E-14	99.9%	9.9559	318.65 ± 0.873
62	4.22641 ± 0.007205	0.42764 ± 0.000800	0.00536 ± 0.000051	-0.00002 ± 0.000092	0.0000288 ± 0.00001143	2.96E-14	99.8%	9.8631	315.92 ± 0.840
63	5.64133 ± 0.003182	0.57649 ± 0.000807	0.00731 ± 0.000056	0.00035 ± 0.000052	0.0001895 ± 0.00001228	3.95E-14	99.0%	9.6886	310.79 ± 0.515
64	4.14596 ± 0.005345	0.41782 ± 0.001060	0.00534 ± 0.000054	0.00030 ± 0.000085	0.0000340 ± 0.00001321	2.90E-14	99.8%	9.8989	316.97 ± 0.953
65	2.85164 ± 0.001974	0.28820 ± 0.000609	0.00372 ± 0.000046	0.00023 ± 0.000066	0.0000389 ± 0.00001135	2.00E-14	99.6%	9.8547	315.68 ± 0.798
66	6.18209 ± 0.005270	0.63077 ± 0.001456	0.00808 ± 0.000067	0.00012 ± 0.000069	0.0000343 ± 0.00001134	4.33E-14	99.8%	9.7849	313.62 ± 0.791
67	6.09409 ± 0.004454	0.60774 ± 0.001343	0.00804 ± 0.000115	0.00619 ± 0.000177	0.0001551 ± 0.00001868	4.27E-14	99.3%	9.9531	318.56 ± 0.802
68	6.73931 ± 0.005852	0.67310 ± 0.001547	0.00866 ± 0.000077	0.00397 ± 0.000087	0.0000562 ± 0.00001136	4.72E-14	99.8%	9.9883	319.60 ± 0.803
69	7.49557 ± 0.005645	0.76812 ± 0.001142	0.00985 ± 0.000103	0.00014 ± 0.000111	0.0000529 ± 0.00001947	5.25E-14	99.8%	9.7380	312.24 ± 0.574
70	7.39283 ± 0.011397	0.75429 ± 0.001681	0.00990 ± 0.000182	0.00039 ± 0.000092	0.0001749 ± 0.00001277	5.18E-14	99.3%	9.7325	312.08 ± 0.867
71	5.17363 ± 0.005773	0.52655 ± 0.001836	0.00669 ± 0.000034	0.00010 ± 0.000091	0.0000434 ± 0.00001689	3.62E-14	99.8%	9.8013	314.10 ± 1.192
72	4.48147 ± 0.002208	0.45427 ± 0.000956	0.00583 ± 0.000085	0.00031 ± 0.000094	0.0000328 ± 0.00001096	3.14E-14	99.8%	9.8438	315.36 ± 0.720
73	5.93250 ± 0.005972	0.60022 ± 0.001618	0.00758 ± 0.000063	0.00040 ± 0.000055	0.0002312 ± 0.00001233	4.15E-14	98.8%	9.7701	313.19 ± 0.932
74	3.75903 ± 0.006372	0.37537 ± 0.000927	0.00479 ± 0.000058	-0.00001 ± 0.000045	0.0000845 ± 0.00001278	2.63E-14	99.3%	9.9477	318.41 ± 1.013
75	6.25691 ± 0.006063	0.62212 ± 0.000731	0.00821 ± 0.000123	-0.00021 ± 0.000124	0.0004846 ± 0.00001562	4.38E-14	97.7%	9.8271	314.86 ± 0.545
76	10.54082 ± 0.004385	1.06891 ± 0.002112	0.01445 ± 0.000188	0.00146 ± 0.000089	0.0000545 ± 0.00001623	7.38E-14	99.8%	9.8464	315.43 ± 0.654
77	4.64796 ± 0.004800	0.47175 ± 0.001190	0.00610 ± 0.000033	0.00019 ± 0.000065	0.0000377 ± 0.00001122	3.26E-14	99.8%	9.8291	314.92 ± 0.890
78	2.22033 ± 0.003182	0.22447 ± 0.000924	0.00288 ± 0.000037	0.00013 ± 0.000050	0.0000703 ± 0.00001039	1.55E-14	99.1%	9.7988	314.03 ± 1.450
79	5.76616 ± 0.003918	0.56088 ± 0.000524	0.00735 ± 0.000085	0.00058 ± 0.000074	0.0001486 ± 0.00001320	4.04E-14	99.2%	10.2023	325.86 ± 0.440
80	3.46833 ± 0.003960	0.35190 ± 0.000609	0.00462 ± 0.000055	0.00014 ± 0.000037	0.0000223 ± 0.00001743	2.43E-14	99.8%	9.8375	315.17 ± 0.805
81	4.71610 ± 0.004115	0.47914 ± 0.000637	0.00626 ± 0.000055	0.00018 ± 0.000057	0.0000660 ± 0.00001757	3.30E-14	99.6%	9.8021	314.13 ± 0.610
82	8.31584 ± 0.006823	0.84844 ± 0.001354	0.01081 ± 0.000108	0.00023 ± 0.000066	0.0000201 ± 0.00001760	5.82E-14	99.9%	9.7943	313.90 ± 0.597
83	3.65247 ± 0.004030	0.36917 ± 0.001074	0.00471 ± 0.000065	-0.00004 ± 0.000076	0.0000065 ± 0.00001261	2.56E-14	99.9%	9.8885	316.67 ± 1.037
84	3.42192 ± 0.003365	0.34739 ± 0.001025	0.00454 ± 0.000046	0.00063 ± 0.000113	0.0000557 ± 0.00001419	2.40E-14	99.5%	9.8033	314.16 ± 1.055
85	3.77832 ± 0.005337	0.38460 ± 0.000727	0.00484 ± 0.000055	0.00019 ± 0.000084	0.0000434 ± 0.00001264	2.65E-14	99.7%	9.7908	313.80 ± 0.805
86	11.32582 ± 0.008491	1.15435 ± 0.001217	0.01493 ± 0.000082	0.00119 ± 0.000119	0.0000164 ± 0.00002013	7.93E-14	100.0%	9.8073	314.28 ± 0.439
87	3.50160 ± 0.003879	0.35551 ± 0.001278	0.00459 ± 0.000067	0.00027 ± 0.000114	0.0000208 ± 0.00000986	2.45E-14	99.8%	9.8323	315.02 ± 1.216
88	14.19876 ± 0.006127	1.44127 ± 0.002192	0.01846 ± 0.000104	0.01474 ± 0.000049	0.0001221 ± 0.00001444	9.94E-14	99.8%	9.8275	314.88 ± 0.508
89	7.65025 ± 0.008311	0.78840 ± 0.001571	0.01020 ± 0.000072	0.00021 ± 0.000085	0.0000012 ± 0.00001045	5.36E-14	100.0%	9.7031	311.21 ± 0.717
90	2.06992 ± 0.001830	0.20881 ± 0.000503	0.00258 ± 0.000033	0.00012 ± 0.000068	-0.0000061 ± 0.00000909	1.45E-14	100.1%	9.9129	317.38 ± 0.912
91	4.84581 ± 0.003861	0.48966 ± 0.001495	0.00631 ± 0.000050	0.00025 ± 0.000076	0.0000084 ± 0.00001349	3.39E-14	99.9%	9.8913	316.75 ± 1.033
92	2.58519 ± 0.001806	0.26064 ± 0.000287	0.00328 ± 0.000044	0.00021 ± 0.000056	0.0000369 ± 0.00000954	1.81E-14	99.6%	9.8769	316.33 ± 0.540
93	4.08916 ± 0.004131	0.41679 ± 0.000950	0.00536 ± 0.000045	0.00024 ± 0.000083	0.0000215 ± 0.00001165	2.86E-14	99.8%	9.7959	313.95 ± 0.827
94	5.78980 ± 0.004686	0.58917 ± 0.000500	0.00752 ± 0.000038	0.00038 ± 0.000081	0.0000415 ± 0.00001112	4.05E-14	99.8%	9.8064	314.25 ± 0.410
95	3.96580 ± 0.004649	0.40515 ± 0.000634	0.00547 ± 0.000103	0.00018 ± 0.000084	0.0000230 ± 0.00001081	2.78E-14	99.8%	9.7717	313.23 ± 0.663
96	3.75187 ± 0.002048	0.37654 ± 0.000672	0.00483 ± 0.000051	0.00018 ± 0.000066	0.0001071 ± 0.00001133	2.63E-14	99.2%	9.8800	316.42 ± 0.660
97	2.30527 ± 0.002501	0.22605 ± 0.000951	0.00292 ± 0.000043	0.00015 ± 0.000072	0.0002974 ± 0.00001225	1.61E-14	96.2%	9.8092	314.34 ± 1.510
98	3.39390 ± 0.003438	0.34700 ± 0.000744	0.00438 ± 0.000056	0.00003 ± 0.000056	0.0000185 ± 0.00001387	2.38E-14	99.8%	9.7649	313.03 ± 0.834
99	1.49906 ± 0.002818	0.15121 ± 0.000359	0.00190 ± 0.000030	-0.00030 ± 0.000146	0.0000343 ± 0.00001198	1.05E-14	99.3%	9.8463	315.43 ± 1.220
100	4.49825 ± 0.004042	0.46001 ± 0.001168	0.00580 ± 0.000058	0.00007 ± 0.000093	0.0000085 ± 0.00000972	3.15E-14	99.9%	9.7731	313.28 ± 0.867
101	1.99281 ± 0.002303	0.20269 ± 0.000722	0.00253 ± 0.000050	0.00008 ± 0.000077	0.0000223 ± 0.00001185	1.40E-14	99.7%	9.7996	314.05 ± 1.304
102	1.84218 ± 0.001786	0.18579 ± 0.000442	0.00234 ± 0.000040	0.00007 ± 0.000075	0.0000189 ± 0.00001054	1.29E-14	99.7%	9.8856	316.58 ± 0.977
103	0.78504 ± 0.001514	0.07969 ± 0.000322	0.00093 ± 0.000027	0.00002 ± 0.000094	-0.0000057 ± 0.00001029	5.50E-15	100.2%	9.8511	315.57 ± 1.869
104	5.15279 ± 0.004715	0.52120 ± 0.001119	0.00730 ± 0.000121	0.00023 ± 0.000112	0.0000154 ± 0.00002059	3.61E-14	99.9%	9.8777	316.35 ± 0.828
105	5.15620 ± 0.004048	0.52613 ± 0.000410	0.00665 ± 0.000060	0.00015 ± 0.000096	0.0000435 ± 0.00001089	3.61E-14	99.8%	9.7759	313.36 ± 0.399
106	2.77588 ± 0.002055	0.28269 ± 0.000863	0.00369 ± 0.000059	-0.00003 ± 0.000048	0.0000266 ± 0.00001034	1.94E-14	99.7%	9.7918	313.82 ± 1.048
107	3.39026 ± 0.003751	0.34187 ± 0.000947	0.00466 ± 0.000066	0.00033 ± 0.000064	0.0000883 ± 0.00001393	2.37E-14	99.2%	9.8407	315.26 ± 1.023

FBR-5 (au21.3i.mus)			310 - 390 Ma						
n	^{40}Ar(*+atm)	^{39}Ar (K)	^{38}Ar (Cl+atm)	^{37}Ar (Ca)	^{36}Ar (Atm)	Moles^{40}Ar	%Rad	R	Age(Ma)
1	9.30485 ± 0.007623	0.93092 ± 0.000922	0.01205 ± 0.000088	0.00547 ± 0.001453	0.0000889 ± 0.00001687	6.52E-14	99.7%	9.9677	318.99 ± 0.446
2	5.01147 ± 0.005477	0.47764 ± 0.000744	0.00642 ± 0.000084	0.00753 ± 0.002479	0.0001257 ± 0.00001453	3.51E-14	99.3%	10.4159	332.09 ± 0.698
3	7.56292 ± 0.011409	0.76079 ± 0.001438	0.00982 ± 0.000119	0.00716 ± 0.001508	0.0001945 ± 0.00001730	5.30E-14	99.2%	9.8663	316.01 ± 0.800
4	6.11701 ± 0.006130	0.54375 ± 0.000492	0.00691 ± 0.000062	0.00850 ± 0.001496	0.0002230 ± 0.00001600	4.28E-14	98.9%	11.1301	352.77 ± 0.555
5	6.88436 ± 0.009955	0.68308 ± 0.000706	0.00892 ± 0.000118	0.01253 ± 0.002125	0.0003369 ± 0.00001368	4.82E-14	98.6%	9.9345	318.02 ± 0.604
6	9.71231 ± 0.009796	0.81577 ± 0.000943	0.01194 ± 0.000151	0.00948 ± 0.002446	0.0003259 ± 0.00001546	6.80E-14	99.0%	11.7888	371.63 ± 0.603
7	7.48338 ± 0.007764	0.74857 ± 0.000956	0.00978 ± 0.000151	0.00499 ± 0.001799	0.0000441 ± 0.00002168	5.24E-14	99.8%	9.9801	319.36 ± 0.593
8	5.56864 ± 0.008072	0.55159 ± 0.000947	0.00689 ± 0.000055	0.00029 ± 0.001882	0.0000265 ± 0.00002773	3.90E-14	99.9%	10.0815	322.33 ± 0.867
9	3.69219 ± 0.004324	0.35546 ± 0.000463	0.00463 ± 0.000075	0.00703 ± 0.002586	0.0000112 ± 0.00002893	2.59E-14	99.9%	10.3797	331.04 ± 0.962
10	8.03048 ± 0.006572	0.79871 ± 0.000860	0.01030 ± 0.000130	0.00734 ± 0.001557	0.0000010 ± 0.00002339	5.62E-14	100.0%	10.0549	321.55 ± 0.516
11	8.59021 ± 0.008803	0.78458 ± 0.000721	0.01026 ± 0.000134	0.00563 ± 0.001998	0.0000755 ± 0.00002204	6.02E-14	99.7%	10.9210	346.74 ± 0.546
12	5.06409 ± 0.007101	0.50584 ± 0.000742	0.00655 ± 0.000092	0.00317 ± 0.003041	0.0000695 ± 0.00003646	3.55E-14	99.6%	9.9713	319.10 ± 0.942
13	8.39251 ± 0.006271	0.80090 ± 0.001506	0.01064 ± 0.000126	0.01072 ± 0.001977	0.0001750 ± 0.00003025	5.88E-14	99.4%	10.4155	332.08 ± 0.764
14	5.20234 ± 0.007592	0.49803 ± 0.001033	0.00627 ± 0.000058	0.00604 ± 0.002223	0.0000676 ± 0.00003573	3.64E-14	99.6%	10.4068	331.83 ± 1.082
15	2.00298 ± 0.002163	0.19854 ± 0.000807	0.00270 ± 0.000054	0.00938 ± 0.001900	0.0000841 ± 0.00003461	1.40E-14	98.8%	9.9679	319.00 ± 2.136
16	6.60688 ± 0.005599	0.65922 ± 0.001050	0.00850 ± 0.000073	0.01241 ± 0.003991	0.0001807 ± 0.00002942	4.63E-14	99.2%	9.9430	318.27 ± 0.717
17	4.31653 ± 0.006563	0.42806 ± 0.000667	0.00542 ± 0.000067	0.00442 ± 0.002285	0.0000751 ± 0.00001834	3.02E-14	99.5%	10.0331	320.91 ± 0.811
18	9.21625 ± 0.012902	0.83483 ± 0.001276	0.01079 ± 0.000096	0.00078 ± 0.002500	0.0000721 ± 0.00002131	6.45E-14	99.8%	11.0143	349.43 ± 0.765
19	7.53942 ± 0.008081	0.71732 ± 0.001272	0.00950 ± 0.000069	0.00402 ± 0.002797	0.0002293 ± 0.00002630	5.28E-14	99.1%	10.4166	332.11 ± 0.776
20	2.63071 ± 0.003574	0.25434 ± 0.000549	0.00329 ± 0.000053	0.00463 ± 0.002028	0.0001352 ± 0.00001980	1.84E-14	98.5%	10.1880	325.44 ± 1.118
21	5.16542 ± 0.004877	0.48237 ± 0.000730	0.00621 ± 0.000073	0.00184 ± 0.002165	0.0000114 ± 0.00002892	3.62E-14	99.9%	10.7018	340.40 ± 0.829
22	3.09679 ± 0.002156	0.29654 ± 0.000719	0.00373 ± 0.000050	0.00376 ± 0.001853	0.0001065 ± 0.00002519	2.17E-14	99.0%	10.3381	329.82 ± 1.162
23	10.17645 ± 0.009059	0.81596 ± 0.001119	0.01075 ± 0.000147	0.01177 ± 0.002174	0.0000331 ± 0.00003520	7.13E-14	99.9%	12.4613	390.69 ± 0.754
24	6.60982 ± 0.005716	0.64793 ± 0.001228	0.00864 ± 0.000096	0.00646 ± 0.002509	0.0001949 ± 0.00003230	4.63E-14	99.1%	10.1136	323.27 ± 0.827
25	4.99035 ± 0.004344	0.46098 ± 0.000738	0.00622 ± 0.000090	0.00376 ± 0.001686	0.0000926 ± 0.00003333	3.49E-14	99.5%	10.7670	342.29 ± 0.925
26	3.68728 ± 0.005331	0.35377 ± 0.000609	0.00459 ± 0.000060	0.00620 ± 0.001853	0.0000437 ± 0.00003433	2.58E-14	99.7%	10.3881	331.28 ± 1.181
27	6.19333 ± 0.005705	0.60517 ± 0.000918	0.00821 ± 0.000102	0.00513 ± 0.001888	-0.0000157 ± 0.00003355	4.34E-14	100.1%	10.2348	326.81 ± 0.781
28	8.17365 ± 0.012884	0.76588 ± 0.001077	0.00983 ± 0.000093	0.00582 ± 0.003102	-0.0000258 ± 0.00003201	5.72E-14	100.1%	10.6729	339.56 ± 0.818
29	5.68671 ± 0.007350	0.55556 ± 0.000948	0.00791 ± 0.000063	0.00387 ± 0.001452	0.0001866 ± 0.00002306	3.98E-14	99.0%	10.1375	323.97 ± 0.802
30	5.15236 ± 0.006601	0.45601 ± 0.000819	0.00594 ± 0.000102	0.00310 ± 0.002937	0.0001089 ± 0.00002474	3.61E-14	99.4%	11.2288	355.61 ± 0.939
31	11.62588 ± 0.004708	1.17846 ± 0.001210	0.01595 ± 0.000150	0.09412 ± 0.002216	0.0004321 ± 0.00003741	8.14E-14	99.0%	9.7646	313.03 ± 0.461
32	5.15125 ± 0.003220	0.51198 ± 0.000582	0.00648 ± 0.000060	0.00140 ± 0.001662	0.0000252 ± 0.00002532	3.61E-14	99.9%	10.0471	321.32 ± 0.627
33	5.62051 ± 0.005145	0.56368 ± 0.001287	0.00737 ± 0.000085	0.00250 ± 0.001523	-0.0000083 ± 0.00002600	3.94E-14	100.0%	9.9716	319.11 ± 0.898
34	5.62377 ± 0.005681	0.55888 ± 0.000948	0.00777 ± 0.000120	0.01080 ± 0.002484	0.0002623 ± 0.00001933	3.94E-14	98.6%	9.9258	317.76 ± 0.715
35	8.22048 ± 0.008560	0.81196 ± 0.001409	0.01005 ± 0.000080	0.00430 ± 0.001600	0.0000493 ± 0.00003010	5.76E-14	99.8%	10.1068	323.07 ± 0.743
36	9.52667 ± 0.009204	0.95039 ± 0.001636	0.01223 ± 0.000139	0.00545 ± 0.002114	0.0000129 ± 0.00002904	6.67E-14	100.0%	10.0205	320.54 ± 0.696
37	8.59087 ± 0.010083	0.86132 ± 0.001552	0.01084 ± 0.000101	0.00191 ± 0.002040	-0.0000571 ± 0.00002758	6.02E-14	100.2%	9.9743	319.18 ± 0.750
38	4.69665 ± 0.005304	0.46401 ± 0.000765	0.00599 ± 0.000074	-0.00208 ± 0.002251	-0.0000634 ± 0.00002974	3.29E-14	100.4%	10.1213	323.49 ± 0.886
39	5.13322 ± 0.006371	0.50902 ± 0.000663	0.00679 ± 0.000072	0.00237 ± 0.002128	0.0000588 ± 0.00001831	3.59E-14	99.7%	10.0507	321.43 ± 0.673
40	6.86822 ± 0.005810	0.63827 ± 0.000860	0.00807 ± 0.000055	0.00503 ± 0.002574	0.0002477 ± 0.00003466	4.81E-14	98.9%	10.6467	338.80 ± 0.747
41	5.95523 ± 0.006600	0.58463 ± 0.001057	0.00775 ± 0.000129	0.00403 ± 0.002079	0.0001358 ± 0.00003338	4.17E-14	99.3%	10.1183	323.40 ± 0.876
42	1.23954 ± 0.000969	0.12461 ± 0.000318	0.00156 ± 0.000027	0.00022 ± 0.002464	0.0000321 ± 0.00003967	8.68E-15	99.2%	9.8711	316.16 ± 3.132
43	7.80975 ± 0.006023	0.77887 ± 0.001391	0.00965 ± 0.000097	0.00399 ± 0.001382	0.0001033 ± 0.00004148	5.47E-14	99.6%	9.9884	319.60 ± 0.802
44	13.27487 ± 0.013648	1.06164 ± 0.001477	0.01446 ± 0.000115	0.09242 ± 0.002428	0.0005277 ± 0.00005330	9.30E-14	98.9%	12.3657	388.00 ± 0.823
45	6.06283 ± 0.005293	0.53758 ± 0.000960	0.00729 ± 0.000053	0.01165 ± 0.001929	0.0001051 ± 0.00004255	4.25E-14	99.5%	11.2223	355.42 ± 1.026
46	5.68633 ± 0.004803	0.56364 ± 0.000997	0.00711 ± 0.000071	0.00564 ± 0.002158	0.0001208 ± 0.00003344	3.98E-14	99.4%	10.0263	320.71 ± 0.846
47	17.87768 ± 0.008716	1.71488 ± 0.001494	0.02391 ± 0.000250	0.09523 ± 0.001661	0.0006542 ± 0.00005302	1.25E-13	99.0%	10.3177	329.23 ± 0.442
48	10.76696 ± 0.008069	0.96516 ± 0.001649	0.01371 ± 0.000263	0.10040 ± 0.003161	0.0006079 ± 0.00004858	7.54E-14	98.4%	10.9797	348.43 ± 0.812
49	5.01067 ± 0.006388	0.50009 ± 0.000584	0.00653 ± 0.000121	0.00356 ± 0.002113	0.0001376 ± 0.00002711	3.51E-14	99.2%	9.9390	318.15 ± 0.755
50	4.82840 ± 0.002528	0.48222 ± 0.000893	0.00618 ± 0.000108	0.00506 ± 0.003114	0.0002626 ± 0.00002839	3.38E-14	98.4%	9.8530	315.62 ± 0.832
51	5.65224 ± 0.003644	0.53704 ± 0.001070	0.00703 ± 0.000135	0.00375 ± 0.001491	0.0003379 ± 0.00002747	3.96E-14	98.2%	10.3396	329.87 ± 0.853
52	11.28418 ± 0.007806	1.09719 ± 0.000995	0.01554 ± 0.000183	0.09038 ± 0.001716	0.0010743 ± 0.00004341	7.90E-14	97.3%	10.0032	320.03 ± 0.530
53	7.74238 ± 0.006261	0.67380 ± 0.001238	0.00844 ± 0.000079	0.00289 ± 0.002321	0.0002384 ± 0.00002890	5.42E-14	99.1%	11.3865	360.14 ± 0.833
54	4.99902 ± 0.004436	0.42814 ± 0.000975	0.00541 ± 0.000053	-0.00983 ± 0.004608	0.0002110 ± 0.00003636	3.50E-14	98.8%	11.5283	364.20 ± 1.201
55	4.45593 ± 0.005607	0.45085 ± 0.000874	0.00596 ± 0.000091	0.00552 ± 0.002765	0.0001271 ± 0.00002812	3.12E-14	99.2%	9.8013	314.10 ± 0.941

FBR-5 (au21.3i.mus)		continued							
n	^{40}Ar(*+atm)	^{39}Ar (K)	^{38}Ar (Cl+atm)	^{37}Ar (Ca)	^{36}Ar (Atm)	Moles^{40}Ar	%Rad	R	Age(Ma)
56	4.09064 ± 0.004848	0.38543 ± 0.001121	0.00512 ± 0.000093	0.00332 ± 0.002307	0.0002931 ± 0.00002711	2.86E-14	97.9%	10.3892	331.31 ± 1.253
57	5.71320 ± 0.006270	0.56344 ± 0.000714	0.00712 ± 0.000080	-0.00073 ± 0.002220	0.0005273 ± 0.00003201	4.00E-14	97.3%	9.8633	315.93 ± 0.765
58	5.94122 ± 0.005870	0.59383 ± 0.000861	0.00785 ± 0.000136	0.00484 ± 0.001537	0.0001926 ± 0.00003654	4.16E-14	99.0%	9.9098	317.29 ± 0.809
59	8.93449 ± 0.013468	0.81569 ± 0.001198	0.01056 ± 0.000072	-0.00053 ± 0.001516	0.0000029 ± 0.00003758	6.26E-14	100.0%	10.9522	347.64 ± 0.850
60	2.58916 ± 0.002006	0.25704 ± 0.000813	0.00326 ± 0.000037	-0.00245 ± 0.002637	0.0001516 ± 0.00003150	1.81E-14	98.3%	9.8979	316.94 ± 1.565
61	5.05858 ± 0.004962	0.49364 ± 0.000859	0.00612 ± 0.000087	-0.00347 ± 0.001495	0.0000040 ± 0.00003407	3.54E-14	100.0%	10.2444	327.09 ± 0.923
62	14.43564 ± 0.009507	1.34084 ± 0.001280	0.01855 ± 0.000136	0.09614 ± 0.002162	0.0006097 ± 0.00004748	1.01E-13	98.8%	10.6387	338.57 ± 0.519
63	5.79820 ± 0.007173	0.55580 ± 0.000782	0.00721 ± 0.000089	0.00351 ± 0.002201	0.0000472 ± 0.00003424	4.06E-14	99.8%	10.4076	331.85 ± 0.852
64	15.84343 ± 0.015772	1.41435 ± 0.001768	0.01941 ± 0.000181	0.09002 ± 0.002931	0.0005335 ± 0.00004854	1.11E-13	99.1%	11.0967	351.81 ± 0.652
65	10.47845 ± 0.018071	1.03101 ± 0.001602	0.01365 ± 0.000072	0.01129 ± 0.001686	0.0001950 ± 0.00002869	7.34E-14	99.5%	10.1084	323.12 ± 0.799
66	5.99914 ± 0.006121	0.60141 ± 0.001020	0.00779 ± 0.000086	0.00678 ± 0.001662	0.0000170 ± 0.00003821	4.20E-14	99.9%	9.9678	319.00 ± 0.872
67	14.06519 ± 0.014387	1.37562 ± 0.002816	0.01900 ± 0.000168	0.09422 ± 0.003474	0.0006055 ± 0.00005375	9.85E-14	98.8%	10.1012	322.90 ± 0.834
68	6.94109 ± 0.009454	0.67826 ± 0.001122	0.00917 ± 0.000111	-0.00131 ± 0.001762	0.0000530 ± 0.00003868	4.86E-14	99.8%	10.2103	326.10 ± 0.883
69	10.25376 ± 0.011564	1.03514 ± 0.001271	0.01331 ± 0.000149	-0.00120 ± 0.002737	0.0001270 ± 0.00003363	7.18E-14	99.6%	9.8693	316.10 ± 0.612
70	10.81029 ± 0.006799	1.10014 ± 0.001705	0.01486 ± 0.000111	0.08939 ± 0.002030	0.0006065 ± 0.00004300	7.57E-14	98.4%	9.6712	310.27 ± 0.645
71	14.62970 ± 0.009726	1.37209 ± 0.001692	0.01946 ± 0.000183	0.09003 ± 0.002778	0.0006789 ± 0.00004678	1.02E-13	98.7%	10.5225	335.19 ± 0.574
72	22.26043 ± 0.016914	1.79569 ± 0.001742	0.02475 ± 0.000186	0.09642 ± 0.002695	0.0005970 ± 0.00003657	1.56E-13	99.2%	12.3036	386.24 ± 0.515
73	19.70037 ± 0.019541	1.88514 ± 0.002269	0.02614 ± 0.000179	0.08642 ± 0.002746	0.0006745 ± 0.00004571	1.38E-13	99.0%	10.3491	330.14 ± 0.568
74	13.67931 ± 0.012139	1.33046 ± 0.001067	0.01857 ± 0.000232	0.09283 ± 0.001089	0.0006962 ± 0.00005236	9.58E-14	98.6%	10.1338	323.86 ± 0.541
75	6.88832 ± 0.007038	0.69120 ± 0.001054	0.00904 ± 0.000117	0.00266 ± 0.001741	0.0002169 ± 0.00002611	4.82E-14	99.1%	9.8734	316.22 ± 0.687
76	2.67917 ± 0.004173	0.26000 ± 0.000656	0.00332 ± 0.000083	-0.00214 ± 0.002560	0.0000613 ± 0.00003010	1.88E-14	99.3%	10.2340	326.79 ± 1.465
77	8.15150 ± 0.004147	0.80721 ± 0.001239	0.01011 ± 0.000108	0.00509 ± 0.001408	0.0001736 ± 0.00002135	5.71E-14	99.4%	10.0355	320.98 ± 0.579
78	5.18947 ± 0.003950	0.48388 ± 0.000516	0.00629 ± 0.000084	0.00190 ± 0.001998	0.0001233 ± 0.00002256	3.63E-14	99.3%	10.6497	338.89 ± 0.626
79	7.30199 ± 0.008171	0.69049 ± 0.000714	0.00868 ± 0.000103	0.01010 ± 0.001813	0.0000677 ± 0.00003097	5.11E-14	99.7%	10.5476	335.92 ± 0.664
80	8.18335 ± 0.006417	0.80588 ± 0.000910	0.01067 ± 0.000135	0.00472 ± 0.002181	0.0000958 ± 0.00003118	5.73E-14	99.7%	10.1200	323.45 ± 0.577
81	10.34139 ± 0.005031	0.96773 ± 0.001042	0.01226 ± 0.000107	0.00942 ± 0.002432	0.0000040 ± 0.00002816	7.24E-14	100.0%	10.6860	339.94 ± 0.486
82	13.59820 ± 0.005632	1.32280 ± 0.001805	0.01868 ± 0.000178	0.09754 ± 0.001597	0.0005147 ± 0.00003535	9.52E-14	98.9%	10.1720	324.97 ± 0.532
83	2.80462 ± 0.001631	0.27458 ± 0.000506	0.00371 ± 0.000074	0.00687 ± 0.001922	0.0000753 ± 0.00002588	1.96E-14	99.2%	10.1355	323.91 ± 1.092
84	6.86680 ± 0.006338	0.69601 ± 0.001096	0.00944 ± 0.000170	0.01021 ± 0.003014	-0.0000272 ± 0.00002877	4.81E-14	100.1%	9.8673	316.05 ± 0.697
85	9.46455 ± 0.012997	0.89677 ± 0.002237	0.01224 ± 0.000160	0.00720 ± 0.001914	0.0000951 ± 0.00003111	6.63E-14	99.7%	10.5234	335.22 ± 1.012
86	14.88108 ± 0.014838	1.41200 ± 0.001297	0.01940 ± 0.000115	0.09810 ± 0.002063	0.0006071 ± 0.00004477	1.04E-13	98.9%	10.4187	332.17 ± 0.545
87	4.18616 ± 0.005133	0.36105 ± 0.000929	0.00445 ± 0.000046	0.00250 ± 0.003177	0.0000480 ± 0.00001672	2.93E-14	99.7%	11.5557	364.98 ± 1.130
88	21.61201 ± 0.013275	2.16535 ± 0.001969	0.02907 ± 0.000261	0.10031 ± 0.002410	0.0006866 ± 0.00002848	1.51E-13	99.1%	9.8916	316.76 ± 0.372
89	9.36591 ± 0.011977	0.87965 ± 0.000733	0.01123 ± 0.000131	0.00613 ± 0.002705	0.0002631 ± 0.00003265	6.56E-14	99.2%	10.5596	336.27 ± 0.624
90	4.92155 ± 0.004396	0.47424 ± 0.000683	0.00592 ± 0.000076	0.00191 ± 0.002209	0.0000691 ± 0.00001654	3.45E-14	99.6%	10.3351	329.74 ± 0.651
91	6.61113 ± 0.006886	0.63544 ± 0.001274	0.00848 ± 0.000171	0.00050 ± 0.002172	0.0001360 ± 0.00002863	4.63E-14	99.4%	10.3408	329.90 ± 0.862
92	7.70767 ± 0.010858	0.76552 ± 0.001387	0.00990 ± 0.000105	0.00029 ± 0.001750	0.0000354 ± 0.00003169	5.40E-14	99.9%	10.0549	321.55 ± 0.836
93	6.47157 ± 0.010039	0.63506 ± 0.000902	0.00840 ± 0.000103	0.00040 ± 0.002490	0.0000928 ± 0.00003969	4.53E-14	99.6%	10.1474	324.25 ± 0.904
94	11.27997 ± 0.009114	1.11767 ± 0.001544	0.01618 ± 0.000220	0.08983 ± 0.001564	0.0007467 ± 0.00004722	7.90E-14	98.1%	9.9027	317.09 ± 0.654
95	10.28471 ± 0.009712	0.96109 ± 0.001289	0.01246 ± 0.000133	0.00143 ± 0.002092	0.0001907 ± 0.00001759	7.20E-14	99.5%	10.6426	338.68 ± 0.585
96	6.73763 ± 0.008104	0.64832 ± 0.001224	0.00860 ± 0.000106	0.00762 ± 0.001448	0.0001478 ± 0.00002563	4.72E-14	99.4%	10.3262	329.48 ± 0.831
97	10.77374 ± 0.007190	1.06553 ± 0.001343	0.01402 ± 0.000133	-0.00025 ± 0.002486	0.0001291 ± 0.00001486	7.55E-14	99.6%	10.0754	322.15 ± 0.480
98	10.62490 ± 0.011246	1.06837 ± 0.001203	0.01378 ± 0.000162	0.00629 ± 0.003436	0.0000969 ± 0.00001494	7.44E-14	99.7%	9.9188	317.56 ± 0.510
99	4.85292 ± 0.005382	0.44224 ± 0.000848	0.00581 ± 0.000133	-0.00106 ± 0.001659	0.0000432 ± 0.00001492	3.40E-14	99.7%	10.9443	347.41 ± 0.834
100	5.78364 ± 0.008005	0.51741 ± 0.000961	0.00675 ± 0.000080	0.00148 ± 0.001808	0.0000077 ± 0.00001636	4.05E-14	100.0%	11.1740	354.03 ± 0.872
101	9.06272 ± 0.005752	0.78146 ± 0.000358	0.01076 ± 0.000113	0.00819 ± 0.002446	0.0001970 ± 0.00002882	6.35E-14	99.4%	11.5237	364.07 ± 0.448
102	6.23014 ± 0.004462	0.59387 ± 0.000825	0.00776 ± 0.000085	0.00169 ± 0.002649	0.0001742 ± 0.00002362	4.36E-14	99.2%	10.4044	331.76 ± 0.643
103	12.49125 ± 0.010315	1.23127 ± 0.002135	0.01725 ± 0.000263	0.08509 ± 0.001989	0.0005856 ± 0.00005274	8.75E-14	98.7%	10.0112	320.27 ± 0.743
104	22.44482 ± 0.018020	2.20294 ± 0.002731	0.03014 ± 0.000174	0.11474 ± 0.002449	0.0008743 ± 0.00002707	1.57E-13	98.9%	10.0764	322.18 ± 0.495
105	19.80325 ± 0.013670	1.91940 ± 0.002366	0.02645 ± 0.000240	0.09042 ± 0.002080	0.0004573 ± 0.00004983	1.39E-13	99.4%	10.2516	327.30 ± 0.526
106	17.41448 ± 0.005795	1.61900 ± 0.001685	0.02291 ± 0.000149	0.09865 ± 0.002792	0.0014500 ± 0.00004775	1.22E-13	97.6%	10.4976	334.47 ± 0.466
107	11.04368 ± 0.007570	0.91946 ± 0.001315	0.01344 ± 0.000213	0.08464 ± 0.002147	0.0004938 ± 0.00004789	7.73E-14	98.7%	11.8613	373.70 ± 0.772
108	8.67718 ± 0.009956	0.82461 ± 0.000771	0.01064 ± 0.000096	0.00590 ± 0.002808	0.0000633 ± 0.00003709	6.08E-14	99.8%	10.5008	334.56 ± 0.653
109	19.06995 ± 0.014095	1.90525 ± 0.001147	0.02575 ± 0.000217	0.10015 ± 0.002114	0.0007536 ± 0.00003257	1.34E-13	98.9%	9.8974	316.93 ± 0.346
110	12.48873 ± 0.013756	1.24682 ± 0.001863	0.01693 ± 0.000158	0.09615 ± 0.001970	0.0006488 ± 0.00005389	8.75E-14	98.5%	9.8701	316.13 ± 0.723
111	5.64334 ± 0.007632	0.54395 ± 0.001254	0.00693 ± 0.000066	0.01022 ± 0.001882	0.0008972 ± 0.00003020	3.95E-14	95.3%	9.8892	316.69 ± 1.033

FBR-10 (au21.3n.mus)		319 - 405 Ma						
n	^{40}Ar(*+atm)	^{39}Ar (K)	^{38}Ar (Cl+atm)	^{37}Ar (Ca)	^{36}Ar (Atm)	Moles^{40}Ar	%Rad	R	Age(Ma)
1	6.73596 ± 0.003665	0.65160 ± 0.000847	0.00854 ± 0.000069	0.00479 ± 0.003012	0.0000437 ± 0.00001754	7.13E-14	99.8%	10.3185	329.25 ± 0.530
2	7.14827 ± 0.004345	0.66594 ± 0.000781	0.00851 ± 0.000081	0.01405 ± 0.003847	0.0000593 ± 0.00002406	5.01E-14	99.8%	10.7099	340.63 ± 0.565
3	3.00281 ± 0.001444	0.26630 ± 0.000649	0.00360 ± 0.000068	0.00722 ± 0.002124	-0.0000057 ± 0.00001612	3.18E-14	100.1%	11.2787	357.04 ± 1.053
4	24.16754 ± 0.014443	2.06363 ± 0.001372	0.02638 ± 0.000310	0.10850 ± 0.009657	0.0004203 ± 0.00005264	1.69E-13	99.5%	11.6562	367.85 ± 0.408
5	8.80270 ± 0.007513	0.76366 ± 0.001825	0.00955 ± 0.000097	0.00729 ± 0.003880	-0.0000349 ± 0.00002597	9.32E-14	100.1%	11.5279	364.19 ± 0.977
6	4.69370 ± 0.004658	0.43502 ± 0.001038	0.00559 ± 0.000081	0.00966 ± 0.006900	0.0000288 ± 0.00002663	3.29E-14	99.8%	10.7721	342.43 ± 1.059
7	4.45067 ± 0.003908	0.40904 ± 0.000911	0.00511 ± 0.000041	-0.00309 ± 0.004082	0.0000429 ± 0.00003888	4.71E-14	99.7%	10.8492	344.66 ± 1.218
8	3.90913 ± 0.003331	0.35868 ± 0.000534	0.00505 ± 0.000134	-0.00434 ± 0.003727	0.0000994 ± 0.00003172	4.14E-14	99.2%	10.8157	343.70 ± 1.022
9	4.19112 ± 0.005287	0.41339 ± 0.000481	0.00538 ± 0.000067	-0.00510 ± 0.003219	0.0001027 ± 0.00003133	4.44E-14	99.3%	10.0637	321.81 ± 0.908
10	6.82266 ± 0.008704	0.67432 ± 0.000979	0.00879 ± 0.000103	-0.00156 ± 0.003889	0.0001696 ± 0.00003244	7.23E-14	99.3%	10.0432	321.21 ± 0.773
11	2.90499 ± 0.002670	0.26870 ± 0.000389	0.00331 ± 0.000042	-0.00679 ± 0.004039	0.0000610 ± 0.00003224	3.08E-14	99.4%	10.7419	341.56 ± 1.274
12	3.21060 ± 0.002778	0.29503 ± 0.000705	0.00367 ± 0.000043	-0.00785 ± 0.003943	0.0000767 ± 0.00003492	3.40E-14	99.3%	10.8029	343.33 ± 1.418
13	2.25714 ± 0.001336	0.21004 ± 0.000427	0.00264 ± 0.000045	-0.00754 ± 0.003497	0.0002341 ± 0.00003180	2.39E-14	96.9%	10.4137	332.03 ± 1.602
14	9.41026 ± 0.009847	0.88951 ± 0.000681	0.01189 ± 0.000099	0.00204 ± 0.003140	0.0000548 ± 0.00003754	9.97E-14	99.8%	10.5612	336.32 ± 0.591
15	6.49379 ± 0.010857	0.57634 ± 0.001177	0.00733 ± 0.000072	0.00084 ± 0.004816	0.0003140 ± 0.00002905	6.88E-14	98.6%	11.1064	352.09 ± 1.055
16	11.42748 ± 0.012268	1.09145 ± 0.001774	0.01408 ± 0.000132	0.07821 ± 0.003823	0.0005330 ± 0.00004779	1.21E-13	98.7%	10.3327	329.67 ± 0.771
17	12.27503 ± 0.005191	1.06725 ± 0.000896	0.01418 ± 0.000082	0.08585 ± 0.003590	0.0002148 ± 0.00002405	1.30E-13	99.5%	11.4499	361.96 ± 0.402
18	4.20260 ± 0.003084	0.40404 ± 0.000910	0.00533 ± 0.000088	0.00891 ± 0.003603	0.0000503 ± 0.00001672	4.45E-14	99.7%	10.3667	330.66 ± 0.879
19	3.56208 ± 0.002875	0.33126 ± 0.000700	0.00408 ± 0.000059	0.00724 ± 0.001666	0.0000372 ± 0.00001559	3.77E-14	99.7%	10.7221	340.99 ± 0.894
20	3.85247 ± 0.003653	0.37188 ± 0.000664	0.00476 ± 0.000051	0.00470 ± 0.002693	0.0000530 ± 0.00001628	4.08E-14	99.6%	10.3186	329.26 ± 0.788
21	5.72510 ± 0.004415	0.52924 ± 0.000636	0.00684 ± 0.000095	0.01425 ± 0.004900	0.0000782 ± 0.00002631	6.06E-14	99.6%	10.7766	342.57 ± 0.679
22	1.80465 ± 0.002250	0.17660 ± 0.000533	0.00223 ± 0.000038	0.00225 ± 0.005570	-0.0000096 ± 0.00003640	1.91E-14	100.2%	10.2200	326.38 ± 2.223
23	3.72210 ± 0.001606	0.35327 ± 0.000655	0.00438 ± 0.000061	0.01128 ± 0.003930	0.0000529 ± 0.00003954	3.94E-14	99.6%	10.4950	334.39 ± 1.234
24	7.94375 ± 0.005293	0.75606 ± 0.001174	0.00950 ± 0.000074	0.01266 ± 0.004267	0.0001109 ± 0.00003145	8.41E-14	99.6%	10.4651	333.52 ± 0.689
25	6.35987 ± 0.005465	0.58988 ± 0.001138	0.00795 ± 0.000147	-0.01320 ± 0.007569	0.0000531 ± 0.00004037	6.74E-14	99.8%	10.7528	341.88 ± 0.970
26	3.73102 ± 0.004604	0.34204 ± 0.000607	0.00450 ± 0.000063	0.00397 ± 0.004998	0.0000643 ± 0.00003420	3.95E-14	99.5%	10.8538	344.80 ± 1.203
27	3.02369 ± 0.001937	0.24004 ± 0.000552	0.00300 ± 0.000045	0.02778 ± 0.005679	0.0000997 ± 0.00002456	3.20E-14	99.1%	12.4854	391.37 ± 1.343
28	3.88458 ± 0.002371	0.29771 ± 0.000856	0.00379 ± 0.000054	0.02378 ± 0.003890	0.0000895 ± 0.00002418	4.11E-14	99.4%	12.9671	404.90 ± 1.416
29	3.68498 ± 0.002535	0.34104 ± 0.000398	0.00445 ± 0.000110	0.02477 ± 0.003408	0.0000332 ± 0.00003088	3.90E-14	99.8%	10.7835	342.77 ± 0.973
30	1.05656 ± 0.001042	0.09634 ± 0.000455	0.00117 ± 0.000044	0.01168 ± 0.005267	0.0000681 ± 0.00002321	1.12E-14	98.2%	10.7701	342.38 ± 2.839
31	7.88063 ± 0.005148	0.77517 ± 0.000940	0.01029 ± 0.000114	0.00104 ± 0.008780	0.0000261 ± 0.00002996	8.35E-14	99.9%	10.1566	324.52 ± 0.579
32	5.77586 ± 0.004322	0.53984 ± 0.001019	0.00734 ± 0.000063	-0.01342 ± 0.007429	-0.0000386 ± 0.00002443	6.12E-14	100.2%	10.6968	340.25 ± 0.813
33	6.28816 ± 0.004903	0.55954 ± 0.000539	0.00699 ± 0.000052	0.00655 ± 0.004047	-0.0000322 ± 0.00002526	6.66E-14	100.2%	11.2392	355.91 ± 0.611
34	6.17055 ± 0.004554	0.60511 ± 0.001027	0.00787 ± 0.000121	-0.01774 ± 0.007406	0.0000412 ± 0.00001517	6.53E-14	99.8%	10.1745	325.05 ± 0.649
35	7.74931 ± 0.008869	0.71388 ± 0.000985	0.00904 ± 0.000062	0.00741 ± 0.003493	0.0001356 ± 0.00001625	8.21E-14	99.5%	10.8001	343.24 ± 0.655
36	4.68470 ± 0.005370	0.41170 ± 0.001020	0.00521 ± 0.000051	-0.00229 ± 0.003887	0.0000143 ± 0.00001621	4.96E-14	99.9%	11.3681	359.61 ± 1.050
37	3.34783 ± 0.001773	0.31658 ± 0.000697	0.00437 ± 0.000091	0.00313 ± 0.002764	0.0000332 ± 0.00002391	3.55E-14	99.7%	10.5450	335.85 ± 1.044
38	3.41221 ± 0.003093	0.29575 ± 0.000522	0.00384 ± 0.000065	-0.00098 ± 0.003021	0.0000240 ± 0.00001724	3.61E-14	99.8%	11.5132	363.76 ± 0.906
39	13.28343 ± 0.008354	1.21721 ± 0.001298	0.01559 ± 0.000100	0.09030 ± 0.002806	0.0002842 ± 0.00002931	1.41E-13	99.4%	10.8512	344.72 ± 0.485
40	3.71358 ± 0.003247	0.36063 ± 0.000564	0.00461 ± 0.000052	0.01375 ± 0.004067	0.0000120 ± 0.00001836	3.93E-14	99.9%	10.2913	328.46 ± 0.761
41	5.68018 ± 0.004382	0.49428 ± 0.000462	0.00620 ± 0.000064	0.00823 ± 0.002693	0.0000113 ± 0.00003106	6.02E-14	100.0%	11.4866	363.01 ± 0.734
42	5.95141 ± 0.004049	0.54928 ± 0.000775	0.00677 ± 0.000054	0.00154 ± 0.004803	0.0000196 ± 0.00003010	6.30E-14	99.9%	10.8248	343.96 ± 0.747
43	5.90684 ± 0.004582	0.49955 ± 0.000650	0.00640 ± 0.000076	0.00452 ± 0.003496	0.0000756 ± 0.00002426	6.26E-14	99.6%	11.7806	371.40 ± 0.724
44	7.28752 ± 0.008243	0.68911 ± 0.001099	0.00885 ± 0.000089	-0.00958 ± 0.005966	0.0000452 ± 0.00003046	7.72E-14	99.8%	10.5546	336.13 ± 0.780
45	4.24820 ± 0.003452	0.38684 ± 0.000756	0.00510 ± 0.000073	0.00726 ± 0.006055	0.0001147 ± 0.00002264	4.50E-14	99.2%	10.8961	346.02 ± 0.922
46	3.56879 ± 0.003796	0.30759 ± 0.000671	0.00390 ± 0.000049	0.00153 ± 0.005035	0.0000834 ± 0.00002332	3.78E-14	99.3%	11.5229	364.04 ± 1.139
47	5.64205 ± 0.004116	0.48644 ± 0.000845	0.00609 ± 0.000045	-0.00668 ± 0.004590	0.0000567 ± 0.00002948	5.98E-14	99.7%	11.5629	365.19 ± 0.893
48	5.69771 ± 0.005966	0.48057 ± 0.001004	0.00594 ± 0.000058	-0.01104 ± 0.004269	0.0000684 ± 0.00002948	6.03E-14	99.6%	11.8118	372.29 ± 1.044
49	8.43001 ± 0.007533	0.83815 ± 0.001086	0.01060 ± 0.000084	0.00943 ± 0.005398	0.0000875 ± 0.00002307	8.93E-14	99.7%	10.0281	320.76 ± 0.570
50	9.20884 ± 0.012907	0.91064 ± 0.001932	0.01168 ± 0.000124	0.00999 ± 0.003838	0.0001607 ± 0.00002223	9.75E-14	99.5%	10.0614	321.74 ± 0.854
51	4.47519 ± 0.003938	0.43888 ± 0.000864	0.00557 ± 0.000047	-0.00156 ± 0.004987	0.0000310 ± 0.00003308	4.74E-14	99.8%	10.1757	325.08 ± 1.001
52	2.39868 ± 0.001862	0.20027 ± 0.000351	0.00255 ± 0.000049	0.00281 ± 0.003594	-0.0000022 ± 0.00003472	2.54E-14	100.0%	11.9785	377.03 ± 1.768
53	2.37514 ± 0.002400	0.22182 ± 0.000445	0.00281 ± 0.000035	-0.00275 ± 0.005898	0.0000392 ± 0.00002475	2.52E-14	99.5%	10.6538	339.01 ± 1.302
54	11.46557 ± 0.005859	1.01347 ± 0.001407	0.01327 ± 0.000077	0.09376 ± 0.005991	0.0003877 ± 0.00004556	1.21E-13	99.1%	11.2092	355.05 ± 0.678
55	3.64220 ± 0.004328	0.34158 ± 0.000618	0.00465 ± 0.000048	0.00667 ± 0.003321	0.0000657 ± 0.00002451	3.86E-14	99.5%	10.6080	337.68 ± 0.999
56	2.98777 ± 0.002025	0.27401 ± 0.000640	0.00361 ± 0.000074	0.00601 ± 0.004386	0.0000840 ± 0.00002444	3.16E-14	99.2%	10.8154	343.69 ± 1.189
57	5.28311 ± 0.002391	0.45463 ± 0.000807	0.00575 ± 0.000089	-0.01922 ± 0.007540	-0.0000488 ± 0.00002955	5.60E-14	100.3%	11.6165	366.72 ± 0.907

FBR-10 (au21.3n.mus)			continued							
n	^{40}Ar(*+atm)	^{39}Ar (K)	^{38}Ar (Cl+atm)	^{37}Ar (Ca)	^{36}Ar (Atm)	Moles^{40}Ar	%Rad	R	Age(Ma)
58	1.13025 ± 0.001715	0.10061 ± 0.000269	0.00120 ± 0.000042	-0.00005 ± 0.002753	0.0000001 ± 0.00001685	1.20E-14	100.0%	11.2333	355.74 ± 1.921
59	5.85630 ± 0.003553	0.57842 ± 0.000725	0.00728 ± 0.000058	-0.00139 ± 0.004992	0.0000040 ± 0.00001743	6.20E-14	100.0%	10.1224	323.52 ± 0.535
60	2.71515 ± 0.002248	0.25827 ± 0.000797	0.00328 ± 0.000056	0.00170 ± 0.002760	0.0000263 ± 0.00001750	2.88E-14	99.7%	10.4836	334.06 ± 1.248
61	4.07838 ± 0.003614	0.39502 ± 0.000465	0.00502 ± 0.000064	-0.00296 ± 0.004351	0.0000102 ± 0.00001918	4.32E-14	99.9%	10.3161	329.18 ± 0.670
62	7.56733 ± 0.003517	0.70448 ± 0.001190	0.00909 ± 0.000084	0.00948 ± 0.003820	0.0001186 ± 0.00002414	8.01E-14	99.5%	10.6932	340.15 ± 0.680
63	4.90013 ± 0.004238	0.40818 ± 0.000431	0.00514 ± 0.000060	0.01300 ± 0.003684	0.0001025 ± 0.00002467	5.19E-14	99.4%	11.9336	375.76 ± 0.764
64	3.83005 ± 0.002416	0.35553 ± 0.000455	0.00443 ± 0.000056	-0.00577 ± 0.004232	-0.0000165 ± 0.00003375	4.06E-14	100.1%	10.7712	342.41 ± 1.018
65	5.67058 ± 0.004476	0.48906 ± 0.000917	0.00612 ± 0.000060	0.00157 ± 0.003082	0.0000607 ± 0.00003116	6.01E-14	99.7%	11.5584	365.06 ± 0.954
66	1.04445 ± 0.001037	0.09298 ± 0.000355	0.00113 ± 0.000040	0.00344 ± 0.004180	0.0000069 ± 0.00003265	1.11E-14	99.8%	11.2151	355.22 ± 3.580
67	2.39082 ± 0.001584	0.21931 ± 0.000765	0.00270 ± 0.000041	0.00266 ± 0.002471	-0.0000057 ± 0.00003665	2.53E-14	100.1%	10.9028	346.22 ± 1.994
68	3.24656 ± 0.002789	0.30743 ± 0.000771	0.00394 ± 0.000051	-0.00484 ± 0.003185	0.0000832 ± 0.00002311	3.44E-14	99.2%	10.4789	333.93 ± 1.140
69	9.93874 ± 0.010718	0.86896 ± 0.001428	0.01126 ± 0.000127	0.01136 ± 0.005948	0.0001182 ± 0.00002398	1.05E-13	99.7%	11.3986	360.48 ± 0.757
70	4.08795 ± 0.003486	0.38995 ± 0.000465	0.00492 ± 0.000052	0.00387 ± 0.004363	0.0000931 ± 0.00002528	4.33E-14	99.3%	10.4136	332.03 ± 0.784
71	6.18157 ± 0.006169	0.56293 ± 0.001206	0.00738 ± 0.000103	0.01321 ± 0.003238	0.0000888 ± 0.00002422	6.55E-14	99.6%	10.9367	347.19 ± 0.918
72	3.05620 ± 0.003054	0.26844 ± 0.000479	0.00331 ± 0.000054	-0.00068 ± 0.002729	0.0000549 ± 0.00002610	3.24E-14	99.5%	11.3243	358.35 ± 1.171
73	4.61861 ± 0.004720	0.39300 ± 0.000904	0.00503 ± 0.000054	0.00042 ± 0.004667	0.0001040 ± 0.00002658	4.89E-14	99.3%	11.6741	368.36 ± 1.128
74	4.02492 ± 0.003002	0.36362 ± 0.000675	0.00452 ± 0.000047	-0.00557 ± 0.004068	0.0000199 ± 0.00001722	4.26E-14	99.9%	11.0515	350.51 ± 0.832
75	2.19049 ± 0.002674	0.20252 ± 0.000670	0.00250 ± 0.000048	-0.00738 ± 0.002668	0.0000106 ± 0.00001685	2.32E-14	99.9%	10.7969	343.15 ± 1.444
76	3.27571 ± 0.002254	0.28884 ± 0.000690	0.00356 ± 0.000044	-0.00530 ± 0.004069	-0.0000008 ± 0.00002366	3.47E-14	100.0%	11.3393	358.78 ± 1.178
77	1.74108 ± 0.001513	0.16300 ± 0.000409	0.00210 ± 0.000044	-0.00487 ± 0.002654	-0.0000459 ± 0.00003169	1.84E-14	100.8%	10.6786	339.73 ± 2.039
78	4.07393 ± 0.002022	0.33593 ± 0.000996	0.00413 ± 0.000043	0.00337 ± 0.005403	-0.0000342 ± 0.00002987	4.31E-14	100.3%	12.1284	381.29 ± 1.414
79	3.04219 ± 0.002439	0.29195 ± 0.000423	0.00369 ± 0.000050	-0.02520 ± 0.006133	0.0000117 ± 0.00001794	3.22E-14	99.9%	10.4001	331.63 ± 0.802
80	3.29680 ± 0.002482	0.30177 ± 0.000909	0.00402 ± 0.000126	-0.00539 ± 0.004029	0.0000226 ± 0.00001912	3.49E-14	99.8%	10.9010	346.16 ± 1.232
81	4.34778 ± 0.003938	0.41522 ± 0.000537	0.00526 ± 0.000062	-0.00284 ± 0.002431	0.0000824 ± 0.00002739	4.60E-14	99.4%	10.4117	331.97 ± 0.816
82	2.99665 ± 0.002355	0.28649 ± 0.000710	0.00354 ± 0.000054	0.00205 ± 0.002149	0.0000757 ± 0.00002433	3.17E-14	99.3%	10.3826	331.12 ± 1.180
83	4.00010 ± 0.003406	0.37793 ± 0.000702	0.00489 ± 0.000064	0.01064 ± 0.003459	-0.0000232 ± 0.00002786	4.24E-14	100.2%	10.5869	337.06 ± 0.978
84	5.62384 ± 0.002395	0.52346 ± 0.000716	0.00690 ± 0.000135	-0.00505 ± 0.007226	0.0000486 ± 0.00003102	5.96E-14	99.7%	10.7151	340.78 ± 0.743
85	7.02780 ± 0.005650	0.67484 ± 0.001132	0.00887 ± 0.000122	0.00929 ± 0.004093	0.0001360 ± 0.00002369	7.44E-14	99.4%	10.3557	330.34 ± 0.701
86	3.23760 ± 0.003796	0.26672 ± 0.000780	0.00373 ± 0.000070	0.00513 ± 0.002783	0.0000780 ± 0.00003552	3.43E-14	99.3%	12.0539	379.17 ± 1.727
87	1.99947 ± 0.001711	0.18529 ± 0.000447	0.00222 ± 0.000044	0.01427 ± 0.004709	0.0000078 ± 0.00001437	2.12E-14	99.9%	10.7859	342.83 ± 1.145
88	1.56947 ± 0.001479	0.14339 ± 0.000547	0.00167 ± 0.000042	0.01522 ± 0.004686	-0.0000025 ± 0.00001378	1.66E-14	100.1%	10.9558	347.75 ± 1.641
89	1.27983 ± 0.001521	0.11597 ± 0.000356	0.00134 ± 0.000037	0.00995 ± 0.003769	-0.0000018 ± 0.00001564	1.36E-14	100.1%	11.0444	350.30 ± 1.716
90	2.61911 ± 0.003941	0.23736 ± 0.000865	0.00288 ± 0.000055	0.00707 ± 0.003185	-0.0000014 ± 0.00001408	2.77E-14	100.0%	11.0374	350.10 ± 1.489
91	4.27448 ± 0.002934	0.34898 ± 0.000745	0.00433 ± 0.000061	0.00907 ± 0.005289	0.0000078 ± 0.00001292	4.53E-14	100.0%	12.2443	384.57 ± 0.930
92	1.52208 ± 0.001282	0.13480 ± 0.000349	0.00169 ± 0.000039	-0.00215 ± 0.002511	-0.0000386 ± 0.00002594	1.61E-14	100.7%	11.2898	357.36 ± 2.048
93	2.70838 ± 0.002072	0.25143 ± 0.000672	0.00331 ± 0.000055	0.00877 ± 0.004717	-0.0000546 ± 0.00002532	2.87E-14	100.6%	10.7751	342.52 ± 1.344
94	2.66560 ± 0.002452	0.26515 ± 0.000442	0.00335 ± 0.000042	0.00283 ± 0.003963	-0.0000429 ± 0.00002841	2.82E-14	100.5%	10.0543	321.53 ± 1.185
95	7.68037 ± 0.006094	0.69276 ± 0.001407	0.00896 ± 0.000067	0.00705 ± 0.002699	0.0000731 ± 0.00001629	8.13E-14	99.7%	11.0564	350.65 ± 0.798
96	2.68653 ± 0.002704	0.26649 ± 0.000434	0.00333 ± 0.000044	0.01156 ± 0.003061	-0.0000015 ± 0.00001618	2.85E-14	100.1%	10.0855	322.44 ± 0.845
97	0.94920 ± 0.001103	0.08799 ± 0.000483	0.00118 ± 0.000033	0.00869 ± 0.003794	0.0000218 ± 0.00001473	1.01E-14	99.4%	10.7238	341.03 ± 2.500
98	2.12966 ± 0.001581	0.20265 ± 0.000379	0.00276 ± 0.000038	0.01360 ± 0.004473	0.0000229 ± 0.00001289	2.26E-14	99.7%	10.4822	334.02 ± 0.910
99	5.18667 ± 0.004573	0.45372 ± 0.000856	0.00608 ± 0.000098	0.01120 ± 0.004464	0.0000375 ± 0.00001578	5.49E-14	99.8%	11.4095	360.80 ± 0.822
100	7.44599 ± 0.007526	0.70105 ± 0.001090	0.00917 ± 0.000141	0.00894 ± 0.005048	0.0000551 ± 0.00001570	7.89E-14	99.8%	10.5992	337.42 ± 0.662
101	9.65830 ± 0.009063	0.86200 ± 0.001758	0.01108 ± 0.000083	0.01456 ± 0.004726	0.0001095 ± 0.00003072	1.02E-13	99.7%	11.1687	353.88 ± 0.864
102	7.13281 ± 0.005308	0.71386 ± 0.000833	0.00903 ± 0.000081	0.00506 ± 0.004573	-0.0000633 ± 0.00002658	7.55E-14	100.3%	9.9926	319.72 ± 0.566
103	6.01688 ± 0.007081	0.57623 ± 0.000706	0.00722 ± 0.000077	0.00596 ± 0.004630	0.0000660 ± 0.00002494	6.37E-14	99.7%	10.4089	331.89 ± 0.698
104	4.46213 ± 0.006517	0.43380 ± 0.001023	0.00574 ± 0.000079	0.00691 ± 0.003924	0.0000574 ± 0.00002313	4.73E-14	99.6%	10.2485	327.21 ± 1.041
105	3.61651 ± 0.002806	0.33647 ± 0.000838	0.00421 ± 0.000054	-0.01692 ± 0.006909	0.0000531 ± 0.00001678	3.83E-14	99.6%	10.6969	340.26 ± 1.011
106	4.99910 ± 0.004258	0.47838 ± 0.001298	0.00610 ± 0.000067	0.00081 ± 0.005134	0.0000815 ± 0.00001683	5.29E-14	99.5%	10.3998	331.62 ± 1.005
107	2.75196 ± 0.002114	0.25753 ± 0.000647	0.00326 ± 0.000041	0.01040 ± 0.003719	0.0000448 ± 0.00002461	2.91E-14	99.6%	10.6385	338.56 ± 1.269
108	1.97233 ± 0.001830	0.18407 ± 0.000505	0.00236 ± 0.000048	-0.01048 ± 0.006899	0.0000389 ± 0.00002868	2.09E-14	99.4%	10.6472	338.82 ± 1.771
109	1.36975 ± 0.001775	0.12559 ± 0.000278	0.00161 ± 0.000047	0.00194 ± 0.006007	0.0001153 ± 0.00001648	1.45E-14	97.5%	10.6371	338.52 ± 1.531
110	9.66316 ± 0.006956	0.92487 ± 0.001187	0.01182 ± 0.000110	0.02332 ± 0.004389	0.0000790 ± 0.00001537	1.02E-13	99.8%	10.4253	332.37 ± 0.515
111	4.50422 ± 0.004097	0.44396 ± 0.000818	0.00589 ± 0.000104	0.00450 ± 0.004265	0.0000736 ± 0.00001634	4.77E-14	99.5%	10.0975	322.80 ± 0.753
112	2.35525 ± 0.002023	0.19532 ± 0.000557	0.00243 ± 0.000062	-0.00197 ± 0.005026	0.0000476 ± 0.00002443	2.49E-14	99.4%	11.9852	377.22 ± 1.625